

2006

Fabrication of Array Microstructures by Localized Electro-Deposition

Nidal Khalaf AlShwawreh

Follow this and additional works at: https://scholarworks.uaeu.ac.ae/all_theses

Part of the [Materials Science and Engineering Commons](#)

Recommended Citation

AlShwawreh, Nidal Khalaf, "Fabrication of Array Microstructures by Localized Electro-Deposition" (2006). *Theses*. 585.
https://scholarworks.uaeu.ac.ae/all_theses/585

This Thesis is brought to you for free and open access by the Electronic Theses and Dissertations at Scholarworks@UAEU. It has been accepted for inclusion in Theses by an authorized administrator of Scholarworks@UAEU. For more information, please contact fadl.musa@uaeu.ac.ae.



**United Arab Emirates University
Deanship of Graduate Studies**

Fabrication of Array Microstructures by Localized Electro-Deposition

By

Nidal Khalaf AlShwawreh

Supervised by

Dr. Ra'a Ahmed Said

Prof. Yousef Haik

Electrical Engineering Department
Faculty of Engineering, UAEU

Mechanical Engineering Department
Faculty of Engineering, UAEU

A Thesis Submitted to the Deanship of Graduate Studies in Partial
Fulfillment of the Requirements for Degree of Master of Science in

Materials Science and Engineering

2005-2006

ES/F11

United Arab Emirates University
Graduate Studies
M.S.c. Program in Materials Science and Engineering



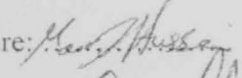
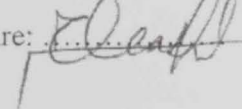
THESIS EXAMINATION REPORT

Student ID : 200350214
Student Name : Nidal Khalaf Hamed Alshwawareh
Title of The Thesis : Fabrication of Array Microstructures by Localized Electro-Deposition.


The Thesis Examination as A Partial Fulfillment of M. Sc. Degree in Materilas Science and Engineering Was conducted on Based on Examining the Thesis and the Students Presentation and the Subsequent Discussion, The Committee Recommends:

- Thesis is Satisfactory as is.
- Thesis is Satisfactory After Minor Modifications.
- Thesis should be Re-Evaluated After Major Modifications
- Thesis is Rejected.

Examining Committee Members:

Thesis Supervisor:	Name: <u>Yousef Haik</u>	Signature: 	Date: <u>10/6/2006</u>
Member:	Name: <u>Khalifa H.K. Haik</u>	Signature: 	Date: <u>10/6/2006</u>
Member :	Name: <u>Mausa I. Hussein</u>	Signature: 	Date: <u>10 June, 2006</u>
Member :	Name: <u>Moh.d. Ameen Jarrak</u>	Signature: 	Date: <u>10-6-06</u>

Approval of Program Coordinator:

Dr. Yousef Haik  Date : 10/6/2006

APPROVAL:
Dean of Graduate Studies

Date :

Dedication

This work is dedicated to my beloved parents, family, my wife and my daughter Luma for their continuous love, support, encouragement and guidance.

Abstract

Localized Electro-Deposition (LED) is now highly receiving scientists and researchers attention for its advantages over conventional fabrication techniques. These advantages include simplicity of the setup thus reducing the overall fabrication cost, capability of producing 2D and 3D high aspect ratio microstructures and its ability to fabricate microstructures from various raw materials. Efforts now are taking place in order to standardize the fabrication by LED to develop a commercial setup that is capable of producing complex microstructures which, in turn, can be integrated in different applications including microelectronics, microelectrochemical systems (MEMS) and sensors applications. The standardization process is performed by studying and optimizing all the parameters that control the LED process. In order to expand the current LED capabilities, this research thesis is investigating the feasibility of fabricating array of microstructures. These micro scale structures can be used as antenna arrays in ultra high frequency applications and also can be integrated in mechanical microsystems.

In this work, two LED fabrication algorithms were introduced and compared to produce arrays of micro scale features: serial deposition and parallel deposition. In serial deposition algorithm, the conventional single tip microelectrode is used to realize high aspect ratio array elements by fabricating them serially (i.e. element by element), while in the parallel deposition algorithm; the same array is fabricated by using multi-tip array microelectrode where the array microstructures are fabricated simultaneously (all array elements grow in parallel fashion). The effects of microelectrode tip material, tip geometry and the used electrolyte (raw material) on the LED fabrication process are also presented.

The new fabrication technology tested in this work enables the advancement of antennas for the upper GHz range. By implementing the parallel deposition technique outlined in this thesis, the resolution and repeatability will be enhanced and the required fabrication time of a microsystem will be shorter thus enhancing the overall production rate.

Acknowledgments

First, I always thank almighty Allah for giving me the opportunity and the well to complete this work.

I would like to express my sincere gratitude to my advisor, Dr. Ra'a Said for his unlimited and continuous support and guidance.

I would like to thank my second advisor Prof. Yousef Haik for his support especially in accelerating the work, reviewing the results and his support while preparing the thesis and publications.

I want to thank CLU unit and the SEM technician at the United Arab Emirates for the assistance in getting the SEM images for the samples.

I want to thank the workshop technicians for their assistance in fabricating the substrates and the electrochemical cell.

No words can express my special thanks to my great family, especially my parents and my wife for her great help and continuous support.

Table of Contents

Chapter	Page
Chapter 1: Introduction to Microfabrication	
1.1 Microfabrication Overview.....	2
1.2 History of Microfabrication.....	3
1.3 Microfabrication Applications and Benefits.....	4
1.4 Applications of electrochemical microfabrication.....	5
1.5 Microstructuring techniques.....	6
1.5.1 LIGA.....	10
1.5.2 Excimer Laser Micromachining.....	11
1.5.3 Micro Electro Discharge Machining.....	12
1.5.4 Laser Assisted Chemical Vapor Deposition.....	13
1.5.5 Micro Stereo Lithography.....	13
1.5.6 LDGW and FGDW.....	14
1.5.7 Laser-induced Forward Transfer.....	14
1.5.8 Shape Deposition Modeling.....	15
1.5.9 Localized Electrodeposition.....	15
1.5.10 Electrochemical Fabrication.....	16
1.6 Comparison between microfabrication techniques.....	17
Chapter 2: Localized Electro-Deposition	
2.1 Introduction.....	24
2.2 Theory of LED.....	25
Chapter 3: Serial/Parallel Fabrication by LED	
3.1 Serial Deposition Using Single Tip Microelectrode.....	38
3.2 Parallel Fabrication Using Array Tip Microelectrode.....	41
Chapter 4: Single and Multi Tip Microelectrode	
4.1 Microelectrode	47
4.2 Single Tip Microelectrode	47
4.3 Multi-Tip Microelectrode	51
4.4 Preparation of Microelectrode	53
4.5 Applications.....	54

Chapter 5: LED Process Simulation

5.1 Simulation of the deposition process.....	57
5.2 Single Tip Microelectrode Simulation	58
5.3 Multi Tip Microelectrode Simulation	60

Chapter 6: Experimental Procedures, Results and Discussion

6.1 LED setup.	67
6.1.1 Electrode fabrication and preparation.....	69
6.1.2 Substrate preparation.....	73
6.1.3 Electrolyte.....	74
6.1.4 Picomotors.....	74
6.1.5 Switching/Gating Circuit.....	74
6.2 Implementing the controlling algorithm by LabVIEW	75
6.3 LED Experiment and results.....	77
6.3.1 Single Tip Microelectrode.....	80
6.3.2 Serial Deposition by single tip microelectrode.....	83
6.3.3 Parallel Deposition by multi tip microelectrode.....	89
6.4 Error Analysis.....	100
6.5 Effect of tip diameter	102
6.6 Effect of tip's material.....	102
6.7 Effect of tips spacing.....	103
6.8 Effect of electrolyte.....	103

Chapter 7: Conclusion and Future Work.....105

7.1 Conclusion.....	107
7.2 Future Work.....	109

References.....110**Appendix.....**114

List of Figures

Figure	Page
1.1: A schematic diagram illustrating the photolithography process	8
1.2: Outline of the micromolding process using LIGA technology	11
1.3: A schematic diagram illustrating the Eximer Laser Micromachining process.....	12
1.4: Microstereolithography.....	14
1.5: LED principle	16
1.6: Microstructures made by different microfabrication techniques	17
2.1: A schematic for the LED deposition at a close distance between the electrode tip and the conducting substrate	26
2.2: A schematic illustrating the concept of the double layer	27
2.3: A schematic illustrating the deposition of the copper ions.	27
2.4: Schematic for the fabrication by Localized Electrodeposition.....	29
2.5: Column structures fabricated by LED.....	30
3.1: LED array microfabrication by Serial/Continuous Deposition algorithm.....	39
3.2: A schematic illustrating the LED array microfabrication by Serial/discrete deposition algorithm.....	40
3.3: LED setup for parallel deposition algorithm.....	43
3.4: A schematic illustrating the LED array microfabrication by Parallel Deposition.....	44
4.1: Most important geometries of microelectrodes and microelectrode arrays.....	48
4.2: Single tip microelectrode.....	48
4.3: A schematic diagram illustrating the concept of diffusion layer.....	51
4.4: General electrical model for the electrode/electrolyte interface.....	51
4.5: Microelectrode arrays.....	53
5.1: Electrical field distribution in the case of single tip microelectrode.....	58
5.2: Electric field computed along imaginary line parallel to the substrate.....	59
5.3: Electrical field distribution in the case of a multi tip microelectrode.....	60
5.4: Electric field computed along imaginary line parallel to the substrate.....	61
5.5: Electrical field distribution in the case of a multi tip microelectrode.....	61
5.6: Electric field computed along imaginary line parallel to the substrate.....	62
5.7: Electrical field distribution in the case of a 3 tips microelectrode	62
5.8: Electric field computed along imaginary line parallel to the substrate.....	63
5.9: Electrical field distribution in the case of a 5 tips microelectrode.....	64
5.10: Electrical field distribution in the case of a 5 tips microelectrode.....	65
6.1: A general photo for the LED setup.....	68
6.2: LED setup.....	68
6.3: 3-D Picomotors.....	69
6.4 A-E: Array microelectrodes.....	70-72
6.5: 55 elements micro array.....	73

6.6 (a)-(b): The calibration process for initial positioning of the microelectrode.....	78-79
6.7: Deposition process as it appears in the microscope.....	80
6.8: Single copper column microstructure.....	81
6.9: Single copper column microstructure.....	82
6.10: Single copper column microstructure.....	83
6.11: 4 microstructures fabricated by serial deposition/discrete algorithm.....	84
6.12: 2 microstructures fabricated by serial deposition/discrete algorithm.....	85
6.13: 4 microstructures fabricated by serial deposition/discrete algorithm.....	86
6.14: 2 microstructures fabricated by serial deposition/continuous algorithm.....	87
6.15: Another failed serial structure.....	88
6.16(A-C): Parallel deposition using heptode microelectrode.....	89-91
6.17: SEM for 2 elements array microstructures fabricated by parallel deposition....	92
6.18: SEM for 2 elements array microstructures fabricated by parallel deposition....	93
6.19: SEM for 4 elements array microstructures fabricated by parallel deposition....	94
6.20: Two-nickel microstructures fabricated by parallel deposition.....	95
6.21: 6-nickel microstructures fabricated by parallel deposition.....	96
6.22: A 6 elements copper array microstructure	97
6.23: A 6 elements copper array microstructure	98
6.24: A 3-elements copper array microstructure.....	99
6.25: A 5-elements nickel array microstructure.....	100

List of Tables

Table	Page
1.1: Comparison between etching techniques.....	9
1.2: Comparison between micromachining technologies.....	18
1.3: Materials used in the various microdeposition techniques	20
1.4: Comparison between deposition techniques.....	21
6.1: Error analysis for single column deposition.....	101
6.2: Error analysis for serial fabrication/discrete algorithm	101
6.3: Error analysis for parallel fabrication algorithm.....	101
6.4: Effect of tip diameter on the fabrication of the array microstructures.....	102
6.5: Effect of electrode tip material on the fabricated microstructure.....	103
6.6: Effect of tip diameter on the fabricated microstructure.....	103
6.7: Effect of electrolyte material on the fabricated microstructure.....	104
7.1: Comparison between parallel and serial fabrication algorithms.....	108

Chapter 1:

Introduction to Microfabrication

1.1 Microfabrication Overview

Scientists, years ago, were convinced that fabrication must be performed in a smaller scale that is in the range of micrometer and nanometer scales in order to maximize the processing speed of the electronics components and microprocessors. Efforts around the globe started to enhance and create new fabrication capabilities that were unimaginable with the traditional technologies, which are suffering from several drawbacks and limitations. An increasing demand to fabricate microstructures that can be integrated in microelectronics, microsystems and microelectromechanical devices was of great influence to start discovering new microscale machining opportunities. As a result of these efforts, new tools and techniques to produce microscale 1D, 2D and 3D structures have come to reality. The term "microstructure" has been used to denote physical devices with minimum dimension much smaller than those of devices such as bipolar or field-effect transistors (FET) used in logic or memory circuits.

In order to comply with the new technologies that are evolving in many applications as: microelectronics, medicine, bioengineering and communication, the optimal fabrication technique suitable for microscale machining must be reliable, able to produce repeatable high aspect ratio microstructures with complex geometry features in 2D and 3D space, produce microstructures from different raw materials, fabricate microstructures with high production rate and must be relatively cheap in order to be commercialized for public use.

For years, there were a variety of fabrication techniques capable of producing microstructures and devices suitable for different challenging applications. LIGA, photolithography, electro discharge machining and laser enhanced chemical vapour deposition are some of these technologies. However, The repaid development of the microelectromechanical systems and their applications and the need for a more advanced microscale components in electronics, medicine and communication have led to expand the scientific research further in order to develop new fabrication techniques with

excellent capabilities or to enhance the current fabrication techniques that have reached their ultimate throughput.

At the beginning, microfabrication has started by implementing microelectronics fabrication techniques. The structures produced using microelectronics technologies were largely of low aspect ratio (height to width ratio), often limited to the use of silicon, equipments are generally expensive and suffering from long development time [1]. As a result, the need for independent techniques to support the rapidly growing microelectromechanical systems (MEMS) and other microscale and nanoscale devices and their applications has led to invent innovative fabrication technologies to overcome the drawbacks of the microelectronics fabrication technology.

1.2 History of Microfabrication

Lithography technique was used to fabricate solid-state devices of limited resolution in 1950s using the planar process for mass production. Research then turned to enhance the fabrication process to improve the resolution. By the nearly 1960s, lithography had progressed to the point where integrated circuits with minimum device line width of $5\mu\text{m}$ were mass-produced using primarily optical-lithography tools and photographic emulsion mask. Improvement of the photoresist material used in lithography process then took place to enhance the resolution further. Few years later Westinghouse developed the first Resonant Gate FET. In 1970, a bulk etched silicon wafers were used as pressure sensors. Later In 1982, Kurt published "Silicon as Structural Material". Electrostatic and comp drivers and micro positioning disk drive heads were the first actuators produced by microfabrication [2]. What considered as a revolution in the research and development of microfabrication industry started in the 80's and 90's of the last century. In 1960s, the minimum dimensions were typically $5\mu\text{m}$; anything below $1\mu\text{m}$ was considered a "microstructure". Today, the minimum size of production devices is down to $1\mu\text{m}$ or less, consequently the term "microstructures" implies devices with dimensions that can reach to $0.1\mu\text{m}$ or less [3]. Starting from the 90s, various microsystems started to appear for the first time including micropumps, micromotors, microgears and microsensors.

For many years, microstructures were limited to 2-D structures. That was due to the fact that early fabrication techniques were borrowed from the microelectronics industry, such as photolithography, wet and dry etching and thin film deposition, which are originally 2-D processes. Research efforts then turned trying to invent new micromachining techniques with broad capabilities allowing a third dimension to be realized. LIGA, electro discharge machining and laser enhanced chemical vapour deposition are some examples of the recently developed techniques suitable for 3D micromachining. Moreover, microfabrication nowadays is not restricted to silicon; microstructures from metals, polymers, ceramics, semiconductors, diamond, glasses, and even organic substances can be produced using one of several available microfabrication techniques [4]. What helped also is that many organizations, especially in the US, have allocated research grants to accelerate the microfabrication technologies and improve the reliability and performance of the micromachining techniques. Nowadays microfabrication is a science of itself, the awareness of this field is now increasing as its applications almost start to enter every aspect of the modern industry.

1.3 Microfabrication Applications and Benefits

From nanoscale to milliscale, microstructures are now playing an important role in instrumentation and microelectronics [5], high-speed processors, medicine, vehicle accelerometers and sensors, surveillance and communication [6]. Micromachining contributed to other wide range of applications as in microrobotics [7], life sciences [8]-[9], integrated hydro- and thermodynamics microsystems [10]-[11] and antenna elements working in Gigahertz and Terahertz ranges [12]-[15].

Microfabrication technologies have resulted in an interdisciplinary field called MEMS, which stands for Micro-Electro-Mechanical Systems. MEMS are integrated microparts including mechanical elements, sensors, actuators and electronics on a substrate fabricated using any of several micromachining technologies available. Micropumps and micromotors are some examples of what microfabrication can offer to MEMS. In their

turn, MEMS have recently being used in many industries starting from automobile to defense and medical industries. Applications of these devices are emerging in a wide variety of industries, such as: pressure, temperature, chemical and vibration sensors, light reflectors, switches, accelerometers (for airbags, pacemakers and games), microactuators for data storage and read/write heads, all-optical switches, and consumer products (thermistors of all kinds) [16]. MEMS also involved in biological application as BioMEMS, which has the growth rate within MEMS market as in biosensors. Biosensors are used as tools to manipulate biomolecules, particularly, for drug discovery and delivery [17], as an example, MEMS based biosensors can be used for intravenous blood pressure monitors [16]. MEMS also started to be a major component in the military applications with primary goal to develop the technology to merge sensing, actuating, and computing in order to realize new systems that bring enhanced levels of perception, control, and performance to weapons systems and battlefield environments [18].

1.4 Applications of Electrochemical Microfabrication

Electrochemical deposition (plating) is the oldest industrial application of an electrochemical reaction. Both electroplating and electroless plating processes deposit pure metals or alloys from metallic ions in solution. Plating also can alter the deposit's electrical, mechanical, magnetic properties, brightness, color, and resistance to corrosion. Storage, packaging, device fabrication, and several other aspects of microelectronics have been affected by electrochemical processing. Electrochemical microfabrication has advanced each level of microelectronic packaging [19].

Copper wiring, introduced by IBM in 1997, uses low-cost electrolytic plating. Copper resistance is 40% less than aluminum wires leading to faster microprocessors. Also electroplating is used for fabrication of copper chip interconnections, void-free deposits in interconnection trenches can be realized by electrodeposition. Internal wiring in the chip becomes very complex in multichip modules. In conjunction with high-aspect-ratio lithography, electrochemical microfabrication offers the possibility of readily producing thick conductors with lateral dimensions in the submicrometer range if required [19].

Electroplated magnetic materials that are used in storage technology are also another application for electrochemical microfabrication. The addition of impurities to nickel-iron alloys in a controlled manner and fabrication of laminated materials by electroplating have led to improved magnetic and related properties [19].

In electrochemical microfabrication, 3D high aspect ratio structures can be realized which in turn could be integrated together to form a 3D micropart suitable for MEMS applications.

1.5 Microstructuring Techniques

Microstructuring or microfabrication techniques originally were borrowed from the microelectronics industry. The use of a mask to produce a pattern on a desired substrate was the standard technique used for long time. Nowadays, various micromachining technologies are being used which have different capabilities and also suffer from different drawbacks. Early fabrication were based on producing 2-D microstructures, however, several technologies have recently proven a strong promise to fabricate standalone 3-D microstructures. However, still there is a limited success in fabricating arbitrary 3-D objects by using a standardized inexpensive technology that can produce desired microstructures with a massive rate. Based on the methodology used, microfabrication technologies can be classified as: photolithography related techniques (ex. LIGA); material removal techniques (ex. Excimer Laser Beams and Electro Discharge Machining) and deposition material techniques (ex. Laser Assisted Chemical Vapour Deposition and Electrochemical Deposition).

In photolithography related techniques, a mask is used to represent a certain geometry that will be transferred to a silicon wafer as shown in figure 1.1. Generally, in the photolithography techniques, SiO₂ barrier layer is deposited on the silicon wafer after the cleaning processes is finished. Then the photoresist layer is added to the surface of the wafer. The user can apply two types of photoresist layers: positive or negative

photoresist. The UV exposure of the sample will change the chemical structure of the photoresist used and make it soluble in a developer solution. Depending on the type of the photoresist used, the resultant structure on the wafer can be either be the same as that of the mask (as in the case of positive photoresist) or it can be the negative or the inverse version of the mask (as the case of negative photoresist). For positive resists, the resist is exposed with UV light wherever the underlying material is to be removed. In these resists, exposure to the UV light changes the chemical structure of the resist so that it becomes more soluble in the developer. The exposed resist is then washed away by the developer solution, leaving windows of the bare underlying material. In other words, "whatever shows, goes". The mask, therefore, contains an exact copy of the pattern, which is to remain on the wafer. Negative resists behave in just the opposite manner. Exposure to the UV light causes the negative resist to become polymerized, and more difficult to dissolve. Therefore, the negative resist remains on the surface wherever it is exposed, and the developer solution removes only the unexposed portions. Masks used for negative photoresist, therefore, contain the inverse (or photographic "negative") of the pattern to be transferred. Figure 1.1 shows the pattern differences generated from the use of positive and negative resist [20].

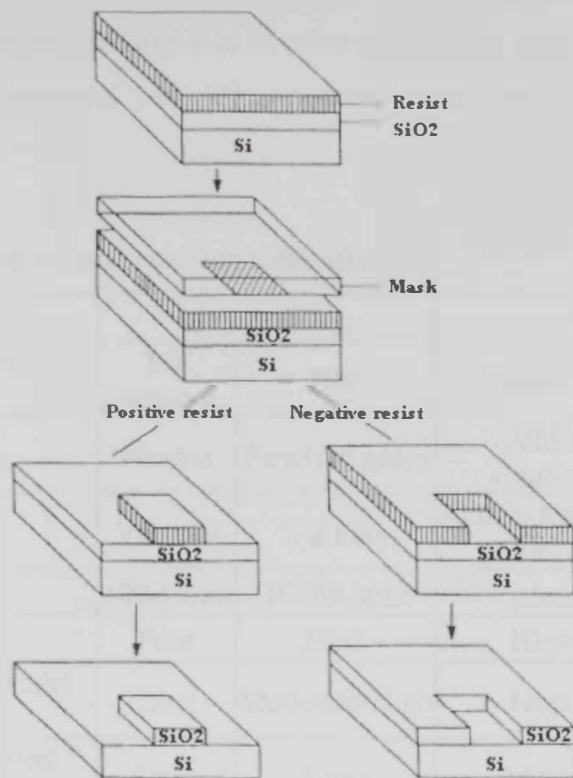


Figure 1.1: A schematic diagram illustrating the photolithography process [20]

Material removal techniques are widely used technologies in the fabrication of microelectronics components. These techniques, which are normally called, etching processes, are based on using a chemical reaction or other means to construct microstructures. Dry vacuum processes for thin-film etching are based on plasma-assisted processes and include ion etching, plasma etching, and reactive ion etching (RIE). Ion etching is a physical process while plasma etching involves a chemical reaction. Reactive ion etching is considered as a combination between the two. Dry-etching techniques are used for precision etching of thin films involving very small amounts of material removal. In the case of wet chemical etching, it involves removal of the unwanted material by exposure of the workpiece to an etchant [21]. The exposed material is oxidized by the reactivity of the etchant to yield reaction products that are transported from the surface by the medium. Chemical etching converts a solid insoluble material to a soluble form by dissolving the extended lattice of metal atoms so that these atoms can

enter the solution as soluble compounds [21]. A comparison of dry and wet thin-film etching processes is shown in table 1.1. In other techniques, ultraviolet laser light can be used to trigger the material removal processes as in the case of Excimer Laser Micromachining.

Table 1.1: Comparison between etching techniques [21].

Etching Factors	Dry Etching		Wet etching	
	Ion etching	RIE	Chemical	Electrochemical
Driving Force	Plasma	Reactive gases	Etching solution	External current
Environment	Vacuum	Vacuum	Acidic/Alkaline solutions	Mostly neutral salt solution
Rate	100Å/min	1000 Å/min	1μ/min	10μ/min
Selectivity	Poor	High	High	High
Safety and environmental concerns	Low	Moderate/High	High	Low
Monitoring and control issues	Some	Some	Many	Few
Cost	High	High	Moderate	Low

In deposition material techniques, the microdeposition requires the ability to move the microparticles and fuse them with a suitable energy source. A variety of materials can be used to create microparts where most advanced techniques use laser as the source to fuse or sinter the material micropowder. Copper and gold for example are widely used in microdeposition techniques. On the other hand, Iron and steels are good to construct functional parts but suffer from high melting temperature limitation. Chemical vapor deposition technique uses metals and ceramics while in laser assisted chemical deposition carbon is used to create carbon fibers [17].

Deposition techniques vary also in the mechanism used to construct a micropart. In the case of electrochemical deposition, an externally applied potential on a tip of sharp needle or microelectrode immersed close to a conducting substrate in an electrolyte solution is used to generate a localized electrical field, which will activate an oxidation-reduction chemical reaction in the electrolytic cell and yield a deposition of the desired

ions crystals present in the electrolyte on the substrate. While in the case of laser assisted chemical vapor deposition LCVD, a laser is used as a heat source to selectively deposit on materials. Shape deposition modeling (SDM) is using also a laser source system with feeding of the micropowder is accomplished using an ultrasonic micropowder feeder. Thin patterns of dry powder can be cladded by a laser beam. In SDM technique, the laser wavelength must be varied according to the material used [17].

Some of the common techniques in each category will be outlined below. A comparison between the advantages and disadvantages of each of these technologies is presented as a guide to compare between the capabilities of these technologies to fabricate microstructures.

1.5.1 LIGA

In 1978 extremely high aspect ratios were attained in polymethyl methacrylate by a process called LIGA, which stands from the German words (Lithographie, Galvanofourmung, Abformung) [22]. Utilizing that the X-ray has a low absorption and diffraction, synchrotron radiation for deep exposure, around several hundred micrometers, is used. As a result, the resolution is submicrometer and the produced aspect ratio was around 1000 [4]. A schematic for LIGA process is shown in figure 1.2.

The X-rays from a synchrotron source is used to hit a thick X-ray sensitive photoresist layer, then the resist is developed and the resultant pattern is then electroplated with metal. The metal structures produced can be the final product or it can be as a universal mold, which can be filled using another material that can't be electroplated as polymers to produce plastic-made structure. A Poor man's LIGA is also a common technique where thick resist is exposed to UV light which enables an increase in the aspect ratio to reach 1200 μm with the SU-8 epoxy based resist [4].

The shortcoming of the LIGA process is that the outcome structure has a lateral features but with less control on the depth features. This can be partially solved by performing multi fabrication steps or layers to add to the depth features. However, this may scarify

the aspect ratio, which is maximized using thick layers instead of using small step sizes [1]. Another major drawback of the LIGA process is the need for a short-wavelength collimated X-ray source like a synchrotron [23].

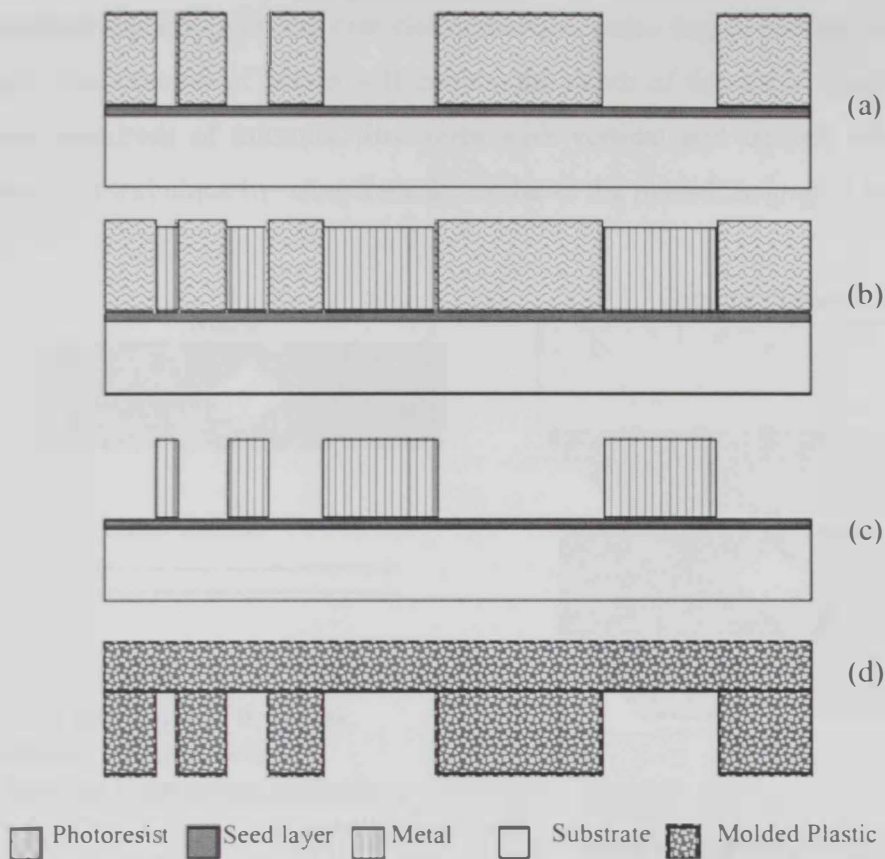


Figure 1.2: Outline of the micromolding process using LIGA technology. (a) Photoresist patterning (b) electroplating of metal (c) resist removal and (d) molded plastic components [23].

1.5.2 Excimer Laser Micromachining

The name of this technique (The Excimer, excited dimer) came from the using of a diatomic molecule such as N_2 as the lasing source. A schematic for this process is outlined in figure 1.3. The advantages of this technique originated from the relatively wide beams of ultraviolet laser light used. Since the wavelength of the excimer lasers are compatible with the chemical bond energies in organic compounds, these lasers can be used in the micromachining of organic materials like polymers and plastics. Also the

material close to the area of interest will not be affected by heating which can cause a significant deformation for the organic material.

In this technique, by pulsing the laser source on and off, the organic material will be removed depending on the material properties, pulse length and the intensity of the laser light. The number of pulses will control the depth of the cut in the material, which can reach hundreds of microns. Structures with vertical and tapered sides can be realized using this technique by using a mask similar to the photolithography-based mask.

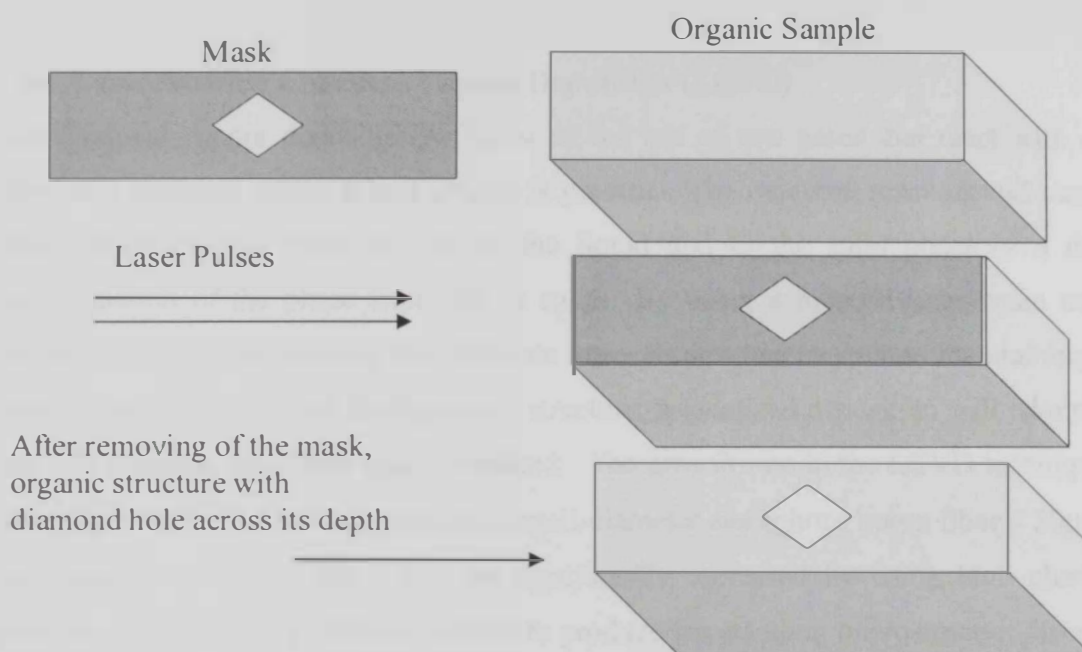


Figure 1.3: A schematic diagram illustrating the Excimer Laser Micromachining process

1.5.3 Micro Electro Discharge Machining (Micro-EDM)

Micro Electro Discharge Machining is a highly repetitive technique to manufacture complex 3-D structures, holes and shafts with high degree of accuracy. Being different from other techniques, Micro-EDM is based on the use of an electrical spark generated between the EDM electrode and the work piece separated by a gap filled with a certain dielectric fluid like oil. The resulting heat will melt small amount of material on both the

tool electrode and the work piece. The erosive fluid will remove some of the melted material and the remaining material will solidify on the electrodes. By using a very high frequency to generate the sparks and a programmed trajectory of the EDM electrode, one can accurately machine complex 3-D structures with high aspect ratios. It is however important to control the gap between the electrode and the work piece and to keep the spark energy small in the range of 10^{-7} J in order to get accurate machining with acceptable surface finish. Micro-EDM can be used to cut and machine hard materials such as steel and carbides. The drawback of this technique is that it is only used for conductive and semi-conductive materials.

1.5.4 Laser Assisted Chemical Vapour Deposition (LCVD)

The chemical vapour deposition is based on the use of two gases that react with each other in a chamber where a heat source is present. The outcome reaction will cause a phase transformation from the gas to the liquid and to the solid phase or a direct transformation of the phase from gas to solid. By using a focused laser beam as the source of heat and by moving the substrate in a certain trajectory while maintaining the laser focused on the tip of the deposited structure, a localized deposition will take place and 3-D complex structures can be realized. The growth rate in the LCVD technique is normally less than $100\mu\text{m/s}$ in case of a small-diameter amorphous boron fiber $< 20\mu\text{m}$ at low chamber pressure, but it can be significantly increased by using high chamber pressure. Also, LCVD process is capable to produce freestanding microstructure from the vapour phase. To construct 3-D microstructures by LCVD, two-beam setup is needed.

1.5.5 Micro Stereo Lithography

The advantage of this technique is that it is capable of manufacturing a curved surface of even dielectric materials. This technique solves the shortcomings of LIGA and Micro Electrical Discharge Machining (Micro-EDM). The Micro Stereo Lithography technique was presented by K Ikuta and K Hirowatari in 1993. A schematic illustrating this process is shown in figure 1.4. The technique mechanism is to repeatedly solidifying a resin layer by layer using UV exposure [4]. Structures like the three-pipe connection and helical springs are some examples of what Micro Stereo Lithography can do. Although

this technique suffers from lower resolution, it has been shown to be complementary to LIGA because of its geometrical flexibility.

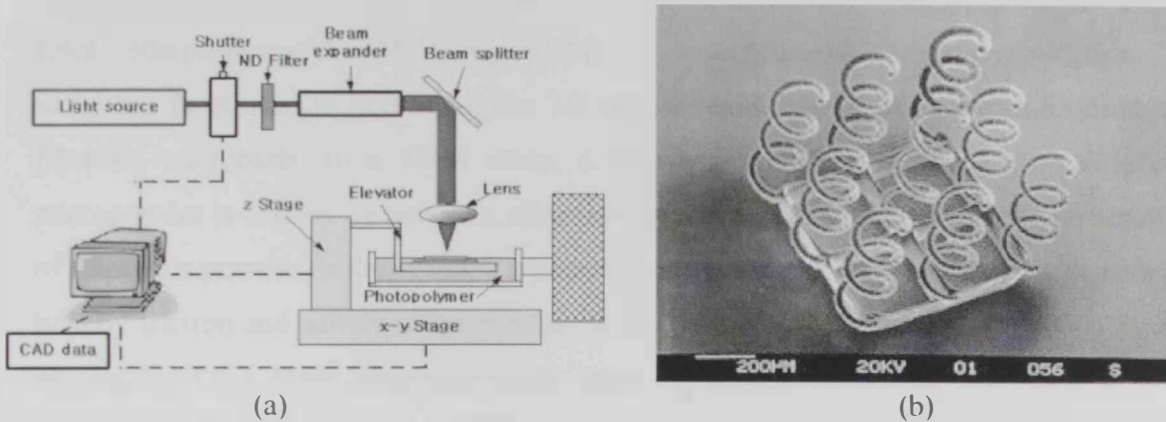


Figure 1.4: Microstereolithography: (a) a schematic of the process (b) a fabricated sample using Microstereolithography technique. Sources: (a) Intelligent Manufacturing Systems Laboratory, Department of Mechanical Engineering, POSTECH, Pohang, Korea. (b) brekely xlab <http://xlab.me.brekely.edu>

1.5.6 Laser-Guided Direct-Write (LDGW) and Flow-Guided Direct-Write (FGDW)

LGDW and FGDW are laser-based processes for dispensing and processing liquid and colloidal materials on virtually any substrate. In both methods, an atomizer is used to produce a dense mist of droplets that contains the material. The particles are fed into either the laser- or flow-guided deposition devices and focused by a narrow laser beam. In LGDW, the particles will travel a distance up to few centimeters into a hollow optical fiber to allow the light and particles to pass together towards the substrate. The deposition rate can reach 10000 particles per second. In FGDW an aerosol-assist method is used to increase the velocity of the particles [17].

1.5.7 Laser-induced Forward Transfer (LIFT)

In this method, a pulsed laser source is used to transfer the desired material from a target to the desired location on the substrate. A target material is kept close to a laser transparent substrate. Low-pressure gas or ambient air can be used in this technique. A vaporization of the target material will take place as a result of the laser source. Some of the material on the target will be expelled away towards the substrate at high speed as a

result of the high vapor pressure. Mixture of solid and melt will be ejected from the target and hit the receiver substrate [17].

1.5.8 Shape Deposition Modeling (SDM)

SDM has been used to build complex 3D macroshapes. This technique can be used to fabricate microparts. In a SDM setup, a laser-based setup is used. The feeding of micropowder is carried by using an ultrasonic micropowder feeder. The main advantage of using this powder feeder is that the powder is driven to the feeding tip of the capillary tube by friction and adhesive forces rather than gravity. Thin patterns of dry powder can be cladded by a laser beam. Different laser wavelength is needed according to the material used. A computer controlled three-axis microstage within a 30nm resolution and a speed of up to 200 mm/s is used. The pulsed laser can be controlled to obtain precise cladding and machining. A camera may be used to monitor the whole process [17].

1.5.9 Localized Electrodeposition (LED)

The process involves localized electrochemical deposition of the desired ions on a substrate. The tip of a sharp pointed electrode is placed in a plating solution and brought near the surface of a substrate where deposition will occur [1]. A schematic for the process is shown in figure 1.5. Upon deposition, an electric field potential is applied between the electrode tip and the substrate through the electrolyte solution. This will lead to an oxidation reaction at the electrode tip, and material deposition resulted from the reduction reaction occurring at the substrate [24]. Since the resulted electrical field will be localized to the area under the electrode tip, the extension of the deposited material, which will grow under the tip, is limited to the dimension of the electrode tip diameter. The electrode motion in the space with respect to the substrate will determine the form of the 3D deposited structure. Various structures can be realized using this technique like straight copper columns, helical structures or even walls and boundaries.

Various phenomena affect the deposition process including mass transport, electron transfer, electrical potential, chemical potential, and crystal growth [1]. A model for the deposition process is available in literature [1]. In this technology, the deposition rate can

be several micrometers per second. Compared to the other techniques, which have limitations on the variety of materials that can be used; the range of materials that can be deposited using this technique is wide containing metals and semiconductors and even conducting polymers [4].

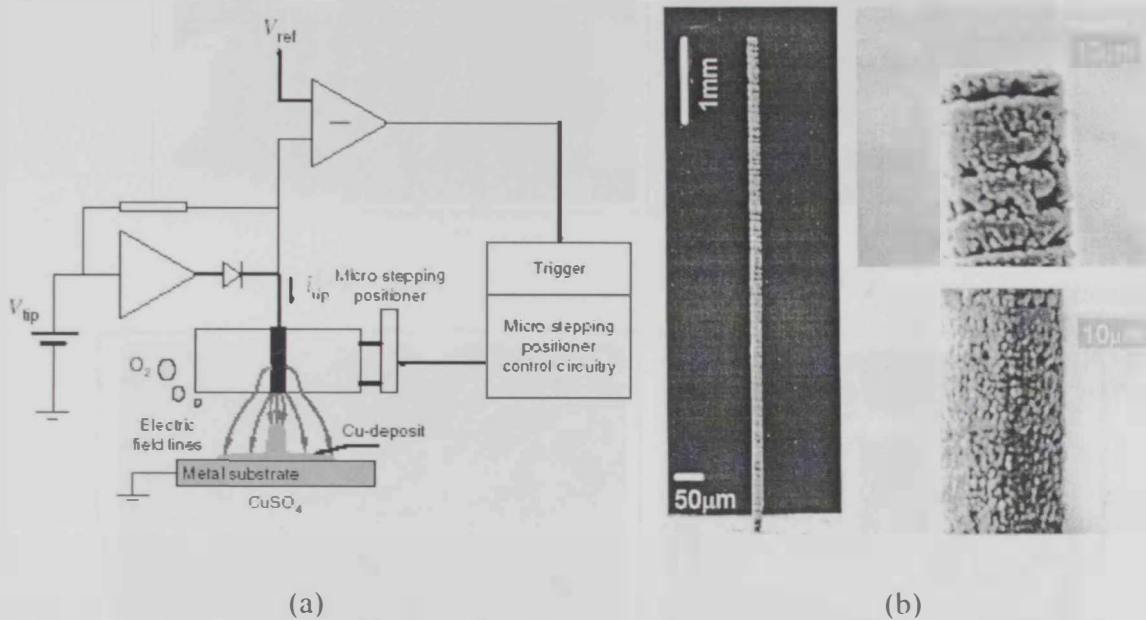


Figure 1.5: LED principle. (a) An illustration of a typical LED arrangement demonstrating the main aspects of the process operation. (b) SEM image of a copper micro-column deposited by LED [24].

1.5.10 Electrochemical Fabrication (EFAB)

EFAB is based on instant mask technology. The cross sections layers of the microdevice are built layer by layer. Using an electrolyte between a cathode and an anode, an instant mask is brought in contact with the substrate. Deposition will selectively occur on the substrate and perform the first layer. Filler that can be removed chemically later is then added and the next layer is built again. This process is repeated layer by layer until the final shape of the microdevice is assembled. The layer thickness can be controlled from 2 to 20 μm ; hence, it is capable of producing substantially large microparts. Some structures like 24-layered nickel structures are realized with geometrical features reach 25 μm [17]. In figure 1.6 below, some of the microparts machined by different micromachining techniques are shown.

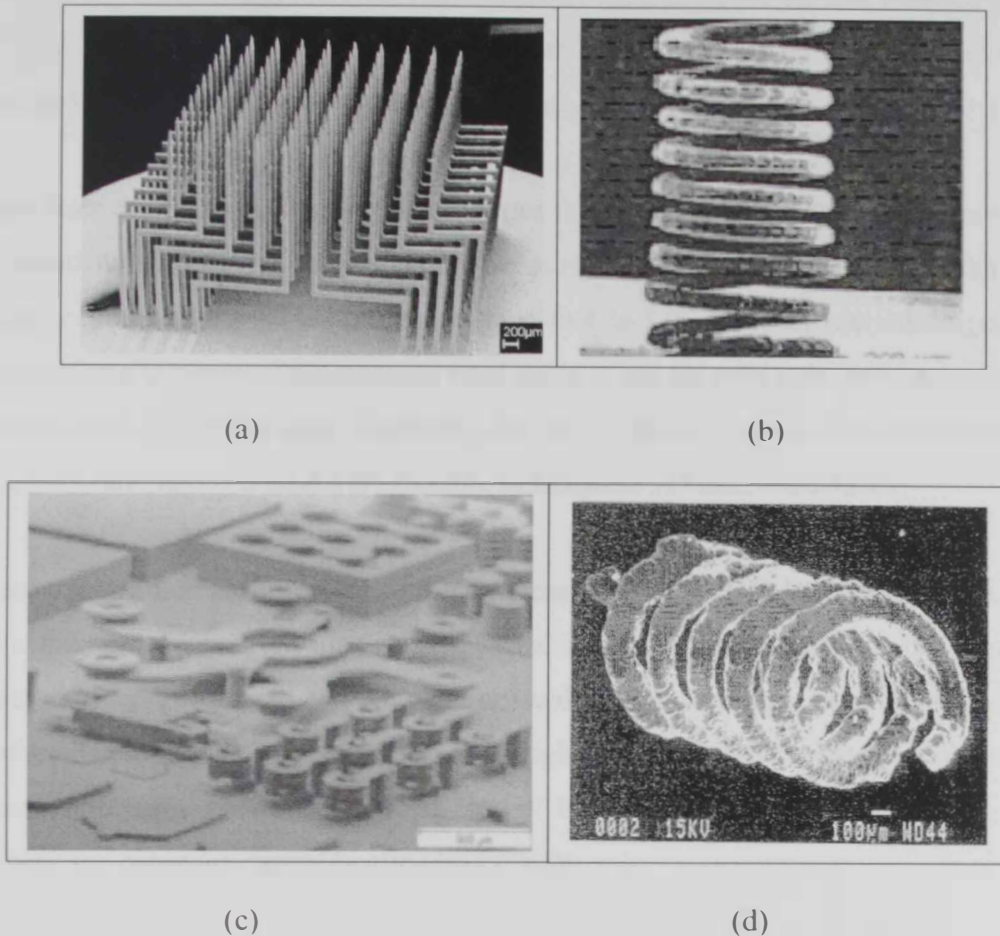


Figure 1.6: Microstructures made by different microfabrication techniques. (a) SEM image of 10*10 array fabricated by electrical discharge machining from titanium alloy [25]. (b) Boron microspring made by LCVD [17]. (c) 24-layered nickel structure built using EFAB [17]. (d) Microspring fabricated by Localized Electrochemical Deposition [1].

1.6 Comparison Between the Microfabrication Techniques

In table 1.2, a general comparison between various micromachining technologies is shown. LIGA process suffers from the geometry freedom related to the difficulty in realizing structures with depth details. However, it is considered as accurate process with excellent ability to fabricate microstructures of minimal dimension having high aspect ratio features. LIGA has a long list of materials that can be used ranging from metals to polymers and ceramics.

Etching technologies accuracy is moderate compared to LIGA. It suffers from that the structures are of low aspect ratio. Also there is less freedom on the geometry to be fabricated and the range of raw materials that can be used. However, the resolution of this technique is moderate and comparable to that in LIGA.

Excimer laser can be used to fabricate structures from metals, polymers and ceramics. The main disadvantages of this technique are the minimum dimension that can be fabricated and the accuracy of the technique is less than that in LIGA. Microstereolithography is poor technique in terms of the material used since it can be used only with polymers. On the other hand, there is a great flexibility for this technique to fabricate structures with high aspect ratio and it is relatively flexible to fabricate 3D microstructures.

The accuracy, minimal dimension and roughness of Micro-EDM technique are moderate but the fabricated geometry has a good aspect ratio with flexibility on the geometry. Metals, semiconductors and ceramics can be used for this technique but not polymers. On the other hand, LCVD is able to produce high aspect ratio structures with moderate minimal dimension. However, the accuracy of the technique is less than that in LIGA. Polymers and ceramics cannot be used by LCVD.

Table 1.2: Comparison between micromachining technologies [26]

Technology	Minimal Dimension	Accuracy	Aspect Ratio	Geometrical Freedom	Roughness	Feasible Materials
LIGA	++	++	++	+-	+	metals, polymers, ceramic materials
Etching	+-	+	-	-	+	metals, semiconductors
Excimer-laser	-	-	+-	+	-	metals, polymers, ceramic materials
Micro stereo lithography	-(+)	-(+-)	++	++	-	polymers
Micro EDM	+	+	++	++	+	metals, semiconductors, ceramics
LCVD	+	+	++	++	+	metals, semiconductors

In table 1.3, a specific comparison between various deposition technologies is shown. The technologies are categorized for the comparison purposes in this table according to the material used in the fabrication process, the type of substrate used and the alternatives of materials that are possible to be deposited. Another comparison between various deposition techniques is shown in table 1.4 where the criteria for the comparison are the advantages and disadvantages of the technique in general.

It is clear from the comparison table shown that a certain fabrication technique may have advantages over other techniques but also may suffer from certain limitations. For example some deposition techniques have a limitation on the type of the material used. It is shown in the tables that EFAB fabrication technique is concerned with the fabrication of metal structures while the fabrication using localized electro-deposition (LED) can yield structures from various materials ranging from metals, metal alloys, semiconductors and even conducting polymers. Also, these fabrication techniques have some variations on the type of the substrate that can be used in the deposition process. The type of ions that can be deposited on the substrate is also varying. For example, selective laser microstructuring uses only Fe particles while localized electrochemical deposition has a wide range of ions that can be candidates for deposition.

From the table 1.4, compared with other deposition techniques, one can observe that localized electrochemical deposition is considered as simple, inexpensive, reproducible and damage free technique. It does not need a mask to generate the desired geometry. However, the limitations shown in the table regarding the resolution of the deposition, which depends on the electrode tip diameter, can be solved by using a multi tip array of variable tip diameter. Although the electrolyte needed in the electrochemical cell must contain conductive ions like copper or nickel, many materials can be deposited even the conductive polymers recently developed.

Table 1.3: Materials used in the various microdeposition techniques [17]

Deposition method		Deposition Material	Substrate/ Precursor material	Material that could be deposited
Particles/ powder	Laser-assisted shape deposition manufacturing (SDM)	Copper Stainless steel	Aluminum	Metallic powder
	Maskless mesoscale materials deposition	Electronic materials	Silicon, glass, plastics, metals, ceramics	Metals, conductors, ferrites and polymers
	Selective laser micro-sintering	Fe particles	Fe	Metallic powder
	Laser guided direct writing (LGDW)	Polystyrene	Glass, Si	Metals, polystyrene, biomaterials
Chemical	Laser assisted chemical vapour deposition (LCVD)	CrO ₂ , Cr ₂ CO ₃ , W, Fe, Ni, Si, Al	CrO ₂ Cl ₂ , W(CO) ₆ , Fe(CO) ₅ , Ni(CO) ₄ , SiCl ₄ , SiH ₄ , Al(CH) ₃ ,	Metals, metal alloys, semiconductors
	Localized electrochemical deposition (LECD)	Al, Au, Pt, Cu	(C ₇ H ₇) ₂ F ₆ , Au	Metals, metal alloys, conducting polymers, semi-conductors
Others	LIFT	Cu	Si, glass	Metals, simple oxides
	EFAB	Ag, Au, Ni, Ag	Metal, ceramic, glass	Metals

Table 1.4: Comparison between deposition techniques [17]

Deposition Process		Advantages	Disadvantages
Particles/ powder	Laser-assisted shape deposition manufacturing (SDM)	<ul style="list-style-type: none"> Combine the additive and subtractive processes Suitable to build 3D heterogeneous structures Possible to create functionally and geometrically complex meso- and microfabrication Could deposit a wide variety of materials 	<ul style="list-style-type: none"> Controlling powder flow rate
	Maskless mesoscale materials deposition	<ul style="list-style-type: none"> Aimed at crucial midsize components Deposit on low-temperature substrate Flexible and effective High-quality thin film with excellent edge definition 	<ul style="list-style-type: none"> Limitations on the aspect ratio and 3D application
	LGDW and FGDW	<ul style="list-style-type: none"> Fiber interior provides a shield from the external environment for the particles Low cost and will deposit virtually any material with micrometer scale accuracy The source and the deposition regions are isolated from each other. 	<ul style="list-style-type: none"> Reflectivity of light is not total as in the solid fibers. Limitations in particle size
	Selective laser microsintering	<ul style="list-style-type: none"> Could control the accuracy by controlling the focus of the laser Not geometry sensitive No additional support is used. 	<ul style="list-style-type: none"> The surface of the parts is always porous
Chemical	Laser assisted chemical vapour deposition (LCVD)	<ul style="list-style-type: none"> Capability of producing highly dense and pure materials Produces uniform films with good reproducibility and adhesion at reasonably high deposition rate Flexibility of using a wide range of chemical precursors. 	<ul style="list-style-type: none"> Chemical and safety hazards caused by the use of toxic, corrosive, flammable and/or explosive gas. Difficult to deposit multicomponent materials with well-controlled stoichiometry The use of a more sophisticated reactor and vacuum system tends to increase the cost of fabrication
	Localized electrochemical deposition (LECD)	<ul style="list-style-type: none"> They are simple, inexpensive, and reproducible and damage free. Maskless deposition of materials 	<ul style="list-style-type: none"> Resolution depends on the tip diameter of the electrode. Materials that conduct electricity can only be deposited.
Others	EFAB	<ul style="list-style-type: none"> It can produce any three-dimensional structure. It can be operated under ordinary room conditions. 	<ul style="list-style-type: none"> It is limited to the deposition of conductors It is a slow process.
	LIFT	<ul style="list-style-type: none"> Easy to build 3-dimensional structures Fabrication of complex micro- and sub-micropatterns Potential of LIFT for fabricating microstructures onto nonplanar surfaces. 	<ul style="list-style-type: none"> Applicable to only limited range of materials The precise control of the distance between target and receiver is crucial Quality of deposited structures depends critically on the thermophysical property of the material.

Localized Electrodeposition (LED) can compete with other techniques to fabricate high aspect ratio 3-D microstructures along with attractive cost. However, still (LED) technique is under development and up to this time, there is no commercial (LED) setup available. Efforts are taking place in order to standardize the process and optimizing the parameters that are affecting its outcome while expanding the technique capabilities. In the following chapter, the LED fabrication process is described and the process parameters are discussed.

Chapter 2:

Localized Electro-Deposition (LED)

2.1 Introduction

Developed and accelerated in 1995 by Madden and Hunter, Localized Electro-Deposition (LED) or sometimes referred as Localized Electrochemical Deposition (LECD) technique has increasingly attracted the researchers' attention for its capabilities in the field of micromachining and microdevices that can be utilized in various applications in the microelectronics industry. Also, the tremendous and rapid development of the field of microelectromechanical systems (MEMS) gave a great boost to the micromachining experts and scientist to develop micromachining techniques and tools with various capabilities to cope with the increased complexity of structures needed by different applications of MEMS like microactuators, microgears and microengines. Compared with the other microfabrication techniques that originally came from microelectronics industry, LED technique has proved to be able to fabricate 2D and 3D microstructures with high aspect ratios (height to width) while using simple and inexpensive setup. Another advantage is that the LED process is classified as maskless fabrication technique, which permits the fabrication of the micropart to be accomplished in one stage process. These mentioned advantages are considered major issues when dealing with high commercial production rates. Moreover, and on the light of the lack of geometrical details in the structures fabricated by the traditional microfabrication techniques, when implementing a carefully controlled LED system, the freedom of fabricating complex geometries will be expanded by adding lateral and depth geometrical details to the microstructure. Another advantage of using LED is that it can be used to fabricate microstructures and microparts from different materials ranging from metals to conducting polymers and semiconductors.

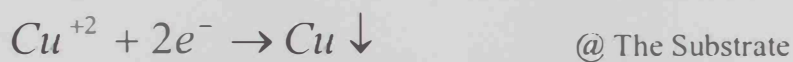
All of these attractive proprieties of the fabrication by LED gave the researchers an opportunity to come up with a superior and simple machining setup that can fabricate various 3D microstructures with unlimited capabilities. However, LED is still under development, up to this time, there is no stand-alone LED setup that is available in the market for commercial use. Global research efforts are taking place in research laboratories in order to enhance and standardize the LED fabrication technology.

2.2 Theory of LED

A. Concept of operation

In a general electrochemical deposition technique, a cathode and anode are immersed in an electrolyte solution containing the material ion that will be deposited (e.g. Cu^{+2}). A potential is then applied between the anode and the cathode causing a current to flow in the electrochemical cell which, in turn, oxidizes the desired ions present in the electrolyte and causes deposition of the oxidized ions on the cathode or the substrate. Electroplating technology is a well-known application for electrochemical deposition technique.

However, in localized electrochemical deposition technique, a sharp electrode normally made from platinum (Pt) wire, representing the anode, is immersed very close to a conducting substrate, representing the cathode, in an electrolyte path containing the material ion of interest as shown in figure 2.1. The sharp electrode, or often-called microelectrode, is isolated by an epoxy or glass material in all directions except at its tip. By applying a potential between the electrode and the substrate, electric field will be generated causing a faradic current to flow through the electrolyte and results in an oxidization reaction at the microelectrode tip and a reduction reaction causing deposition of the metal ions at the substrate [27]. In the electrochemical cell shown in figure 2.1 below, copper sulphate solution is used in order to build structures made from copper material. The oxidization reaction at the tip will result in extra electrons that will be attracted to the Cu^{+2} ions present in the cell. Because only the tip of the electrode is exposed in the electrochemical cell, a concentrated high intensity electric field will take place only in the area beneath the electrode tip and causes a localization of the ions deposition to the desired location on the substrate surface. The equations modeling the process are:



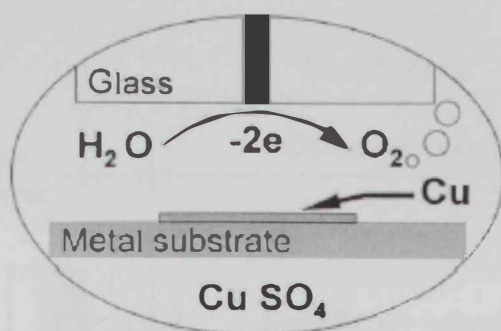


Figure 2.1: A schematic for the LED deposition at a close distance between the electrode tip and the conducting substrate [27].

The mechanism of deposition is controlled by the electrical double layer and ion migration. In the presence of the applied potential, the electric charges located on the surface of the electrode and the ions in the electrolyte make electrical double layer. The anions are adsorbed on the metal electrode surface by chemically mutual reaction. This is called specific adsorption, the locus of the electrical centers of the specifically adsorbed anions is called inner Helmholtz plane (IHP) [28]. Cations are hydrated by the water molecules. Water molecule also adsorbs at metal electrode surface. Therefore, solvated cations can approach the metal surface only to a distance of about two water molecules size. The locus of centers of these nearest solvated cations is defined outer Helmholtz plane (OHP) [28]. The region from metal surface to OHP makes the compact double layer and its thickness is about 3 \AA . The region from OHP to ions layer that electrically distributed in bulk electrolyte by charged electrode makes diffuse double layer. The thickness of the diffuse double layer depends on the total ionic concentration in the solution. This electrical double layer has similar properties with that of a capacitor in electrical circuit. The copper ion is moved to diffuse double layer by electrical migration that is caused by the polarized metal substrate. Copper ion reaches OHP by diffusion caused by concentration difference, and it is deposited on copper substrate after getting over the activation energy barrier [28], copper ions are then crystallized and the structure begins to grow. A schematic of the deposition mechanism is shown in figures 2.2 and 2.3 below.

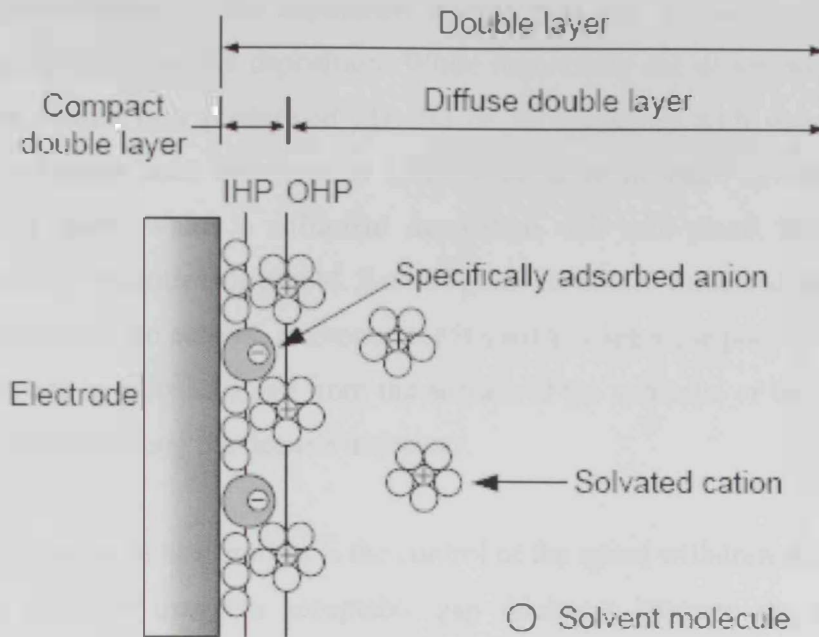


Figure 2.2: A schematic illustrating the concept of the double layer at the electrode /electrolyte interface [28].

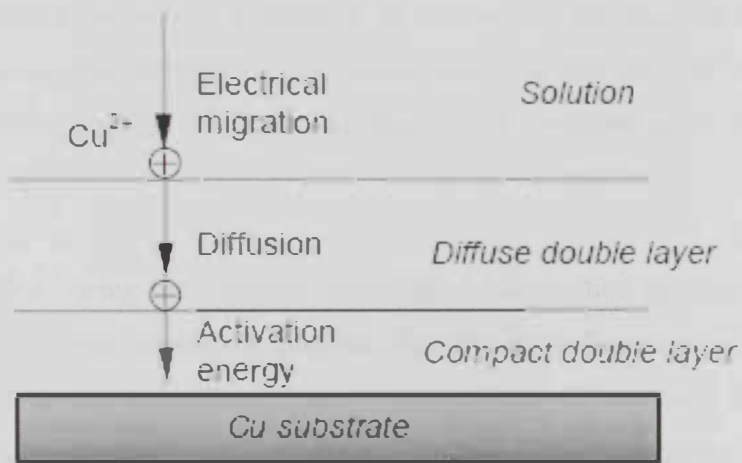


Figure 2.3: A schematic illustrating the deposition of the copper ions on the conducting substrate [28].

As the deposition grows in the vertical direction, the reaction current will increase because of the decrease in the resistance of the electrolyte surrounding the electrode. The

current will reach its maximum value once touched the electrode tip. The deposition rate in this case is proportional to the deposition current that will act as an eye on the continuity and progression of the deposition. While monitoring the deposition rate, the electrode is then moved in a predefined 1D, 2D or 3D trajectory with respect to the substrate. The technique used in a typical LED setup is to measure or estimate the deposition current above which a sufficient deposition will take place, this value is recorded as a process deposition threshold. Based on this threshold value and the value of the instantaneous deposition current, a comparator is used to trigger the positioner system holding the electrode in order to move from the surface of the substrate or the surface of the newly built structure along the desired trajectory.

One important parameter in this process is the control of the speed withdrawal away from the substrate in order to maintain acceptable gap thickness between the tip of the electrode and the deposited surface. This gap should not be large making the tip being away from the structure surface, which may cause a discontinuity in the deposition process. On the other hand, the gap should be kept not too small causing ions crystals to block the electrode tip from the cell electrolyte. While moving the electrode in the space away from the substrate, this trajectory can be programmed so that the deposition beneath the electrode can result into the fabrication of the desired structure as shown in figures 2.4.b and 2.5.

It is worth noting that during the chemical reaction and deposition process, some extra components will affect the deposition process like the air bubbles resulted from the oxidization reaction at the electrode tip as shown in figure 2.1 shown above. These bubbles can have a significant effect in slowing down the deposition rate and sometimes blocking the electrolyte away from the electrode tip. Optimal controlling of the applied potential can minimize the effect of this phenomenon on the deposition process.

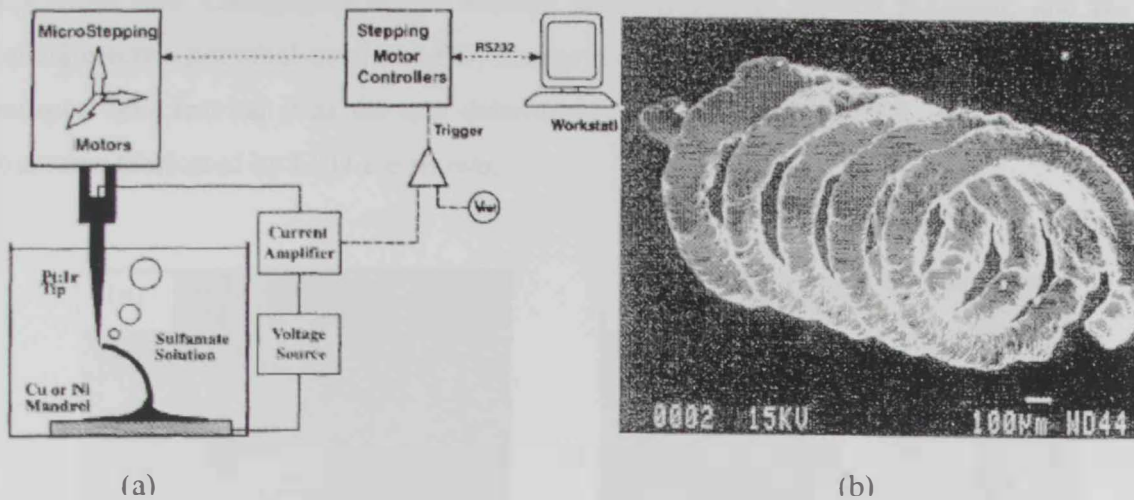


Figure 2.4: (a) Schematic for the Localized Electrodeposition (LED) process (b) A nickel spring made by LED [1].

The outcome of the microfabrication by LED process can be a various range of structures from 1D vertical microcolumn and walls to square, rectangular, elliptical and other 2D structure as well as 3D structures like helical shapes and springs as shown in figure 2.4.b. When using one electrode in the fabrication process, the structure resolution will be limited by the electrode diameter. Thickness issue may be controlled by using multiple sharp electrodes with different tip diameters bundled together or by using single microelectrode containing more than one tip having different diameter sizes (array microelectrode). During the fabrication process, these tips in the array can be independently toggled on or off using a control algorithm depending on the thickness of the desired section or micropart.

Various parameters affect the deposition process in the electrochemical cell including: mass transport, electron transport, electrical potential, chemical potential and crystal growth [1]. The understanding of these parameters on the deposition process is well established in literature [1]. Essentially, an ion must have enough energy to transport through the bulk electrolyte and reach the electrode/solution interface, overcome the potential barrier at the interface, receive an electron to neutralize as an atom, and incorporate itself within the crystal of other atoms reduced from the electrolyte. In this

series of events, mass transport and charge transfer are generally the limiting factors of deposition rate. Charge transfer is directly affected by the applied potential, and for typical electric potential used in LED, charge transfer rates greatly exceed that of mass transport thus leaving it as the rate determining process. In figure 2.5, some deposited structures fabricated by LED are shown.

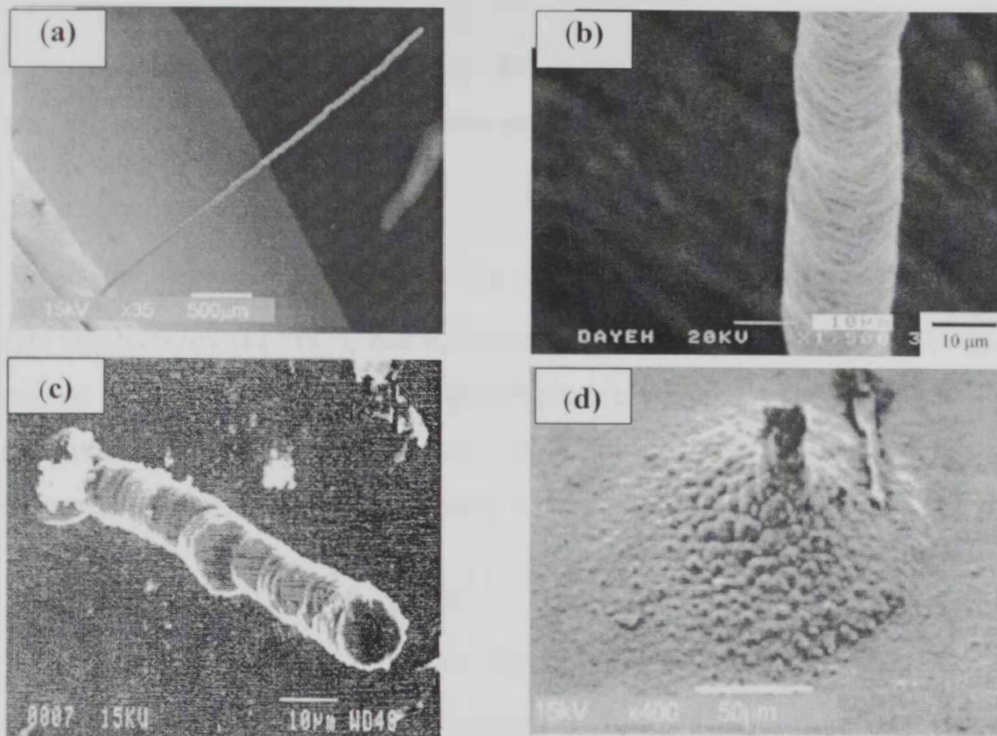


Figure 2.5 (a)-(d): Column structures fabricated by Localized Electro-Deposition (LED) [27], [1], [29].

B. Mathematical modeling of LED process

The ability to model the fabrication by LED process will certainly lead to enhance the technology and contribute to the optimization of the process, which ensures a proper fabrication of the desired microstructure in terms of repeatability, accuracy and resolution. By using a simulation model, various parameters affecting the fabrication rate and the characteristics of the deposition profile can be studied.

As mentioned earlier, the mass transport is the factor that determines the deposition rate. The mechanisms that determine the mass transport profile are the diffusion, which is driven by the concentration gradient, convection, which is driven by the pressure gradient (natural and forced convection), and migration, which is driven by electric potential gradient. Also, the presence of an external magnetic field founded to affect the flow of the electrolyte and influence the deposition process has been studied in [30].

In LED process, the migration force, which is proportional to the applied electric field, dominates; the normal current density can be determined as a special case of Ohm's law:

$$J_n = \sigma E_n \quad 2.1$$

where J_n is the deposition current density normal to the surface ($A\ m^{-2}$), σ is the electrolyte conductivity ($\Omega^{-1}\ m^{-1}$), and E_n is the component of the electric field intensity (V/m) normal to the deposition surface. In LED process containing dynamic flow, Ohm's law can be extended to account for the convection and induction mechanisms that might affect the process giving the full form of Ohm's law:

$$J_n = \rho_q v_q + \sigma(E_n + v_q \times B) \quad 2.2$$

where v_q is the flow velocity ($m\ s^{-1}$) of the depositing species contributing to convection transport, ρ_q is the species density ($g\ m^{-3}$) and B is the intensity of the applied magnetic field (T). A more general equation taking the account of diffusion which can be the process limiting factor in situations where the spacing between the tip and the substrate is small compared to the tip diameter, this equation is a modified version of Nernst-Planck equation taking the effect of magnetic intensity that might be present in the process:

$$J_n = -D_q \nabla C_q + C_q v_q + \frac{z_q F}{RT} D_q C_q [E_n + v_q \times B] \quad 2.3$$

where D_q is the diffusion coefficient ($m^2\ s^{-1}$) of the depositing species within the electrolyte, C_q is the concentration ($mol\ m^{-3}$) of the depositing species in the electrolyte solution, z_q is the number of electrons in the deposition reaction, F is a Faraday (96 500 C), R is the gas constant ($8.314\ J\ mol^{-1}\ K^{-1}$), and T is the absolute temperature (K).

In literature, effort were carried to simulate the deposition growth by computing the electrical field which is proportional to the deposition current as shown in equation 2.3.

C. Process resolution

The resolution of the LED process is mainly determined by two factors: the minimum dimension that can be fabricated and the minimum spacing between the adjacent structures in order to avoid overlapping. The minimum dimension that can be fabricated is limited to the tip diameter. In order to determine the resolution, it was found in the literature that the value of S/R is a measure of the resolution of the process, where S stands for the deposit radius at half maximum and R is the tip-apex radius of curvature related to the electrode geometry thus higher values of S/R indicates lower resolution.

Although the deposition extent can be confined to an area determined by the tip radius, undesired deposition outside such an area would occur due to stray field lines coupling to the substrate from the tip edges and sides. Thus to prevent adjacent structures from contacting, it was determined from the calculations done in literature that a minimum spacing of at least $6R$ from the centers of two adjacent structures would be required where R is the radius of the tip. It is also found that by decreasing the spacing between the tip and the deposit surface, and by reducing the insulation material surrounding the tip; the resolution of the process will be enhanced [24]. The effect of the tip insulation on the deposition profile was studied in literature [24].

D. Process repeatability

The repeatability of the LED process is related to the success rate of the deposition process. In any experiment of LED, failure may happen due to the disturbance of the process caused by the air bubbles generated at the surface tip which will reduce the amount of the electrolyte coming to the tip and will act as an insulation between the tip and the deposit surface, as a result, air bubbles cause a significant reduction in the deposition rate. Also the failure may happen due to the misalignment issues between the tip and the deposit end at any time in the process, especially, the failure rate is higher

when the substrate and the electrode surfaces are not aligned initially (at the beginning of the deposition). As mentioned earlier and in order to ensure a proper performance, the overlapped area between the tip and the deposit end must be maximized during the whole process. Because of the large insulation around the tip, it is hard to maintain this maximum overlapped area especially during a 3-D fabrication where the microelectrode has to move in a predefined 3D trajectory.

In literature, a proposed solution for the first issue was to control the distance between the electrode tip and the deposit surface by utilizing an adaptive feedback control algorithm. In this way the withdrawal speed is set in proportional to the detected current gradient thus maintaining a constant deposition rate during the process, which will enhance the repeatability of the LED process [24].

E. Process automation

Two important issues are related to the process automation: the initial placement of the tip close to the desired location on substrate and the ability to track and determine the instantaneous location of the deposit. The first issue is very critical. It is found that the success rate highly depends on the initial positioning. This stage is performed by monitoring the tip current while positioning the microelectrode close to the substrate at the desired location using the aid of a microscope. The general behavior of the tip current is as follows: when the microelectrode is far from the substrate, the diffusion will be constant due to the mass amount of electrolyte available, and the tip current will remain constant accordingly. As the tip approaches the substrate, the current will be reduced due to the less amount of the electrolyte available and also due to the effect of air bubbles occupying more volume than the electrolyte. The tip current will stabilize again at a certain distance from the tip reaching its minimum value. In the literature, it was found that by monitoring the current gradient and not the current itself, one can predict the optimum spacing between the tip and the substrate. When the measured current reaches a constant value close to the substrate, the current gradient will reach a null value. Thus by monitoring the current gradient, the positioning must be stopped when the gradient of the tip current reaches a null value close to the substrate. After this initial

positioning stage, the deposition process can start [24]. The controlling code will compare the acquired current with the threshold value set by the user. This threshold corresponds to the state when enough deposition has occurred underneath the tip. The threshold value is a function of the microelectrode geometry, potential used and the electrolyte (type and concentration) available in the cell and must be carefully determined by the user prior to starting of the deposition. Once this threshold is achieved; the controller will trigger the positioner to move away from the substrate along the desired trajectory.

The height of the tip surface depends on the withdrawal increments of the microelectrode away from the substrate. The controlling code will keep track of these withdrawal increments and accumulate them. Once the accumulated increments reached the desired height, the deposition process will be stopped producing the desired microstructure deposited on the substrate.

F. LED current and anticipated capabilities

Theoretically, LED is able to fabricate any microstructure. However, most of the previous research in this field was concentrated in the fabrication of 1-D and 2-D microstructures. Examples of these possible LED structures include column structures, horizontal line segments, helical structures, vertically crossing line segments and vertical tube structures. These structures can be used in various applications as a simple monopole and helical antennas in communication systems working in terahertz range, realization of electrically conducting objects for integrated circuit interconnects and rerouting, microrobotics, and integrated bio- and hydrodynamic microsystems. LED has proven its capability to fabricate 2D and 3D high aspect ratio structures from various materials like nickel and copper. The ability to fabricate 3D complex structures is the core and the prime requirement for microelectromechanical applications like micromotors, micropumps and microgears. Currently, various research efforts are taking place in order to expand the capabilities of the LED processes. The flexibility, repeatability, reliability, and accuracy of the technique are the major process parameters

that must be optimized in order to introduce LED as standard fabrication technique capable of competing with advanced high-tech technologies.

In the literature, some requirements for the development of the LED process were identified [11]. One of these requirements is the dynamic control of the tip withdrawal mechanism and speed. The optimal control mechanism must be intelligent to track the deposit end and maintain a maximum overlap area between the effective surfaces of the tip and the deposit end. The other requirement is addressing the microelectrode itself. The geometry of the microelectrode certainly affects the behavior of the deposition process and eventually controls the final outcome. All of the previous experiments in this field have used a non-specialized microelectrode borrowed from other fields like scanning electrochemical microscopy (SECM), neuroscience and biological applications. These microelectrodes are not designed for LED process and accordingly their performance will not be optimum. Integrated microelectrodes and microelectrode arrays for LED application have been suggested as possible solution to expand the capabilities of the LED process. However, none of these suggestions was implemented previously.

In this thesis work, we are investigating and demonstrating the idea of parallel deposition technique by using multi-tip microelectrode or sometimes referred as microelectrode array and compare it with the serial deposition technique in fabricating array microstructures. The array microelectrode is basically a number of independently addressable tips separated by a certain distance thus forming a specified geometry; these tips are sufficiently insulated from each other. Arrays of similar type have been used in bioscience. However, several limitations prohibited the use of these microelectrodes in the LED process including geometry and material limitations. Also, some of the arrays available were not independently addressable (all of the tips are reading a signal from several location and the individual signals are then combined to form the final measured signal).

As an example of a microelectrode array, a geometry of 4*4 array (4 rows and 4 columns) will contain 16 tips that can be activated at the same time; in this case, 16

similar structures will be deposited in parallel, as it is a 16-times repeated deposition using one single-tip microelectrode (i.e. serial deposition technique). The relatively large insulation around the microelectrode tip (resolution issue), poor repeatability (accuracy) and long fabrication time to produce the array microstructure (production rate) are the drawbacks of serial deposition technique. It is expected that the parallel fabrication will enhance the capabilities of the LED process and will reduce the time required to produce a microsystem that contains multi-structures with identical geometries. Also, the effect of adjacent tips on each other and a proposed algorithm for the parallel deposition are presented.

Chapter 3:

Serial/Parallel Fabrication by LED

3.1 Serial Deposition Using Single Tip Microelectrode

Previously, 2-D and 3-D structures (like copper or nickel vertical segments and helices) were realized by localized electrochemical using a single tip microelectrode. The deposition current is measured so that it will be an indication on the amount of the instantaneous deposition taking place under the microelectrode tip. Once the deposition current reaches an acceptable threshold value, the tip is withdrawn away from the substrate allowing more deposition to take place under the tip. The shape of the final structure will follow the route or the trajectory of the tip in the space. During this procedure, the LED process parameters must be carefully monitored and implemented; for example, the tip withdrawal speed must be optimized so that the output of the deposition process is a solid and confined structure. Also the applied potential, level of the deposition threshold, electrolyte concentration and microelectrode geometry must be studied and optimized in order to fabricate the desired structure without any defects or irregularities.

It is known that microfabrication processes can be effectively applied to yield a single device or thousands of devices as in batch processing [31]. In LED, possible solutions for this application are to use a single tip microelectrode and run a serial deposition process to fabricate the structures one by one or to use a multi tip microelectrode and run a parallel deposition process to fabricate all the structures at once. In serial deposition process, two different algorithms might be adopted to accomplish this fabrication requirement: continuous and discrete algorithms.

In LED serial deposition technique/discrete algorithm, the master structure is first fabricated at a certain location on the substrate. Once this step is accomplished, the electrode is moved to a new location on the substrate where a copy of the master structure will be fabricated again and so on. If the separation between elements and the structure height are programmed, the expected outcome of this algorithm is an array of elements having the same/different heights or aspect ratios separated by a defined distance. The drawbacks of this technique are that it is time consuming, poor repeatability and its

resolution (density of the structures on the substrate) is limited by the tip geometry and its surrounding insulation. A single failure in depositing one column will result in a complete failure in the fabrication of the whole structure. This is shown in figure 3.1 below.

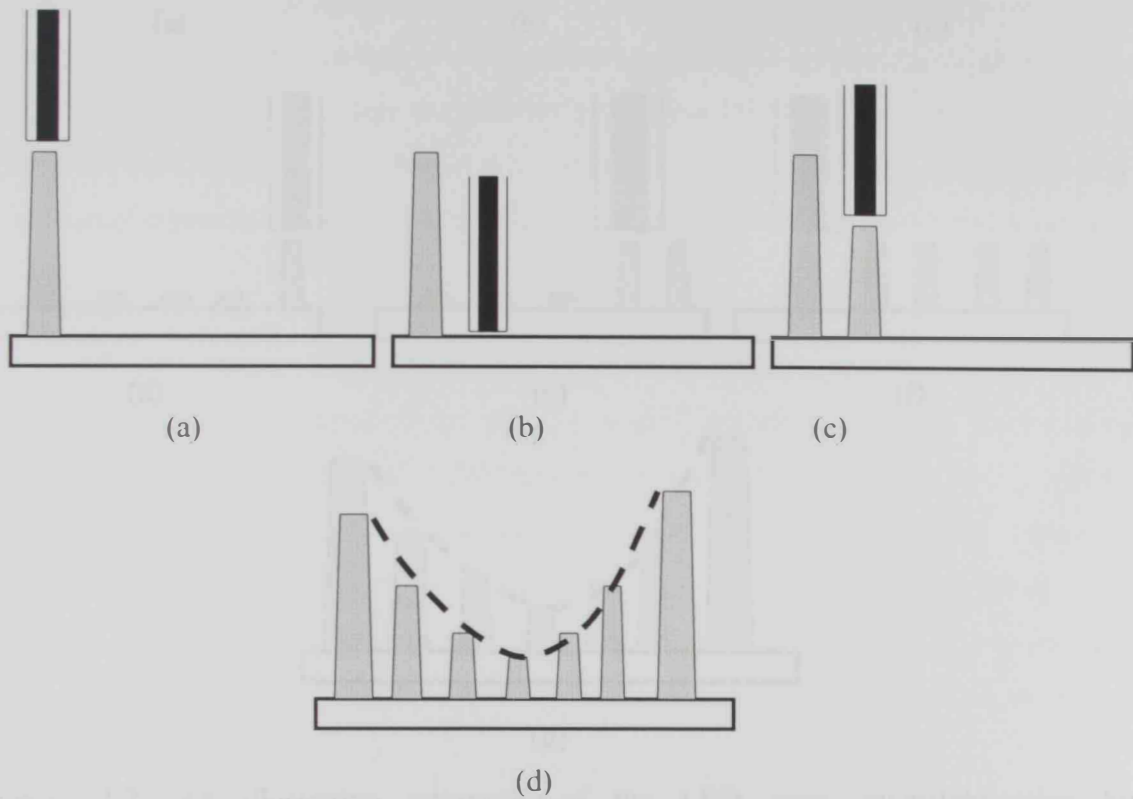


Figure 3.1: An illustrative schematic of the LED array microfabrication by Serial/Discrete Deposition algorithm using single tip microelectrode. (a) The deposition algorithm starts on the first location and fabricate the first structure (a master copy) (b) the tip is then moved to another location and the deposition process is then repeated again to fabricate another structure. (c) The process is repeated sequentially until all elements in the array are fabricated. (d) The array elements can be of a similar height or having different heights thus allowing 3D discrete surface realization.

On the other hand, in LED serial deposition/continuous algorithm, the fabrication algorithm is quite different. A schematic diagram for the process is shown in figure 3.2. First, the tip is brought close to the substrate, potential is then applied to the tip and the reaction current is monitored as in a typical LED process. Once enough deposition is achieved under the microelectrode tip, the microelectrode will not be drawn away from

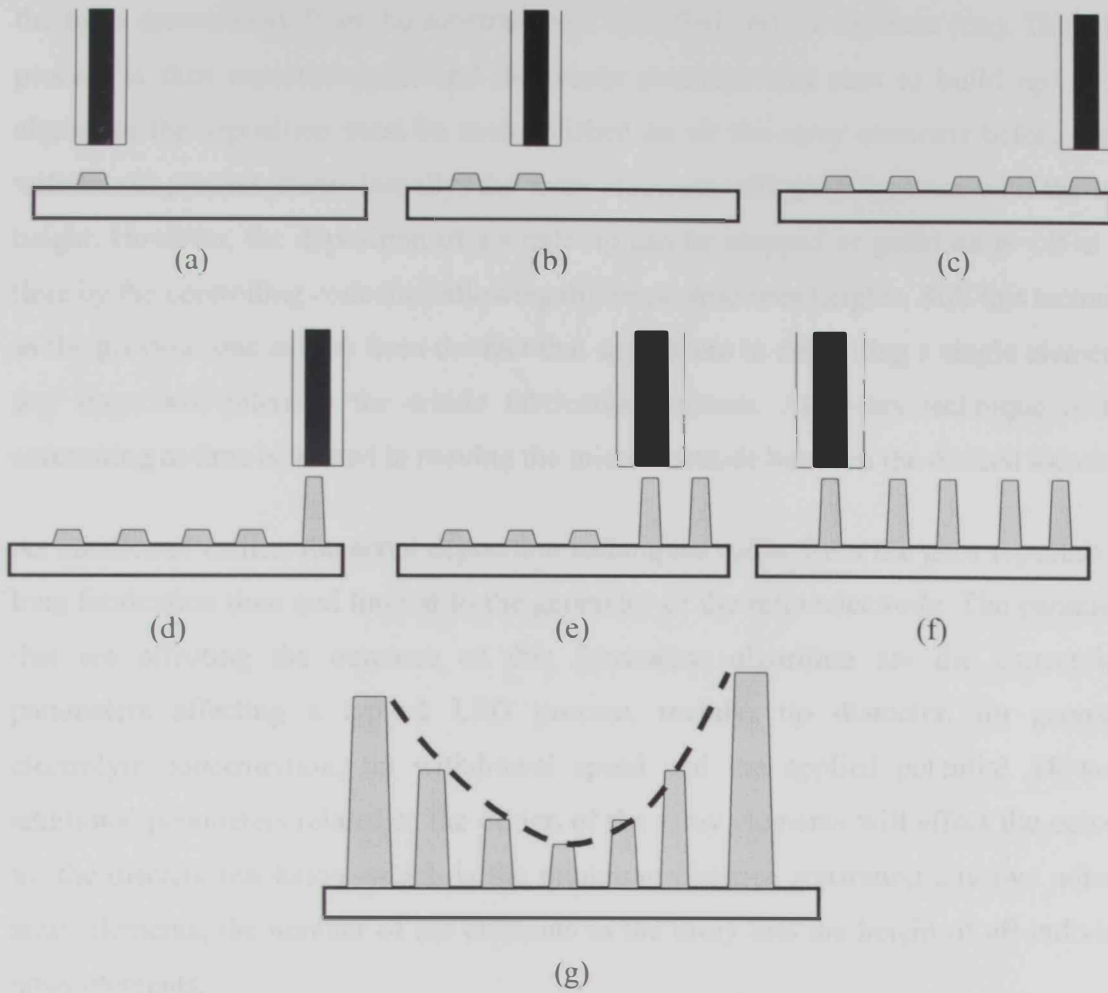


Figure 3.2: An illustrative schematic of the LED array microfabrication by Serial/continuous deposition algorithm using single tip microelectrode. (a) The deposition algorithm starts on the first location to fabricate the master structure (b) Once enough deposition is achieved on the master structure, the tip is then moved to another location and the deposition is then repeated again for another structure. (c) The process is repeated sequentially until enough deposition is achieved on all the elements in the array. (d) The tip then moved away from the deposited structure and the deposition will build up. (e) & (f) the process is then repeated on all the elements. (g) The array elements can be of a similar height or having different heights as shown thus allowing 3D discrete surface realization.

the substrate as in the serial deposition/discrete algorithm but it will move to the adjacent location where to fabricate the second element of the array. The tip will move to all points where these structures elements will be fabricated and ensure that enough deposition is realized on each location before the tip is drawn away from the substrate. Once the whole set of elements in the array achieved enough and equal deposition levels,

the tip is drawn away from the substrate by a specified vertical distance (Δz). The whole process is then repeated again and the whole structure will start to build up. In this algorithm the deposition must be accomplished on all the array elements before the tip withdrawal process starts. Initially, the array elements will grow together with the same height. However, the deposition of a single tip can be stopped or gated on or off at any time by the controlling code thus allowing different structures heights. Still this technique as the previous one suffers from the fact that any failure in depositing a single element at any stage will interrupt the whole fabrication process. Also this technique is time consuming as time is wasted in moving the microelectrode between the desired locations.

As mentioned earlier, the serial deposition techniques suffer from the poor repeatability, long fabrication time and limited to the geometry of the microelectrode. The parameters that are affecting the outcome of this fabrication algorithm are the conventional parameters affecting a typical LED process, mainly: tip diameter, tip geometry, electrolyte concentration, tip withdrawal speed and the applied potential. However, additional parameters related to the design of the array elements will affect the outcome as: the discrete resolution, which is the minimum distance separating any two adjacent array elements, the number of the elements in the array and the height of all individual array elements.

3.2 Parallel fabrication using Array Tip Microelectrode

A new methodology to fabricate array structures using Array Tip Microelectrode is presented in this thesis. These array microelectrodes are now widely implemented in the biological application especially in neuroscience field for signal recording. The Array Tip Microelectrode is basically a multi-tip microelectrode containing independently addressable tips separated by a certain distances (normally equally spaced in the simplest design). There is infinite number of geometries that can be constructed using a given array design, for example a 4*4 array contains 16 tips arranged in 4 rows and 4 columns can be used to realize 16 microstructures on the same substrate simultaneously. Similarly, the same configuration can be used to realize 4 microstructures arranged in 2 rows and 2 columns by activating only 4 elements in the array. The distance between adjacent array

tips will determine the maximum resolution of the fabricated structures. In this thesis, we are implementing the fabrication of array microstructures by tip array microelectrode through using the parallel deposition algorithm that can be described as follows:

Suppose we have a 4*4 array. First, the array is brought close to the substrate, and then the same potential is applied to all of the 16 tips in the array. The deposition process of the 16 tips is monitored by acquiring the reaction current for each element independently as in a conventional fabrication by single tip microelectrode. The individual tip current is then compared with a threshold value set earlier by the user. Once enough deposition is achieved underneath any tip in the array (tip current exceeds the threshold), that specific element will be inactivated by removing the potential applied to it without interrupting the other active elements in the array. This must be done automatically by installing a gating mechanism, which will act as On/Off switch. In this mechanism, a transistor is used as a digital switch. The controlling signal (On/Off) for this switch comes from the controlling code to activate or deactivate a specific tip. The controller code will wait for the case when all the tips are switched off (enough deposition achieved on all concerned tips). Once all elements achieve enough deposition, the potential will be returned back to all the tips involved in the process and then the positioner is triggered to pull the array away from the substrate by a certain distance (Δz) in the vertical direction away from the substrate. The whole process is repeated and the active tips will start depositing on the deposited surface produced in the previous stage and so on. This process will continue until the total accumulated increments equal the desired height. A possible output of this algorithm is 16 structures of similar heights. Another possible output is a parabolic structure where the deposited segments have variable heights. The LED setup for parallel deposition is shown in figure 3.3. A schematic diagram illustrating the process of parallel deposition algorithm is shown in the figure 3.4 below.

To control the process, an algorithm is written in LabVIEW, where the user has the option to specify the geometry of the desired structure by choosing the elements involved in the process, (for example all of the 16 elements or just 8 of them), height of the vertical segments (which can be independently variable for each segment), electrode potential, enough deposition threshold and tip withdrawal speed. First the code will generate the

required potential and send it to the array by the aid of data acquisition unit. Then, the code will keep monitoring the deposition currents of all active tips in the process, compare them with the threshold value, isolate tips that achieved enough deposition, trigger the actuator to move the microelectrode when enough deposition is achieved on all participating tips and repeat the process until the accumulated increments equals the total desired height.

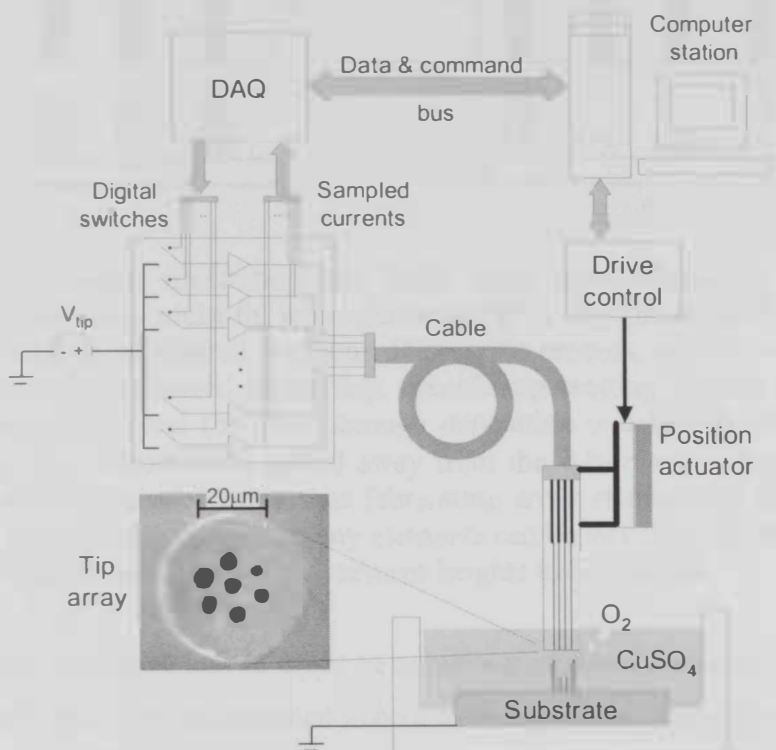


Figure 3.3: LED setup for parallel deposition algorithm, it consists from a microelectrode array connected to an array of digital switches. Each tip is independently connected to a digital switch. The process is monitored and controlled by the LabVIEW code using the aid of a data acquisition unit.

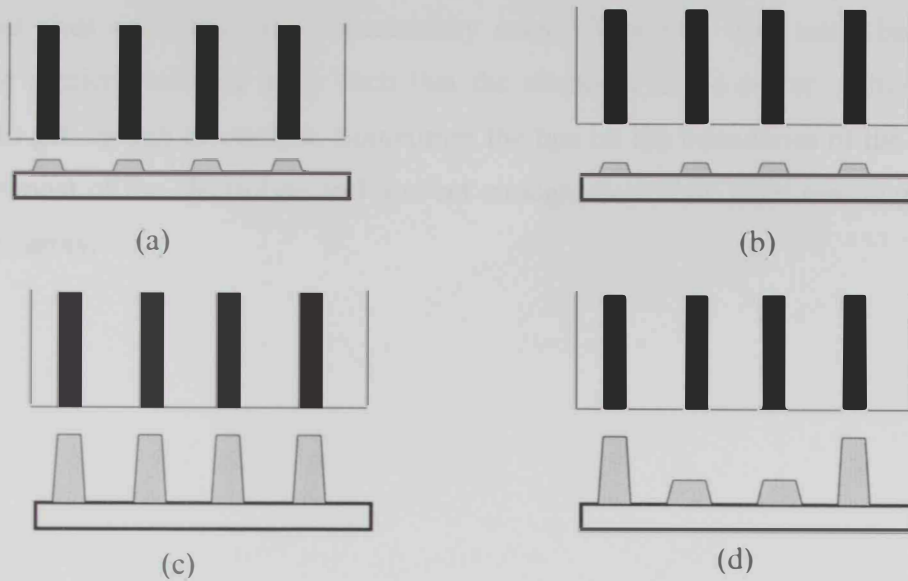


Figure 3.4: A schematic illustrating the LED array microfabrication by Parallel Deposition algorithm using multi-tip microelectrode (4*1). (a) The deposition algorithm starts simultaneously on all desired locations. During the process, any tip is switched off if enough deposition is achieved under that specific tip waiting for the other tips to achieve same deposition level (b) Once enough deposition is achieved under all array tips, the multi-tip microelectrode is pulled away from the substrate by an amount of Δz (c) the process will be repeated again thus fabricating array elements of similar heights (d) Also, during the fabrication process, any elements can be switched off permanently at a specific height thus allowing variable structures heights to be realized

In this fabrication algorithm, and in order to achieve a confined symmetrical structure, the final deposited structures are expected to be a true copy of the master structure except the element height, which can be either fixed or variable in order to construct the final discrete surface. Various discrete surfaces and structures can be achieved using this technique, for example a parabolic dish or hemispherical structure can be constructed using this methodology. Also some microelectrode arrays can be designed with tips of different diameter sizes. This will result in microstructures with variable thickness (which is controlled by the tip diameter). If we let the height also to be variable, then structures with different aspect ratios can be realized on the same sample.

The deposition rate of parallel deposition algorithm using tip array microelectrode is much greater than that of serial deposition algorithm since there is no time wasted to move to another location on the substrate and all of the structures are living the same

conditions thus enhancing the repeatability issue. However, care must be taken in designing a microelectrode array such that the elements in the center of the array are assured to get enough electrolyte. Sometimes the tips on the boundaries of the array will consume most of the electrolyte and prevent enough electrolyte from reaching the inner tips in the array.

Chapter 4:

Single and Multi Tip Microelectrodes

4.1 Microelectrode

If the geometric dimensions of an electrode become very small, the behavior of this electrode will be different from the behavior of large electrode with infinite dimensions. The differences are caused by the change in the mass transport which causes several changes such as decreased ohmic drop of potential, fast establishment of steady-state signal, a current increase due to the increase of the mass transport at the electrode boundary and increased signal to noise ratio. The beneficial properties of small electrodes have been recognized since the time of description of the mass transport in the vicinity of voltammetric electrodes, but only during the 1980s, when the development of microelectronics industry made it possible to measure low current and to construct small-size electrodes. The small-size electrodes are then used in many applications including analytical chemistry and biochemistry [32].

The small-size electrode is called microelectrode. However, in the literature, the term ultramicroelectrode is used. It is now conventionally assumed that the microelectrode has dimensions of tens of micrometers or less. Now carbon multi-wall nanotube electrode with diameter of 100nm is found in the literature. The microelectrode is fabricated either mechanically or photolithographically. The microelectrodes are either single tip microelectrode or multi-tip microelectrode (microelectrode arrays). Some of the most common types of electrodes and electrode arrays are shown in figure 4.1.

4.2 Single-Tip Microelectrode

A typical single-tip microelectrode consists of an insulated microwire of a diameter of about few microns usually made from platinum, iridium, tungsten or their alloys as shown in figure 4.1. Normally the insulation material is glass or polyamide matrix. Unfortunately, there is no specialized microelectrode for the LED system. Most of the microelectrodes used in this work are borrowed from the neuroscience and biological applications. However some successful trials were attempted to build a special microelectrode for localized electrochemical deposition process as shown in figure 4.2.

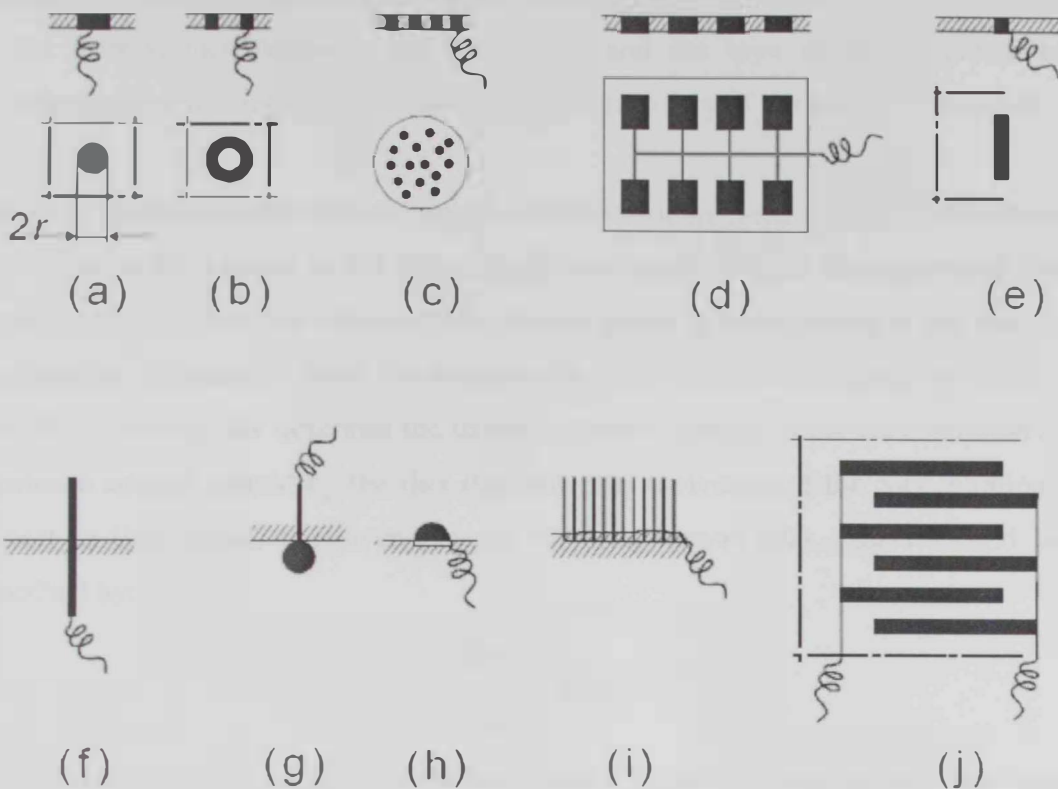


Figure 4.1: Most important geometries of microelectrodes and microelectrode arrays (a) microdisk (b) microring (c) microdisk array (d) lithographically produced microelectrode array (e) microband (f) single fiber (microcylinder) (h) microhemisphere (i) fiber array (j) interdigitated array [32].

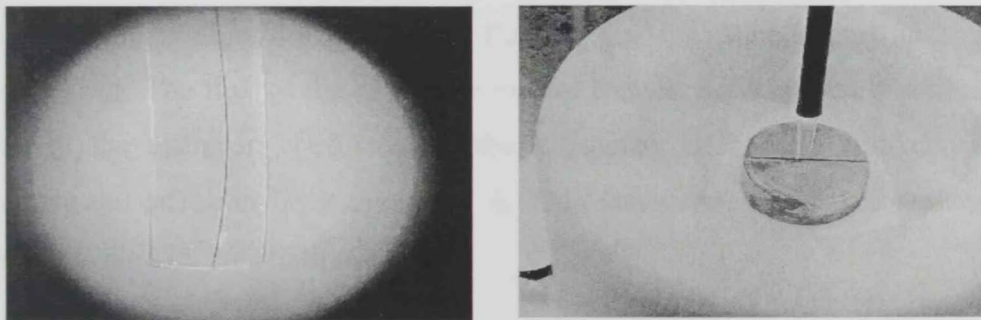


Figure 4.2: Single tip microelectrode: 25 μm diameter insulated Pt wires in a glass matrix. The shaft of the microelectrode is protected to ease the attachment of the microelectrode to an actuator.

The Single Tip Microelectrode is widely used in the neuron-engineering systems for either to transduce neuronal activity into an electrical signal or uses an electrical energy to excite or suppress neuronal activity. Since neuroscience is dealing with small number

for neurons, miniaturized electrodes with dimensions on the scale of neurons are used. In the neuroscience research, the application and the type of the specimen to be investigated by the microelectrode determine the geometry of the electrode required.

The most important factor determining the behavior of an electrode is the mass transport in solution in the vicinity of the electrode. When considering an uncomplicated charge-transfer reaction, then the voltammetric current signal is proportional to the flux of the electroactive substance toward the solution-electrode interface described by Fick's first law. Fick's second law describes the time-dependent changes in the concentration of the substance amount caused by the flux (the potential derivative of the concentration with respect to time equals the divergence of the flux vector) [32]. Fick's second law is described by:

$$\frac{\partial c}{\partial t} = D\Delta c \quad 4.1$$

When the electrode potential is switched from a value at which no electrode reaction occurs to that corresponding to the limiting current of the electrode reaction, then the concentration of the electroactive substance at the electrode surface decreases to zero and a concentration gradient develops over a certain distance from the electrode surface into the bulk of the solution; this distance increases with increasing electrolysis time. The solution volume within the diffusional flux of the substance occurs is termed the diffusion layer. The flux of the substance toward the electrode is then described by the product of the diffusion coefficient of the substance, D , and its bulk concentration divided by the diffusion layer thickness, δ . This quantity is defined, for planar semi-infinite diffusion, by the relationship:

$$\delta = \sqrt{\pi Dt} \quad 4.2$$

If the electrode geometry is approximated by the model of an infinitely large planar electrode with the substance flux perpendicular to the electrode plane, then the flux is uniform over the entire electrode surface and the substance concentration attains the bulk value at a distance of a few diffusion layer thickness values. However, the flux is not

uniform over the electrode surface due to the edge effect for other geometries [32]. A graph indicating the diffusion layer of two adjacent electrodes is shown in figure 4.3.

In the case when $\delta \ll r$, where r is the radius of the electrode, the electrode can be modeled as infinite electrode model. However, when $\delta \gg r$, the edge effect plays a predominant role, and the diffusional flux toward the electrode is constant with time but inhomogeneous over the electrode surface; it increases with decreasing distance from the electrode edge [32].

After sufficient time, a steady state is established for the electrode of certain geometries (planar or spherical). Spherical electrode has a simple flux pattern described by the following equation:

$$\left(\frac{\partial c(x,t)}{\partial x} \right)_{x=r} = c^0 \left[\frac{1}{\delta} + \frac{1}{r} \right] \quad 4.3$$

where $\left(\frac{\partial c(x,t)}{\partial x} \right)_{x=r}$ is the concentration gradient, c^0 is the bulk substance concentration, r is the electrode radius. The first term predominates at short time where $\delta \ll r$, while the second will predominates at long time ($\delta \gg r$). It can be seen that the time required to reach the steady state phase is strongly dependent on the electrode geometry. Thus, the smaller the electrode, the shorter the time required reaching steady state.

In the case of LED system, the electrode is attached to an actuator with a fine resolution. Normally a micro stepper motor with step size of around 30nm is used to move the microelectrode in the 3D space. The mechanical design of the microelectrode is important in order to ease its movement in the 3D space and is also important to minimize the vibrations of the electrode shaft during the fabrication process, which certainly will affect the accuracy of positioning of the microelectrode at the desired location on the substrate.

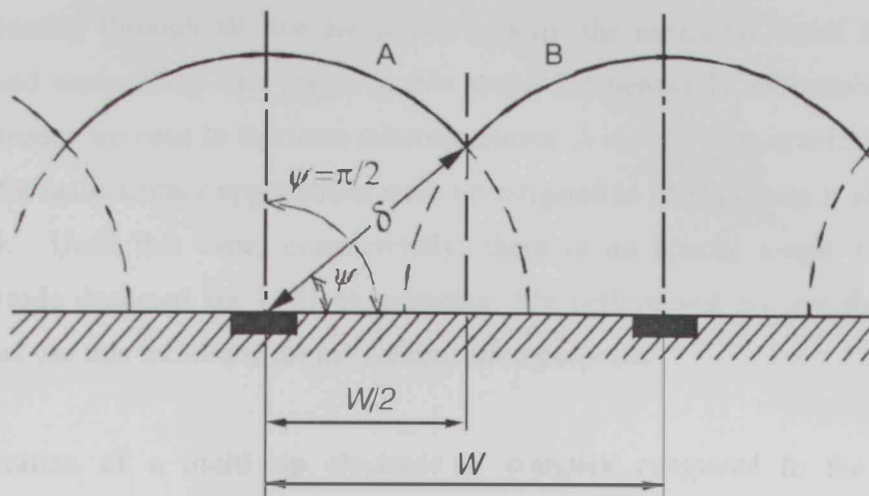


Figure 4.3: A schematic diagram illustrating the concept of diffusion layer for two adjacent electrodes [32].

In general, the LED process consists of a metal-electrolyte interface. Metal-electrolyte model is complex compared to the ohmic metal-metal model. An electrode surface can be modeled with a capacitance C_e and resistance R_e of the metal-electrolyte interface in parallel, and a potential V_e dropped across the interface in series as shown in the figure 4.4. The value of each component depends on the frequency, material, electrolyte and temperature [33].

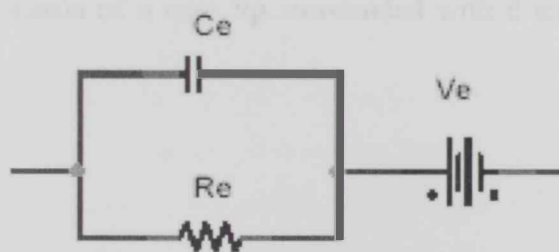


Figure 4.4: General electrical model for the electrode/electrolyte interface [33].

4.3 Multi-Tip Microelectrode (Microelectrode Array)

The multi-tip microelectrode is a microelectrode with more than one tip. These tips can be independently addressable (i.e. independent signal for each tip) or it can be an extension to one tip (one tip with multi heads). In neuroscience, sometimes they use this multi tip array to record the current from different locations of the sample then the

currents passing through all tips are added to form the measured signal that will be acquired and analyzed at later stage. In this study, independently addressable multi tip microelectrodes are used to fabricate microstructures. A sample of microelectrode arrays available for neuroscience applications were investigated in LED process is shown in the figure 4.5. Until this time, commercially, there is no special single tip or array microelectrode designed for LED experiments. We believe that we are the first who propose and use this technique for microfabrication purposes.

The fabrication of a multi tip electrode is complex compared to the single tip microelectrode. In single tip microelectrode, the positioning of the tip in the glass matrix is not very important. Normally, the location of the tip is selected to be in the center of the surface of the microelectrode. However, in the case of multi tip microelectrode, it is essential to maintain a fixed distance between tips, which is the case in almost all of the current applications of the microelectrodes. For example a 16 (2 rows * 8 columns) elements array used in neuroscience found in the literature is designed with a fixed distance between the adjacent elements as shown in figure 4.5. Sometimes the fabrication technique limits the minimum distance between the tips. However a gap distance of about the tip diameter or greater can be realized. The geometry also can be flexible, for example, a heptode consists of a core tip surrounded with 6 smaller tips is shown in figure 4.5.

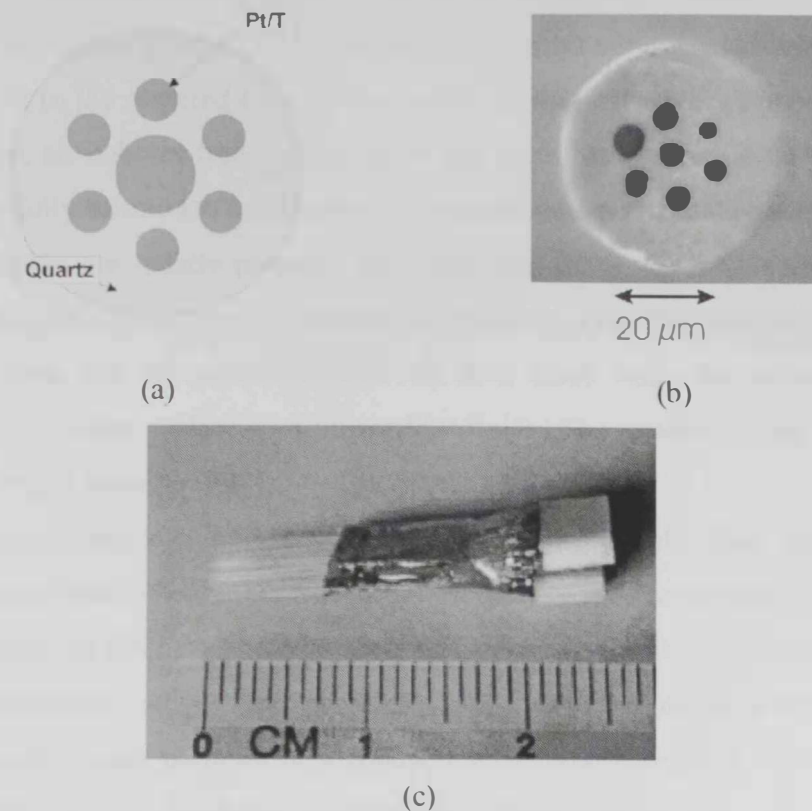


Figure 4.5: Microelectrode arrays (a) Cross section of a multicore fiber containing 7 Pt/T cores. The outer fiber diameter is about $100\mu\text{m}$. These seven tips are independently addressable (b) a microscopic graph for the real heptode array in part (a). (c) Array used for chronic recording composed of 2 rows of independently addressable electrodes.

To operate the microelectrode array in a similar way to a single tip microelectrode, the distance between adjacent tips must be greater than the diffusion layer. If the diffusion layers overlap as can be seen in the figure 4.3, then the tips will induce a mutual effect and it will certainly affect the final microstructure.

4.4 Preparation of Microelectrodes

Microelectrodes and their arrays are usually prepared in the laboratory for a given purpose. The preparation process is not complicated but requires very careful work and experience. Some of these approaches are outlined below:

- Microcylindrical electrodes are obtained by sealing thin metal wires or carbon fiber in tapered glass capillaries (micropipettes). The protruded wire or fiber is then cut to the required length. The quality of the seal is very important; it must be tight, air bubbles free. Epoxy resins that are most often used for sealing must be carefully selected to be chemically resistance and noncontaminating [32].
- Microdisks are mostly prepared by fixing thin metal wires or carbon fibers in tapered glass capillaries by carefully melting the glass. The disk is then obtained by cutting off the protruded wire or fiber flush with the surface thorough polishing of the surface to a mirror-like finish. The quality of the seal and the polishing is important [32].
- Band electrodes can be prepared by sealing thin metals films into a suitable insulator. Photolithographic techniques are widely used to produce a broad range of shapes and sizes, both single electrodes and electrode arrays [32].
- Microelectrode arrays are prepared in a very simple way by dispersing sufficiently small particles of a conductive material (usually a very fine graphite powder) in an insulator. Of course, these arrays are poorly defined electrochemically. Well-defined arrays are now almost exclusively prepared by photolithography [32].
- Like all solid electrodes, microelectrodes require suitable pretreatment and activation prior to measurements. The first step always involves the obtaining of smooth surface (usually mechanical polishing), followed by chemical or electrochemical conditioning, or by the combination of the two [32].

4.5 Applications

The application of the microelectrodes and microelectrode arrays include:

- Electrochemical reaction mechanisms and kinetics. The study of reaction mechanisms makes primary use of the decreased resistance and capacitance at microelectrodes permitting the use of various voltammetric techniques with very fast potential scans, measurements in a steady state and application of a great

variety of solvents and supporting electrolytes including solvents of low relative permittivity values or samples without a supporting electrolyte added [32].

- Trace electrochemical analysis [32].
- Electrochemical reaction in solution of very high resistance. In the absence or at a very low concentration of a supporting electrolyte, electrochemical investigations can be performed on systems of high resistance [32].
- Analytical sensing. Many sensors for gaseous substance employ microelectrode systems with liquid or solid-polymer electrolytes. The main advantage of microelectrodes here are small dimensions, which also permit construction of multisensor arrays [32].
- Biosensors. Microelectrodes offer advantages over conventional larger working electrodes within biosensors since they experience hemispherical solute diffusional profiles, and it is this phenomenon that can impart stir-independence to sensor response, whilst also offering lowered limits of detection. Individual microelectrodes offer very small responses and one approach for overcoming this problem is to use microelectrode array to allow cumulative and so larger response to be measured [34].
- Scanning electrochemical microscopy (SECM). The SECM techniques are becoming an increasingly important area of microelectrode application for imaging redox centers present in thin films [32].
- Micro arrays can be used in heavy metal detection [35].
- Microfabrication. The single tip microelectrode is used to fabricate high aspect ratio microstructures. The fabrication of multi tip array microelectrode is investigated here in this thesis.

Chapter 5:

LED Process Simulation

5.1 Simulation of the deposition process

In order to investigate the process of the parallel and serial deposition, simulation analysis was performed to study the possible outcome of the fabrication process in case of single and multi tip microelectrodes. It is well known that for the LED process, the deposition profile is proportional to the strength of the electrical field applied between the tip and the substrate [27]. First, the case of a single tip microelectrode was simulated by defining the geometry and boundaries of the system (microelectrode, substrate and the surrounding) and then the electric field distribution is calculated numerically. In the simulation, the tip material is copper and the substrate material was copper while the surrounding was estimated as vacuum. The tip is insulated with a glass matrix. The diameter of the tip used in simulation was $100\mu\text{m}$. The microelectrode tip was positioned $5\mu\text{m}$ above the substrate. Due to the fact the strength of the electric field underneath the tip of the microelectrode is proportional to the amount of deposition that may take place; the magnitude of the electric field along the substrate surface was extracted and plotted.

To simulate parallel deposition, a microelectrode array composed of a 3 adjacent tips made of nickel placed in a glass matrix is brought close to the copper substrate. The diameter of the micro tips used in simulation was $100\mu\text{m}$ and the tip-substrate distance is kept $5\mu\text{m}$ as in the case of single tip simulation. The horizontal distance between the tips within the array (center to center) was set to $100\mu\text{m}$. The electric field simulation was performed using Ansoft software. Ansoft uses finite element method to compute the electric field distribution for a defined geometry. In this problem, the electric field, which is representing the deposition profile, was computed at all surfaces and on an imaginary line placed $0.1\mu\text{m}$ above the substrate. To study the effect of any mutual coupling between array tips, the separation distance between the tips was changed to $200\mu\text{m}$ and $400\mu\text{m}$, the simulation process was repeated. Simulation results for these cases are shown below.

5.2 Single Tip Microelectrode Simulation

The electric field simulation below was conducted for the case of tips potential of 3.8V. Ansoft software was used to simulate the magnitude of the electrostatic fields. The insulation material surrounding the 25 μm copper tip was glass performing a cylindrical microelectrode of diameter of 1000 μm . Vacuum was used to simulate the background however; this is a simplification of the simulation as in the real case the electrolyte is used instead of vacuum. The result for the simulation is shown in figures 5.1 and 5.2.

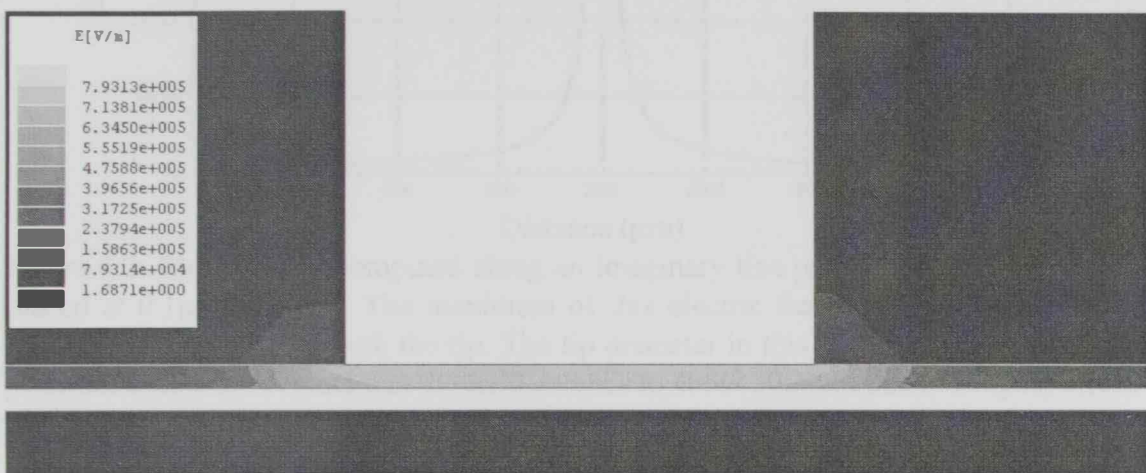


Figure 5.1: Electric field distribution in the case of single tip microelectrode, note that the electrical field inside the substrate and the electrode is zero and its maximum is located underneath the tip. Also the electrical field inside the glass matrix is small compared to the field beneath the tip. The tip diameter in this case is 100 μm and the tip potential equals 3.8V.

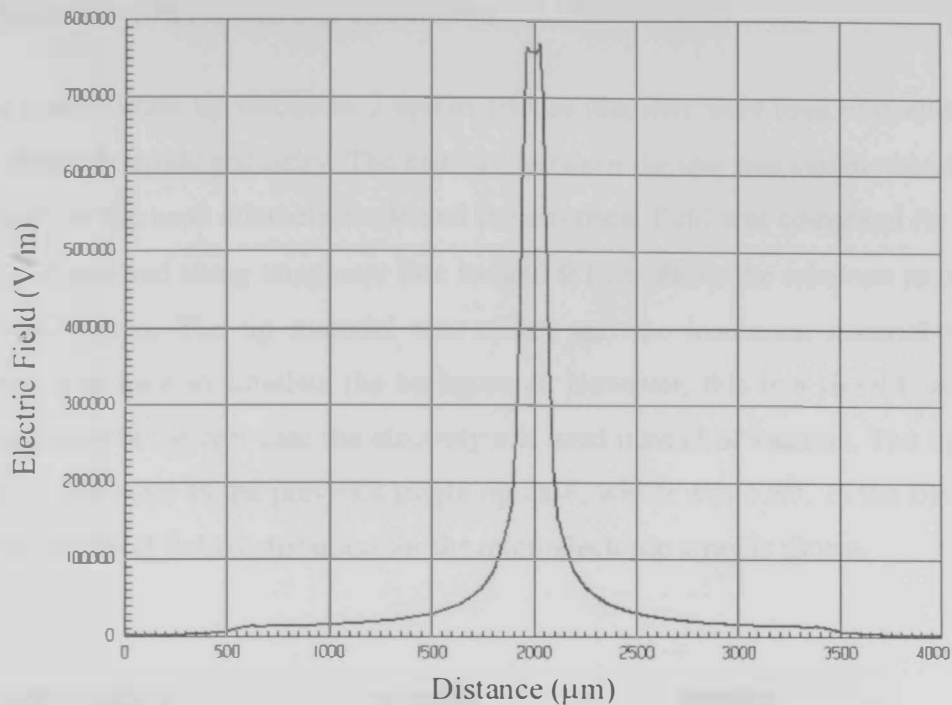


Figure 5.2: Electric field computed along an imaginary line parallel to the substrate and placed at $0.1\mu\text{m}$ above it. The maximum of this electric field along the line is at the middle of the line underneath the tip. The tip diameter in this case is $100\mu\text{m}$ and the tip potential equals 3.8V . Note that the field extends to about $3000\mu\text{m}$ due to fringing effect.

It can be seen from figures 5.1 and 5.2 that the field is maximum in the area beneath the tip (where the field is localized) and the field strength is negligible in the glass matrix away from the substrate. Also because they are modeled as perfect conductor, the field inside the microelectrode tips and the conducting substrate is zero. In the deposition process, the deposited structure will likely take similar profile of figure 5.2. Due to the electrical field distribution around the microelectrode, the fringing effect is clear. The fringing effect shown in figures 5.1 and 5.2 has to do with the geometry of the insulation surrounding the array as studied in the literature [36]. In real deposition experiment, this fringing phenomenon will result in a deposition of the crystals on the substrate around the electrode tip forming a relatively large base compared with the diameter of the tip. This deposition base is unwanted and can be minimized by proper design of the microelectrode. In the literature, it was shown that when the insulation material surrounding the tip is less, the deposited base would be minimized [36].

5.3 Multi Tip Microelectrode Simulation

In the case of multi tip electrode, 3 tips of $100\mu\text{m}$ diameter were used to simulate general array microelectrode geometry. The distance between the tips was varied according to the geometry of the used microelectrode and the electrical field was computed for each case in all surfaces and along imaginary line located $0.1\mu\text{m}$ above the substrate as done in the previous section. The tip material was nickel and the insulation material was glass. Vacuum was used to simulate the background. However, this is a simplification of the simulation as in the real case the electrolyte is used instead of vacuum. The tip potential was kept the same as the previous single tip case, which was 3.8V . In the figures 5.3 to 5.8, the electrical field distribution for the microelectrode array is shown.

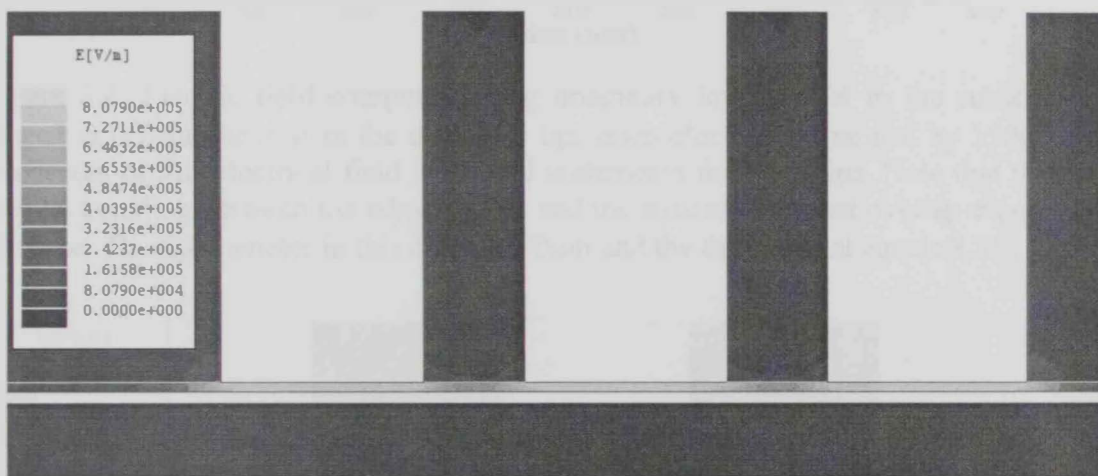


Figure 5.3: Electric field distribution in the case of a multi tip microelectrode separated by a distance of 1.5 times the tip diameter (center to center, $150\mu\text{m}$); note that the electrical field inside the substrate and the electrode tips is zero. Also the electrical field inside the glass matrix is small compared to the field beneath the tip where it is localized. The tip diameter in this case is $100\mu\text{m}$ and the tip potential applied equals 3.8V .

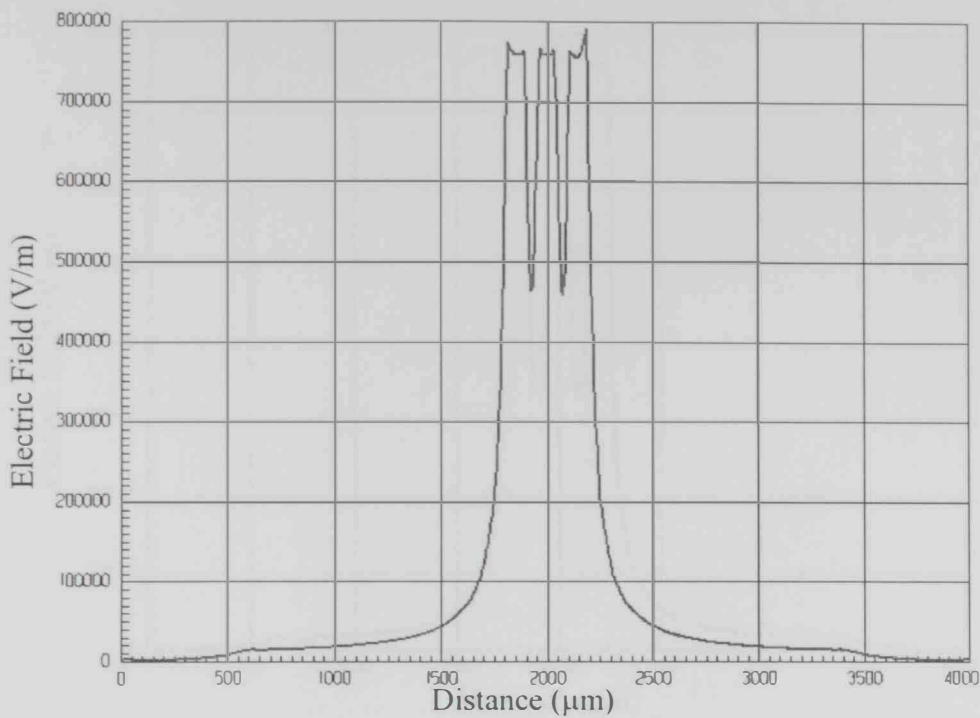


Figure 5.4: Electric field computed along imaginary line parallel to the substrate and placed at $0.1\mu\text{m}$ above it in the case of 3 tips microelectrode separated by $150\mu\text{m}$. The maximum of this electrical field is located underneath the three tips. Note that there is a mutual coupling between the adjacent tips and the structures almost overlap especially at the base. The tip diameter in this case is $100\mu\text{m}$ and the tip potential equals 3.8V .

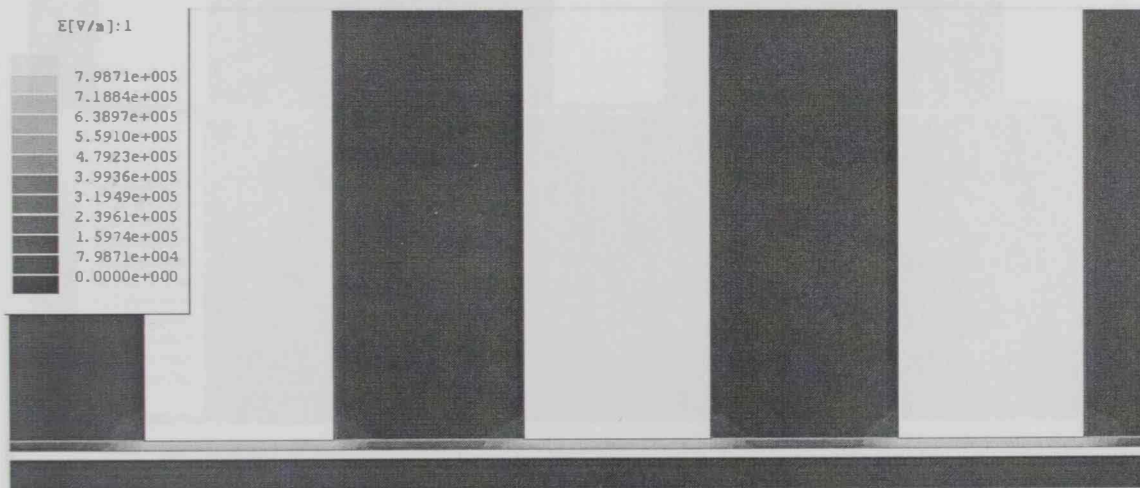


Figure 5.5: Electrical field distribution in the case of a multi tip microelectrode separated by 2 times the tip diameter (center to center, $200\mu\text{m}$); note that the electrical field inside the substrate and the electrode tips is zero. Also the electrical field inside the glass matrix is small compared to the field beneath the tip. The tip diameter in this case is $100\mu\text{m}$ and the tip potential applied equals 3.8V .

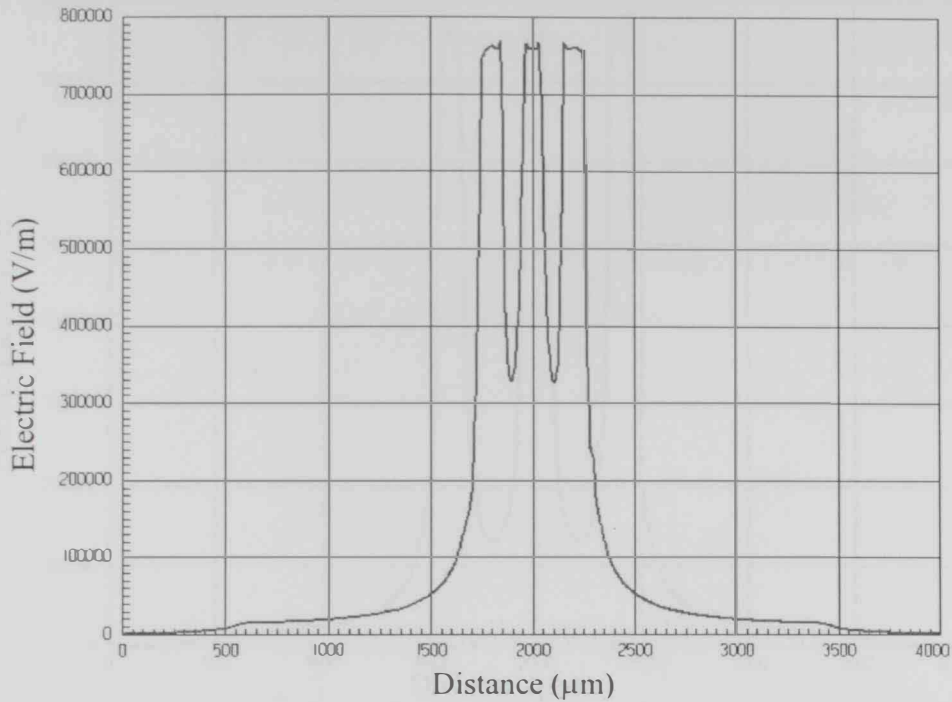


Figure 5.6: Electric field computed along imaginary line parallel to the substrate and placed at $0.1\mu\text{m}$ above it in the case of 3 tips microelectrode array separated by $200\mu\text{m}$. The maximum of this electrical field is along the three tips. Note that there is a mutual coupling between the adjacent tip, which is less than the previous case. The tip diameter in this case is $100\mu\text{m}$ and the tip potential equals 3.8V .

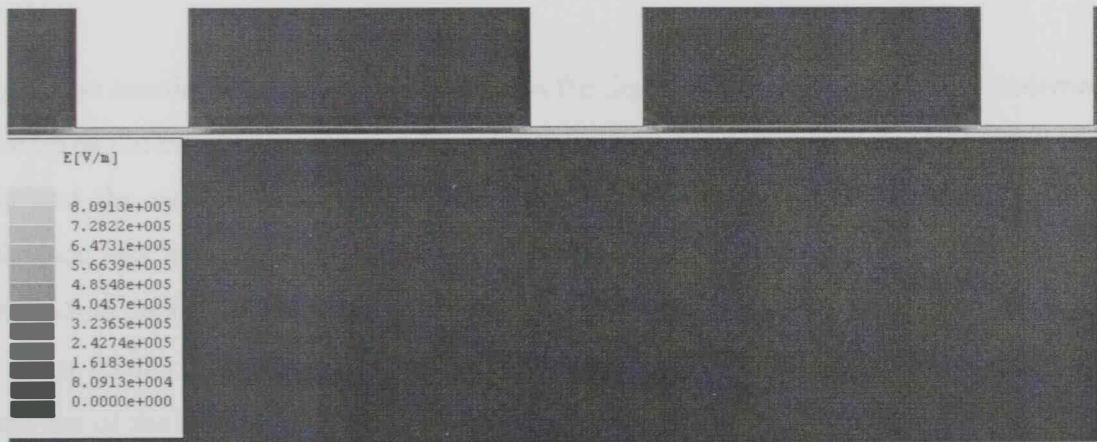


Figure 5.7: Electrical field distribution in the case of a 3 tips microelectrode separated by $400\mu\text{m}$. Note that the electrical field inside the substrate and the electrode tips is zero. Also the electrical field inside the glass matrix is small compared to the field beneath the tip. The tip diameter in this case is $100\mu\text{m}$ and the tip potential equals 3.8V .

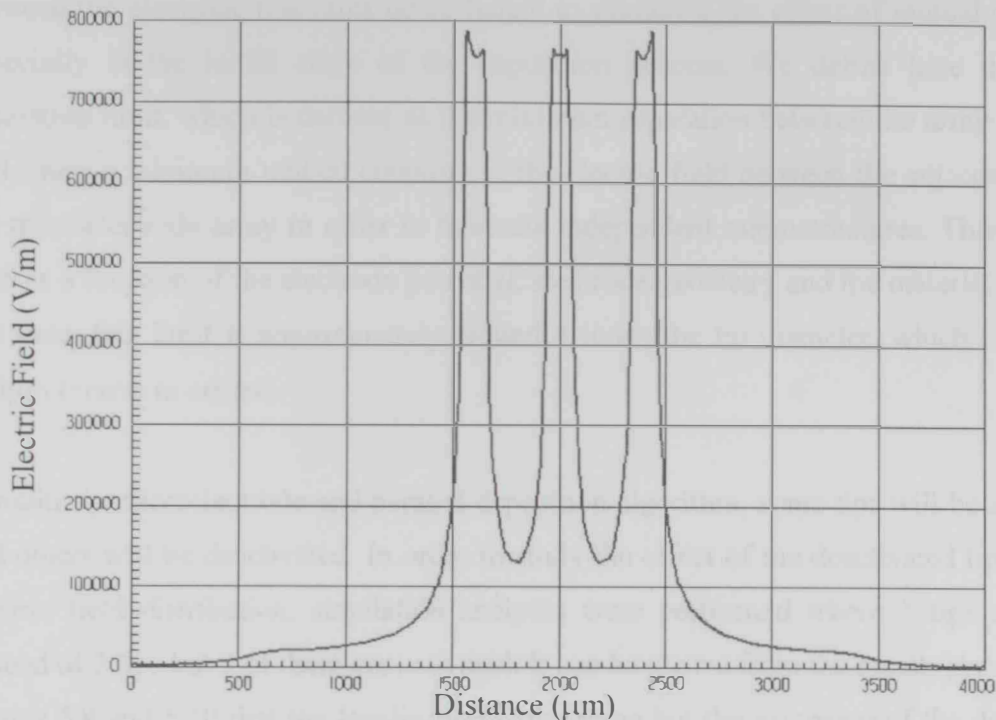


Figure 5.8: Electric field computed along imaginary line parallel to the substrate and placed at $0.1\mu\text{m}$ above it in the case of 3 tips microelectrode array separated by $400\mu\text{m}$. The maximum of this electrical field is along the three tips of the microelectrode array. Note that there is mutual coupling between the adjacent tips. This mutual coupling is less than that in case of separation distance equals $150\mu\text{m}$ or $200\mu\text{m}$ and the structures look more independent. The tip diameter in this case is $100\mu\text{m}$ and the tip potential equals 3.8V .

From the simulation results, it is shown that the deposition profile is localized underneath the tip of the microelectrode and its geometry is mainly controlled by the geometry of the tip and the surrounding insulation. When the tips within the array are separated by distance less than $200\mu\text{m}$, the mutual effect of the electric field will heavily affect the individual deposited structures. As can be seen in the case when the separation distance is $150\mu\text{m}$ (center to center), there is a high degree of overlap between the electrical field profiles of the adjacent three tips. It is expected that in such a case, the tips will start to act as one big tip and the resulting structures underneath these tips will tend to have a form of one structure having a diameter larger than a single tip diameter instead of an array of individual microstructures. This effect is highly obvious at the initial stage of the deposition process where a wide base will be formed first. In order to fabricate a micro array with independent structures using parallel deposition algorithm, the distance

between the electrode tips must be sufficient to minimize the effect of mutual coupling especially at the initial stage of the deposition process. We define here the array separation limit, which is defined as the minimum separation between the array tips that will cause a minimum mutual coupling of the electric field between the adjacent tips in the microelectrode array in order to fabricate independent microstructures. This defined limit is a function of the electrode potential, electrode geometry and the material used. In this case, this limit is approximately around 4 times the tip diameter, which is around $400\mu\text{m}$ (center to center).

In multi tip microelectrode and parallel deposition algorithm, some tips will be activated and others will be deactivated. In order to study the effect of the deactivated tips on the electric field distribution, simulation analyses were performed where 5 tips are used instead of 3 tips but 3 of them are activated. It can be shown from the results presented in figures 5.9 and 5.10 that the localization is the same but the extension of the deposition base is less, which is considered an added advantage of parallel deposition.

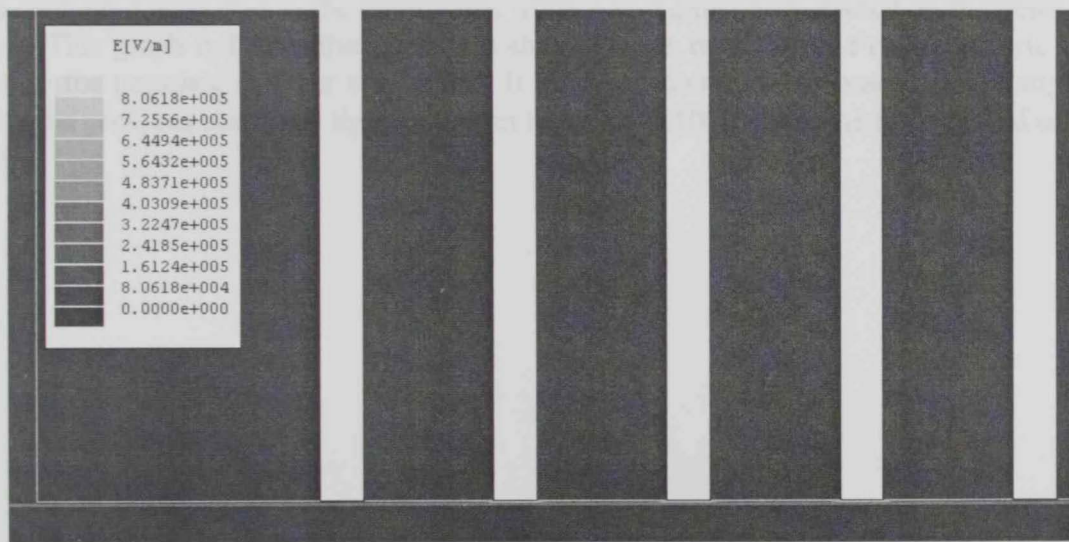


Figure 5.9: Electrical field distribution in the case of a 5 tips microelectrode separated by $400\mu\text{m}$. Only 3 tips were activated. The tip diameter in this case is $100\mu\text{m}$ and the tip potential equals 3.8V.

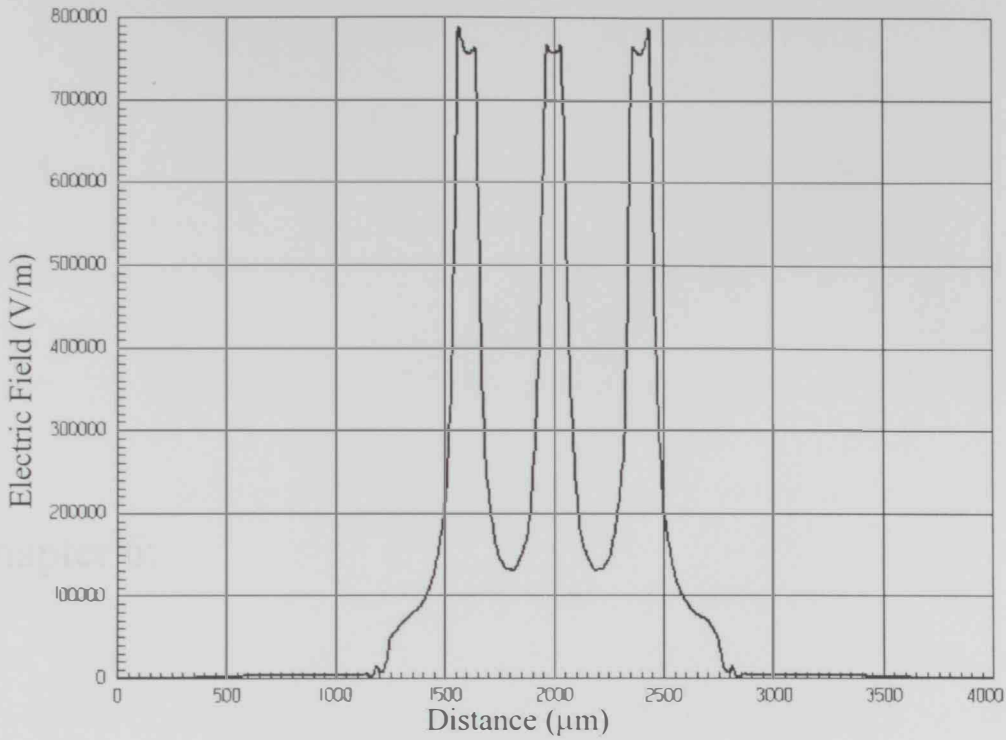


Figure 5.10: Electric field computed along imaginary line parallel to the substrate and placed at $0.1\mu\text{m}$ above it in the case of 5 tips microelectrode array separated by $400\mu\text{m}$. The potential is applied to the inner 3 tips while maintaining no potential on the other two tips. This graph indicates that there is a slight change in the profile of the electric field due to the presence of other conductors. It can be shown that the base is less compared with the previous case. The tip diameter in this case is $100\mu\text{m}$ and the tip potential equals 3.8V .

Chapter 6:

Experimental Procedures, Results and Discussion

6.1 LED setup

The process of microfabrication by LED involves the use of a suitable microelectrode according to the geometry of the desired microstructure, an electrochemical cell filled with the electrolyte containing the species to be deposited, a conducting substrate where the microstructure will be built, a highly accurate 3D actuator to move the microelectrode array in the 3D space and a controlling algorithm that will control the whole fabrication process. Also in the case of parallel deposition, a set of digital switches is used to activate or deactivate any tip in the array at any time. The integration of all of these key elements forms the general setup of the LED process. To visually follow the fabrication process instantaneously, a microscope with a good zooming capability is normally used. In literature some researchers used X-ray to monitor the microstructure growth by time. Using the microscope instead of the X-ray will keep the advantage of simplicity of the setup still valid. Also, the microscope will allow the user to see the air bubbles as a result of the oxidization reaction at the tip surface but the final geometry will not be followed by a simple microscope as the initial distance between the tip and the substrate is very small compared to the microelectrode insulation dimension.

The LED setup used in this work is shown in figures 6.1 to 6.3. 3-axis picomotors are used to hold the microelectrode array allowing it to move in the space with a resolution of about 30nm. The copper-made substrate is put in a hole in an electrochemical cell made from Teflon. The microelectrode array is then brought by the aid of the picomotors to a distance very close to the substrate. A microscope is used to help in monitoring the initial positioning of the microelectrode array close to the substrate. The controlling code of the deposition process was written in LabVIEW. The function of the code is to control the parameters of the deposition process like tip voltage, withdrawal speed and height of the desired microstructure. In the following sections, the elements of the LED setup that were used are presented in more details.

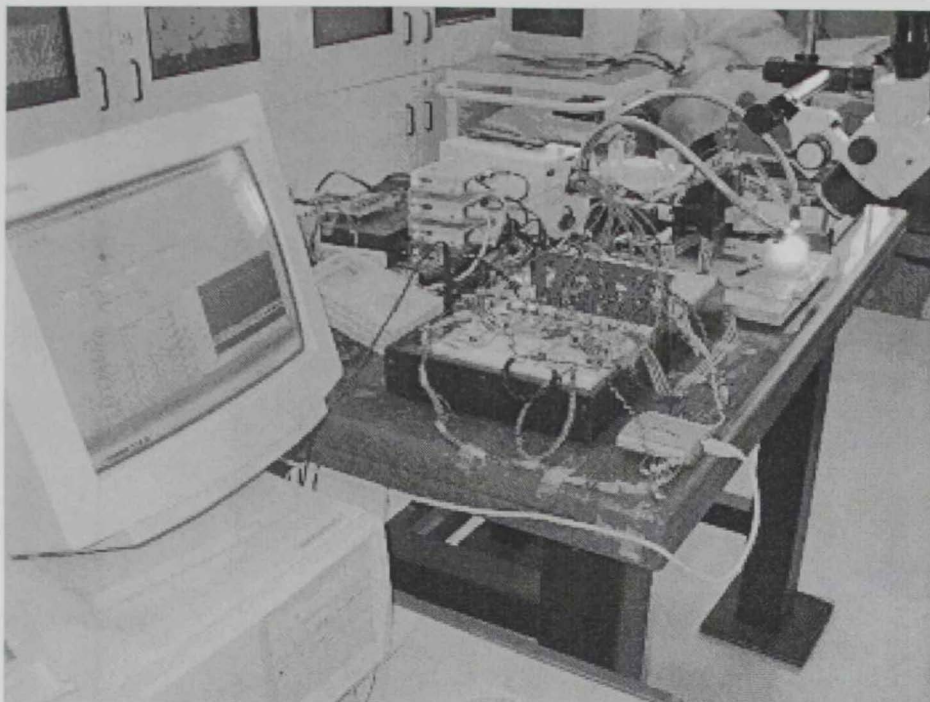


Figure 6.1: A general photo for the LED setup showing the controlling code written in LabVIEW running parallel deposition experiment. Data acquisition unit is used to provide the potential required and monitor the deposition current (deposition rate).

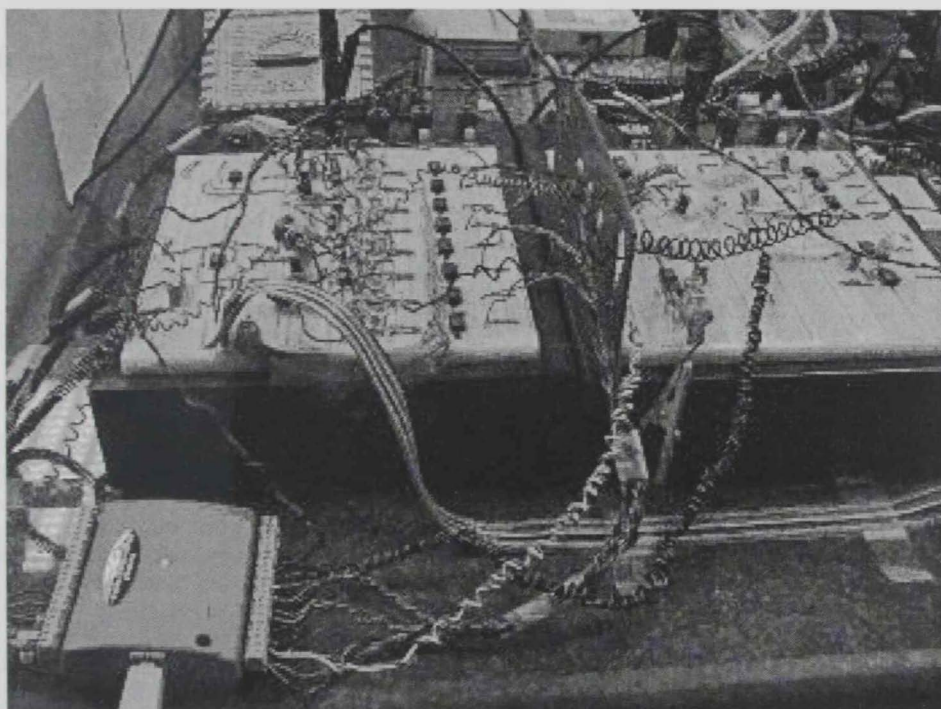


Figure 6.2: LED setup, in this photo, the gating/switching circuit used in parallel deposition is shown as well as the data acquisition unit used to acquire the deposition current of the array tips.



Figure 6.3: 3-D picomotors (from Newfocus Inc.) of resolution about 30nm per step is used to move the microelectrode array in the space. The movement of the picomotors is programmed by LabVIEW code according to the user requirements.

6.1.1 Electrode fabrication and preparation

Several electrode designs were investigated in this work; these electrodes were borrowed from neuroscience field and designed originally for biological applications, as there were no microelectrodes designed specially for LED technique. However, the performance of these microelectrodes was not promising. Several limitations of these microelectrodes prohibited a good integration of them in the LED setup. Of these limitations: the design of some of these microelectrodes is fixed and not flexible either in the geometry side or on the material of the microelectrode used (tip and insulation). Sometimes the material used is not inert in the electrolyte used. Another limitation is the high cost of these microelectrodes and microelectrode arrays and the long time required to design and fabricate the required geometry. Some of these electrodes were insulated by a non-rigid epoxy like polyamide matrix, which cause a difficulty in an accurate positioning of the electrode in the 3D space. Other types of microelectrodes arrays use a very thin insulation matrix of outer diameter being about $100\mu\text{m}$, which complicates the handling and integration of these arrays in the LED setup.

A microelectrode array was self-made in the lab by embedding a number of micro wires in a glass micropipette. The microwires used in this work were made from copper, nickel and platinum/Iridium materials insulated with a thin polyamide layer supplied by California Fine Wires Company. The diameters of the microwire used were $25\mu\text{m}$ made from Pt/Ir material as shown in figure 6.5. Also $100\mu\text{m}$ microwires made from copper and nickel materials were used. In order to maintain a close distance between the array tips, the microwires were twisted together prior to inserting them in the micropipette. The microwires were then pulled from the side of the glass micropipette ensuring enough wire length to work with at a later stage. An adhesive material is then used to fill the micropipette from one end. In our case, a super-glue material available in the supermarkets was used. The adhesive material was sucked from the other end to ensure that the adhesive material is fully filling the micropipette around the microwires to an acceptable level. In this process, care must be taken in order to minimize the chance for any air bubbles to be present in the micropipette during the sucking of the adhesive material. The microelectrode was put aside for about 24 hours until the epoxy material is set and well distributed around the microwires. The surface of the microelectrode was then cleaned and polished. Photos for some of these self-made micro arrays are shown in figure 6.4.A to 6.4.E below were the tips were made from copper or nickel. Pt/Ir microelectrode is shown in figure 6.5.

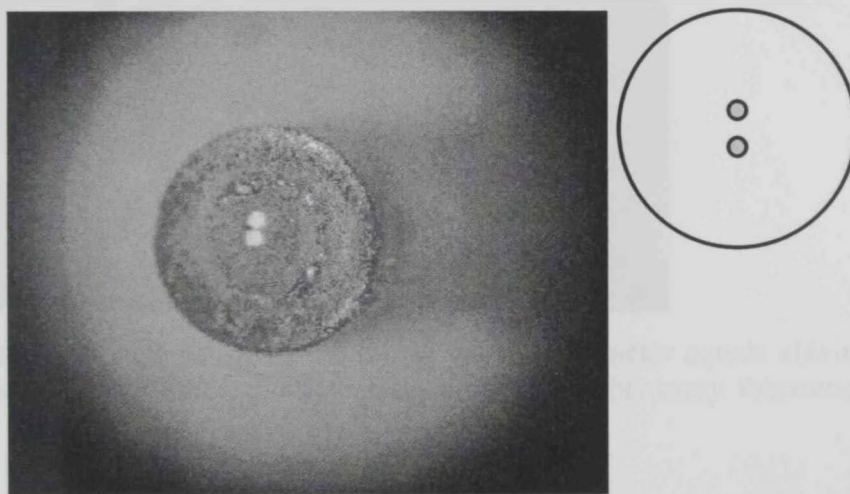


Figure 6.4.A: A micro array composed of two $100\mu\text{m}$ copper microwires. The microwires are insulated by polyamide material. Only the tip of the micro wire is exposed at the end of the microelectrode. Note the distance between the tips is less than the tip diameter.

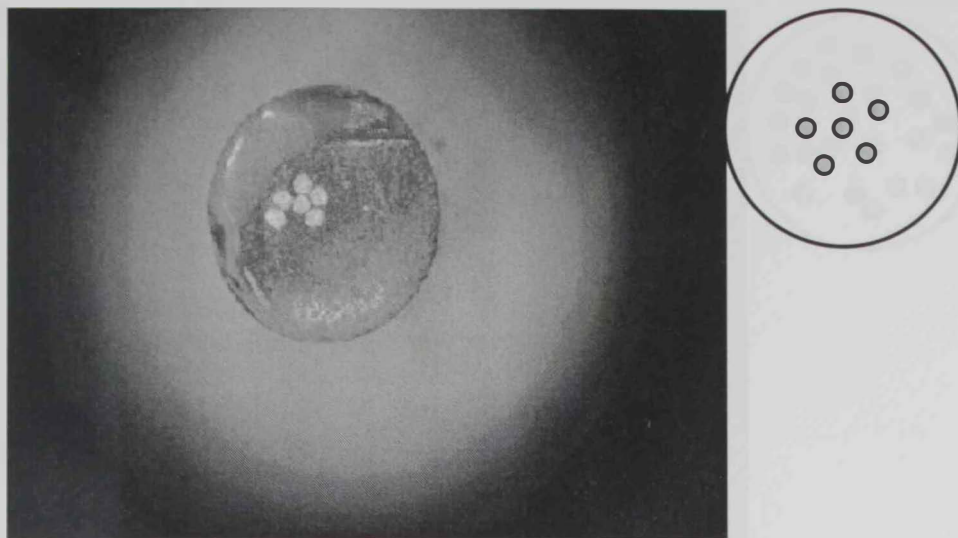


Figure 6.4.B: Flower type of copper micro array fabricated by twisting 5 microwires on another microwire and then embedding them in a glass micropipette. A glue matrix is used to fill the volume between the microwires and the inner diameter of the micropipette. The material is copper and the tip diameter is $100\mu\text{m}$.

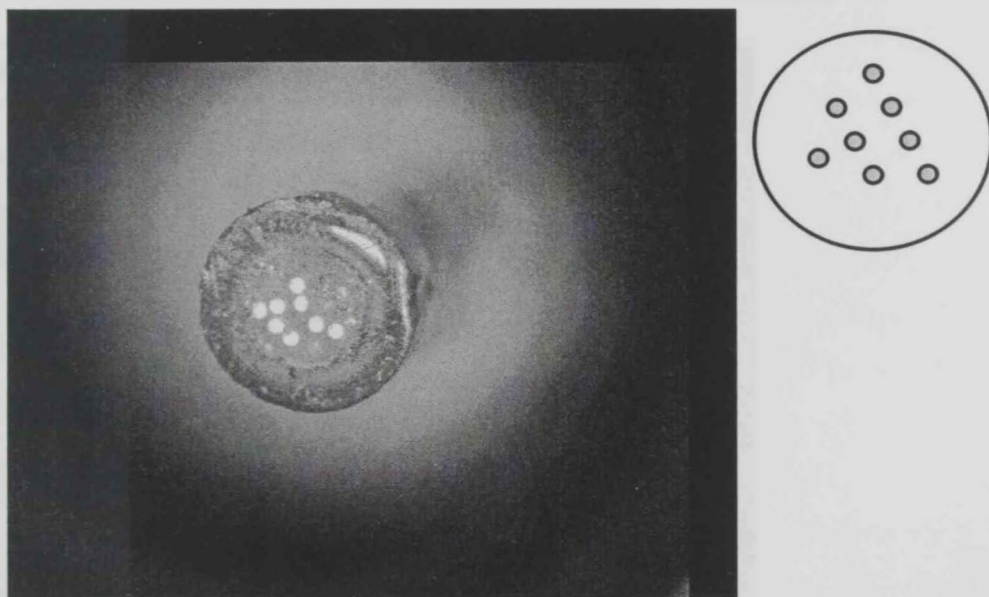


Figure 6.4.C: A micro array of 8-tips made of nickel with tip diameter equals $100\mu\text{m}$. Note that the distance between tips is hard to control by using this array fabrication technique.

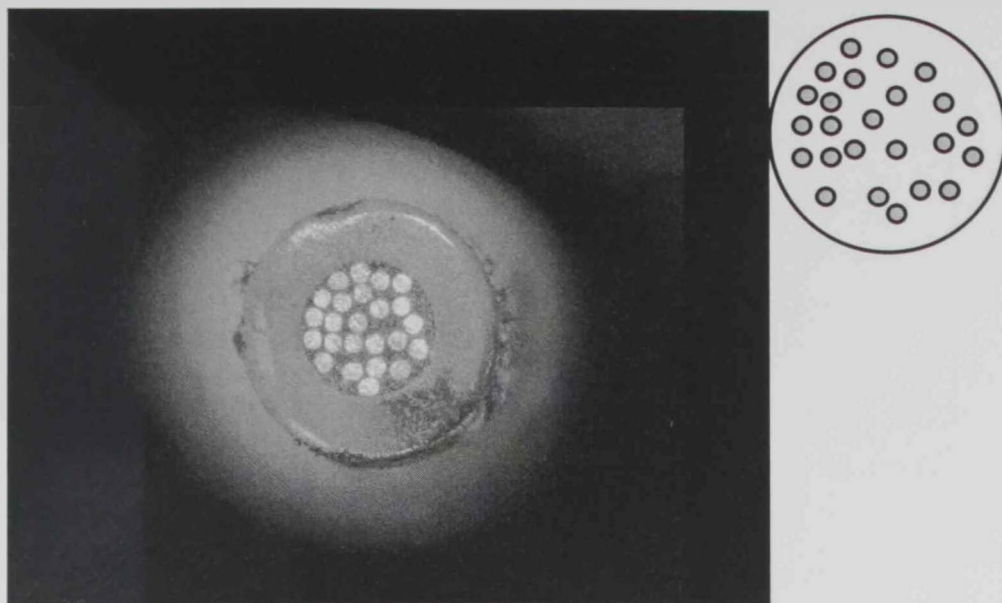


Figure 6.4.D: 24 elements micro array. Note that there is almost no touch between the elements of the array. The tip material used here is nickel with tip diameter of $100\mu\text{m}$. In this array, the amount of glue is less and the bonding of array elements is improved.

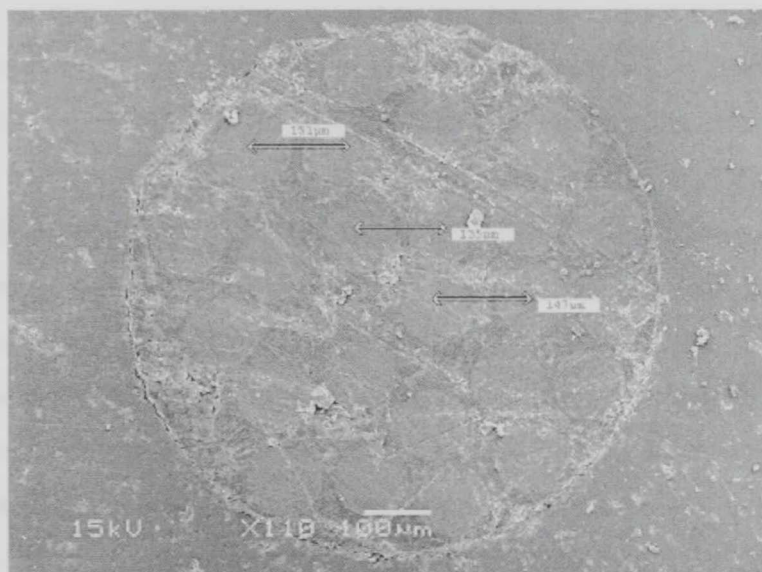


Figure 6.4.E: SEM image of 24 elements micro array made of $100\mu\text{m}$ nickel tips inserted in a glass micropipette. Note that there is almost no touch between the elements of the array.

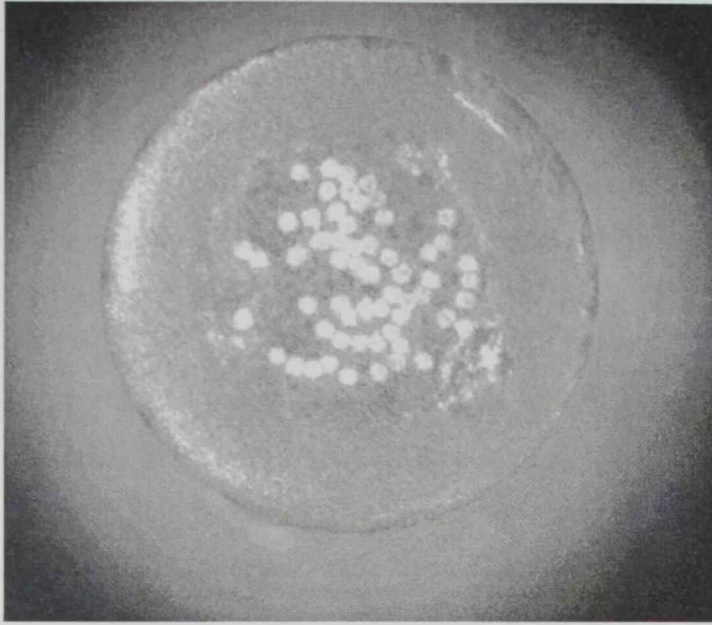


Figure 6.5: 55 elements micro array. The tip material used here is Platinum/Iridium (Pt/Ir 90%-10%) that is commonly used in the LED technology. The tip diameter is $25\mu\text{m}$.

The drawback of this simple technique is that it is hard to control the distance between the tips precisely during the fabrication of the microelectrode array. The other limitation of this fabrication methodology is that it is hard to identify the exact location of a microwire by just looking to the tip especially after cleaning and polishing; this is because that the arrangement of the tips within the microelectrode array is unknown and the tips are almost randomly distributed in the micropipette. However, the advantage of this technique is the low cost and simplicity of fabrication. In this methodology, the microelectrode array was built in this way to ease the investigation of the parallel microfabrication by array microelectrode, as the microelectrodes available in the market were not suitable for this purpose. Advanced design and fabrication of the microelectrode array with controlled geometry have to be done at a later stage.

6.1.2 Substrate Preparation

The substrate used in the LED technique in this work was made of copper material. The substrate was designed with a shaft from one end to ease the removal of the substrate from the cell when the experiment is finished. Prior to the experiment, the copper substrate was cleaned and polished to a mirror like finish. The substrate was then placed

in the electrochemical cell as shown in the LED setup figure 6.1. The substrate must be placed horizontally so that it will be parallel to the tip surface. Any misalignment in the substrate will likely cause a failure in the deposition. It is believed that the success rate of the deposition experiments is highly dependent on the initial placing of the microelectrode on the substrate. The substrate was connected from the other side to a negative potential with respect to the electrode tip potential.

6.1.3 Electrolyte

In this work, the materials of interest to be deposited were copper and nickel. As a result, the electrolytes used in this work were copper sulphate ($\text{CuSO}_4 \cdot 5\text{H}_2\text{O}$) and nickel sulphate ($\text{NiSO}_4 \cdot 6\text{H}_2\text{O}$). Also some rare earth metals electrolytes were investigated. The deposition process is dependent on the concentration of the ions in the electrolyte. The concentrations used in this study were 0.25 and 0.75 moles. Other materials electrolytes can be used as LED is a flexible technique able to fabricate microstructures from various materials.

6.1.4 Picomotors (3-D Actuator)

In this work, the Model 8310 closed-loop picomotorTM actuator (from Newfocus Inc.) was used. This actuator is ideal for applications where closed-loop control and absolute position calibration is required. With an integrated rotary encoder and forward and reverse limit switches, this device offers around 30nm resolution. Two closed-loop picomotors were installed in X and Y directions to navigate the array in the space above the substrate. Open loop actuator was used in the Z direction. The motion of these picomotors was automatically programmed by using LabVIEW with the aid of a special hardware driver and control library supplied by the company. These picomotors are shown in the LED setup figures 6.1 and 6.3 above.

6.1.5 Switching/Gating Circuit

The switching/Gating circuit is shown in figure 6.2. It contains 8 digital switches controlled by LabVIEW code. These gating elements are actually transistors acting as digital switches. The function of this circuit is to switch the array tips on by forwarding

the tip potential coming from the LabVIEW code (assigned by the user). This is done by sending a signal (Digital Low) to the transistor base. If enough deposition is achieved underneath a specific tip, the switching circuit will switch that tip off and remove its potential. The controlling signal for these digital switches comes from the LabVIEW code, which either enable or disable these switches based on its deposition performance. LabVIEW code is continuously sensing the deposition current for each tip involved in the process. The code is designed to send an activation signal (Digital High) to the switch to turn it off and isolate it from the process if it achieved enough deposition while keeping the other switches on. When all the tips achieved enough deposition, all the transistor switches will be disabled and the LabVIEW code will send an activation signal to trigger the picomotors to move in the Z-direction.

6.2 Implementing the controlling algorithm by LabVIEW

A set of controlling codes for the LED deposition process was written in LabVIEW. The first code controls the deposition process of a single microcolumn using single tip microelectrode. The controlling parameters in this code are: the electrode potential, the desired column height, the deposition threshold value (as a reference of the desired deposition level) and the withdrawal increment and speed of the actuator while moving the microelectrode away from the substrate. Single tip microelectrode was used to realize high aspect ratio structures using this developed code. However, a multi tip microelectrode can be also used to realize single column by just activating one tip in the array.

In the second code, the serial deposition algorithm is controlled by a set of extra parameters, which are: the number of microstructures desired and the distance between them. In the serial deposition, the single tip microelectrode was used to deposit more than one structure serially. The motion of the microelectrode is programmed to scan all the locations where the deposition is to be realized on the substrate. When the microelectrode achieved enough deposition on one location, it moves to the other location and so on. Once all the location achieved enough deposition, the tip will be moved in the vertical

direction and the whole process is repeated again. In this algorithm, the microstructures are fabricated serially. Another algorithm of serial deposition was also implemented by a LabVIEW code where the microstructures in the array are fabricated individually (one by one).

LabVIEW code was also used to control the parallel deposition process with the aid of the switching/gating circuit mentioned above. In the parallel deposition code, the user has the freedom to choose which tips in the array to be activated according to the desired geometry. LabVIEW will generate the required microelectrode potential assigned by the user to the tips involved in the process and monitor the deposition current for each of these tips with the aid of the data acquisition unit. Initially, the activated tip will start to build the deposition underneath it, based on the threshold value put by the user in the code, the code will switch a specific tip off when enough deposition is achieved, this done by deactivating a digital switch circuit connected in series to each tip in the array thus disconnecting the applied potential. The code will then wait until all the tips involved in the process achieved enough deposition (i.e. the deposition current measured is above the threshold value) and that all of tips are switched off. The code will then put the electrode potential on again on all the involved tips (to ensure continuity of the deposition) and trigger the Z-axis picomotor to increment a certain distance in the vertical direction. This increment is a user-defined variable in the code. It is very important to optimize this value so that there will be no large gap between the deposition surface and the array tips which may cause a failure in the deposition growth. The user also has the freedom to set the withdrawal speed of the picomotor. Also optimizing the speed of the withdrawal has an effect on enhancing the continuity of the deposition. The whole process will be repeated again until the accumulated increments reach the desired height set by the user in the beginning of the process. The expected outcome of this procedure is a number of columns of equal heights and of a diameter around the tip diameter. However, the same program can be used if variable segments heights are to be realized by switching the code off at a certain stage and isolate a specific tip permanently from the deposition process when the deposition underneath it reached a desired height and continue the process with less number of tips. The written LabVIEW codes controlling

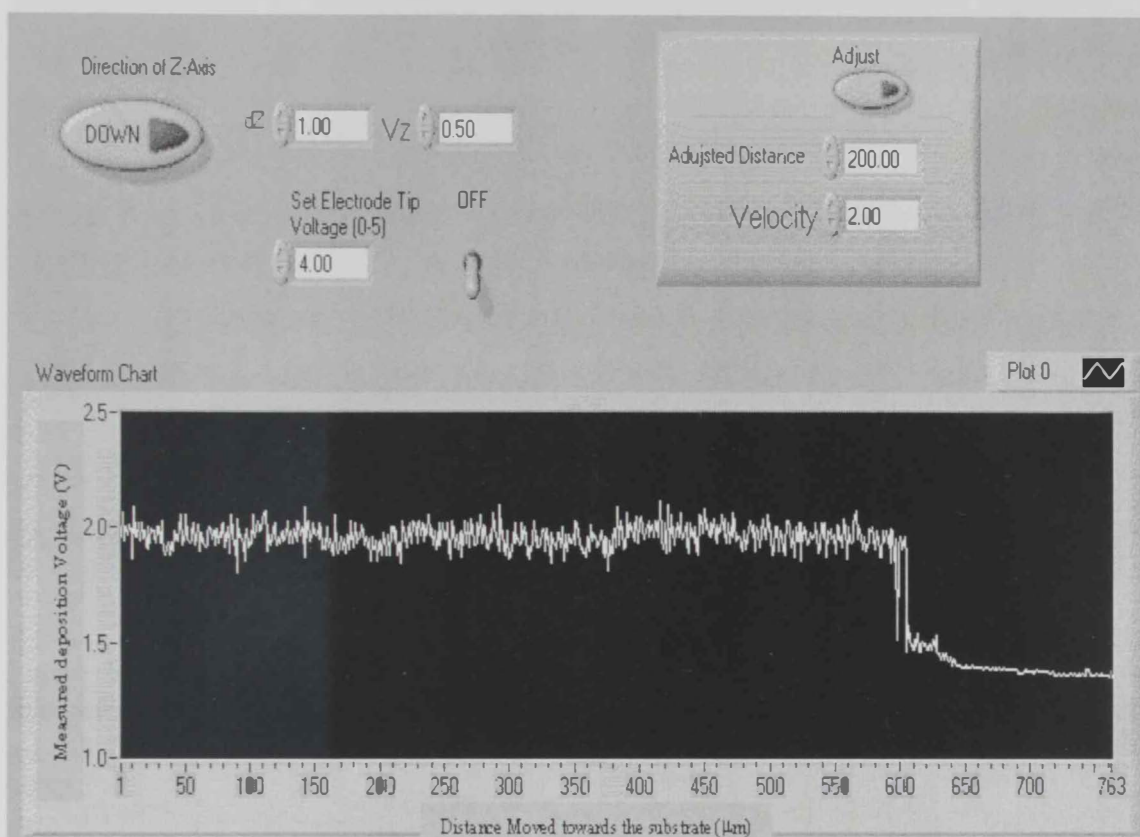
the process are shown in the appendix. Two other LabVIEW codes were written to support the algorithms above. The first code is used to navigate the microelectrode in the space above the substrate. This code was very useful during the experimental work. The second code is used to assist in the initial positioning of the microelectrode at a distance very close to the substrate.

6.3 LED Experiment and Results

In the LED experiment, a substrate was polished and positioned in the electrochemical cell. The microelectrode surface was polished and cleaned. A suitable microscope was used to check that the surfaces of the microelectrode tips were clean. The electrolyte was then put in the cell. With the aid of the microscope, the microelectrode was positioned first at a very close distance to the substrate; often, it was hard to know the distance accurately between the microelectrode and the substrate due to the presence of the relatively large glass insulation. To accurately determine the optimal position of the microelectrode on the substrate, the following algorithm was followed:

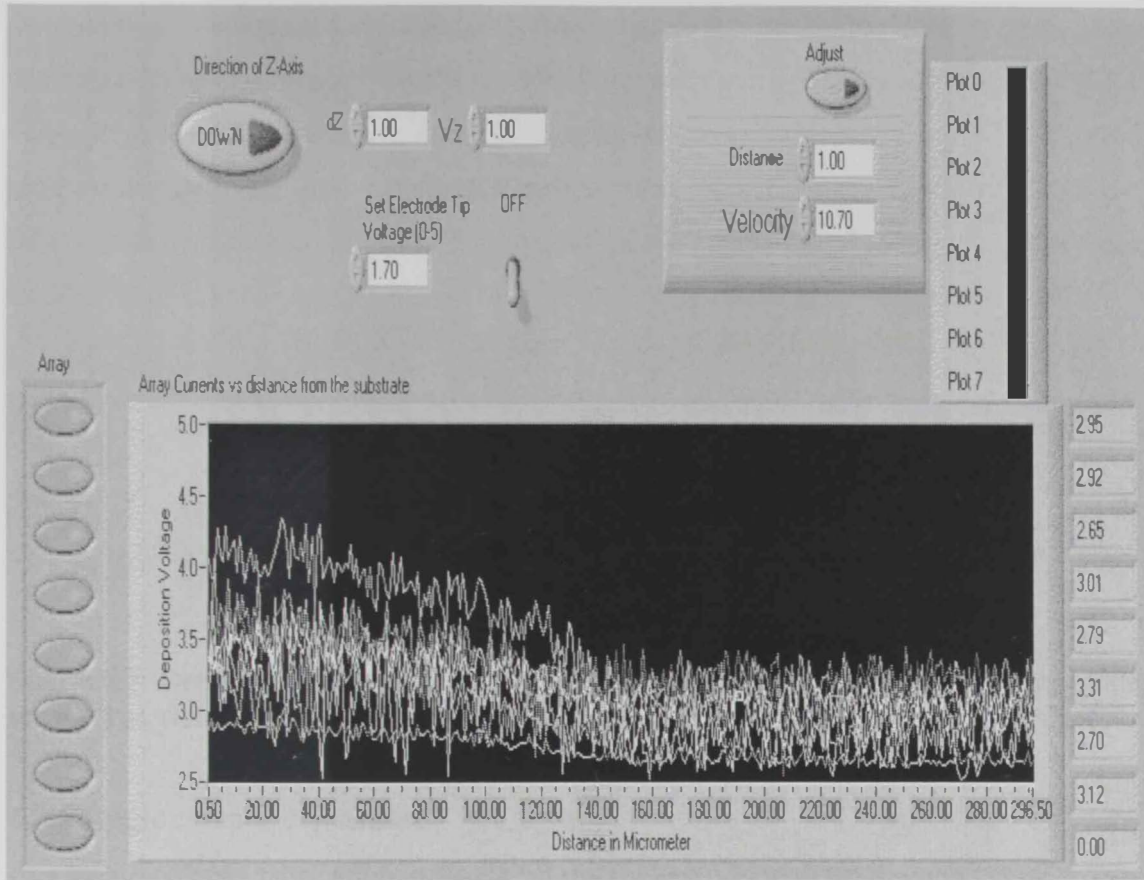
First, the microelectrode was brought away from the substrate and activated by putting the desired voltage on it, and then, a written LabVIEW code was used to move the microelectrode down towards the substrate. During this movement the current of the reaction was measured and recorded as well as the distance moved towards the substrate. The graph of the current against the moved distance was monitored during the process, when the microelectrode start to be close to the substrate, the volume of the electrolyte will be less and thus the measured reaction current will drop, that current will then stabilize to a steady state value. The distance at which this steady state begins was assumed to be zero (i.e. the tip touches the substrate). If an initial gap between the tip and the substrate is required, then it will be easy to reverse the motion of the microelectrode and adjust it to the distance required. It is of great importance to position the microelectrode accurately in a very close distance to the substrate in order to increase the success rate of the deposition. In the figure 6.6, a sample for this calibration is shown for the case of single tip microelectrode and for the case of mutli-tip microelectrode.

When the positioning process is finished, the deposition process will start by running the LabVIEW code. The deposition will start and controlled by the computer according to the desired geometry and the algorithm to be used. A microscope can be used to monitor the reaction in the cell. Air bubbles are used as indication that the deposition process is taking place as shown in figure 6.7.



(a)

Figure 6.6.a: The calibration process for initial positioning of the case of single tip microelectrode. Note that at about 700 μm , the electrode tip touches the substrate.



(b)

Figure 6.6.b: The calibration process for initial positioning for the case of multi tip microelectrode. Note that at about $200\mu\text{m}$, the microelectrode touches the substrate. Note also that the current of the tips are different according to the location of the tip in the array.

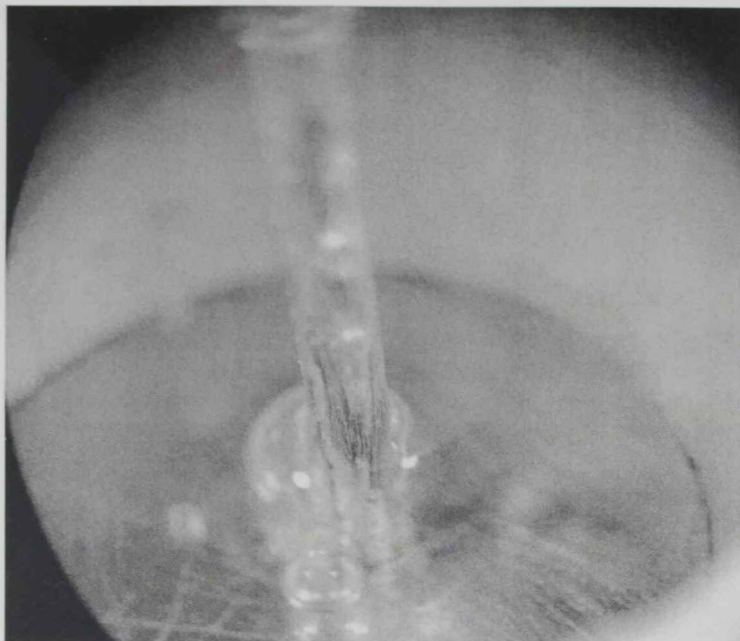


Figure 6.7: Deposition process as it appears by the microscope. Note that the air bubbles are used as visual indicator that the deposition process on the substrate is taking place.

6.3.1 Single column deposition

In a single column fabrication, a single tip microelectrode with tip diameter equals $25\mu\text{m}$ is used. The length is set to be $400\mu\text{m}$. From the figure 6.8, it is clear that LED can produce high aspect ratio structures. Here in this case, the aspect ratio value is about 8. Note that the diameter of the column is about the 25μ and almost equals to the tip diameter. However, this diameter is not constant along the height of the structure; also the porosity of the structure is higher. This is due to the fact that the withdrawal speed and the vertical increment were set to a high value.

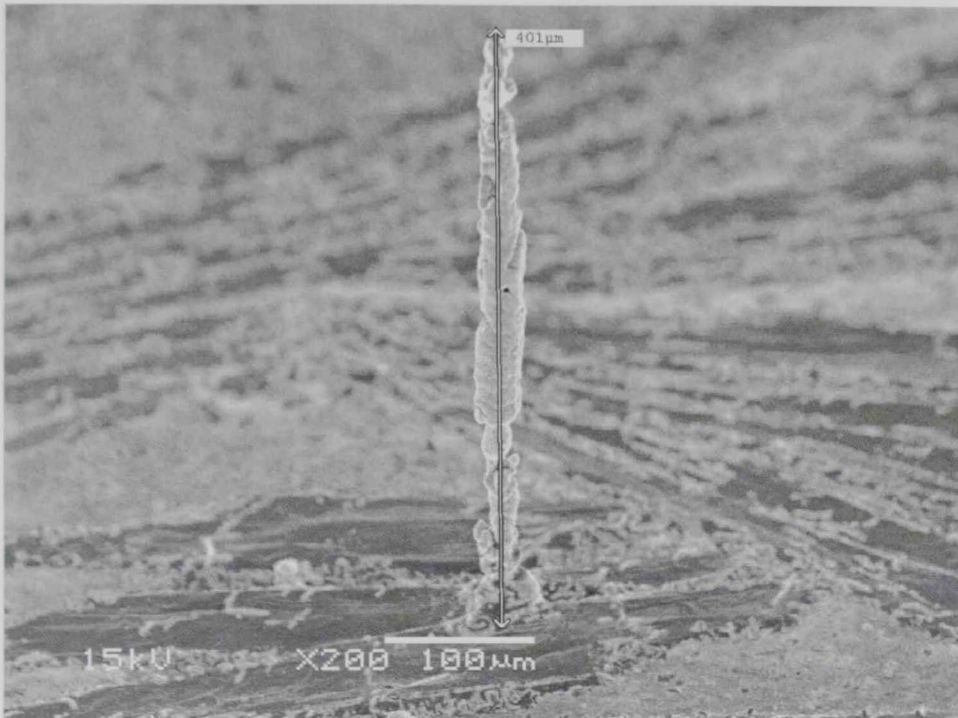


Figure 6.8: SEM image for a single column microstructure made from copper using the single tip microelectrode shown in figure 4.2, the height is programmed to be $400\mu\text{m}$; the thickness of the column equals $25\mu\text{m}$, which is about the same as the tip diameter used. As stated previously, the tip diameter is controlling the resolution of the process. However, there is some degree of porosity in the microstructure. In this case the withdrawal speed and vertical increments were set to be high.

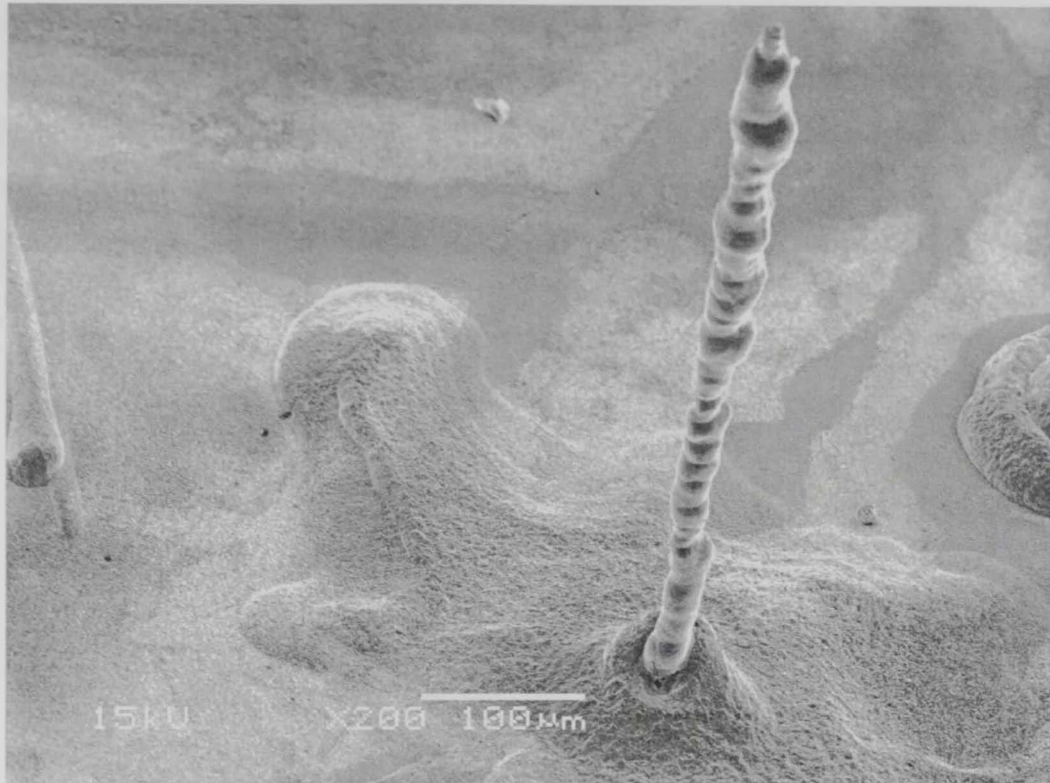


Figure 6.9: SEM image for a single copper column microstructure using the single tip microelectrode shown in figure 4.2, the height is programmed to be $800\mu\text{m}$; the thickness of the column equals $25\mu\text{m}$, which is the same as the tip diameter used. Note the large base due to the fringing effect of the electrical field generated by the tip. The structure is better than the previous one because of the less vertical incremented and withdrawal speed used. however, the diameter of the structure is still not constant along the structure.

In the figure 6.9, the micro column has a height of about $800\mu\text{m}$ and aspect ratio of about 16. The structure is almost straight with a large base compared to the tip diameter as expected. The porosity is improved as the withdrawal speed and the vertical increment was less compared to the previous figure. This structure can be used as antenna in the GHz range. If we consider the fact that the antenna length is proportional to quarter the wavelength, then the frequency corresponding to this length ($800\mu\text{m}$) is about 90 GHz. However, the geometry of the structure is not confined along its height.

The structure shown in figure 6.10 is an improved version of the structures shown in figure 6.8 and 6.9. The structure is confined and symmetrical. The resolution and the porosity are clearly enhanced. If the same structure will be used as a radiating antenna or

transceiver in a micro-electronic system, its center frequency will be of about 180 GHz. The withdrawal speed is less than the previous cases and the vertical increment was kept to $0.5\ \mu\text{m}$, which maintained a better situation for the deposition to grow symmetrically. It is shown that the parameters of the process must be optimized to improve the final microstructure geometry features.

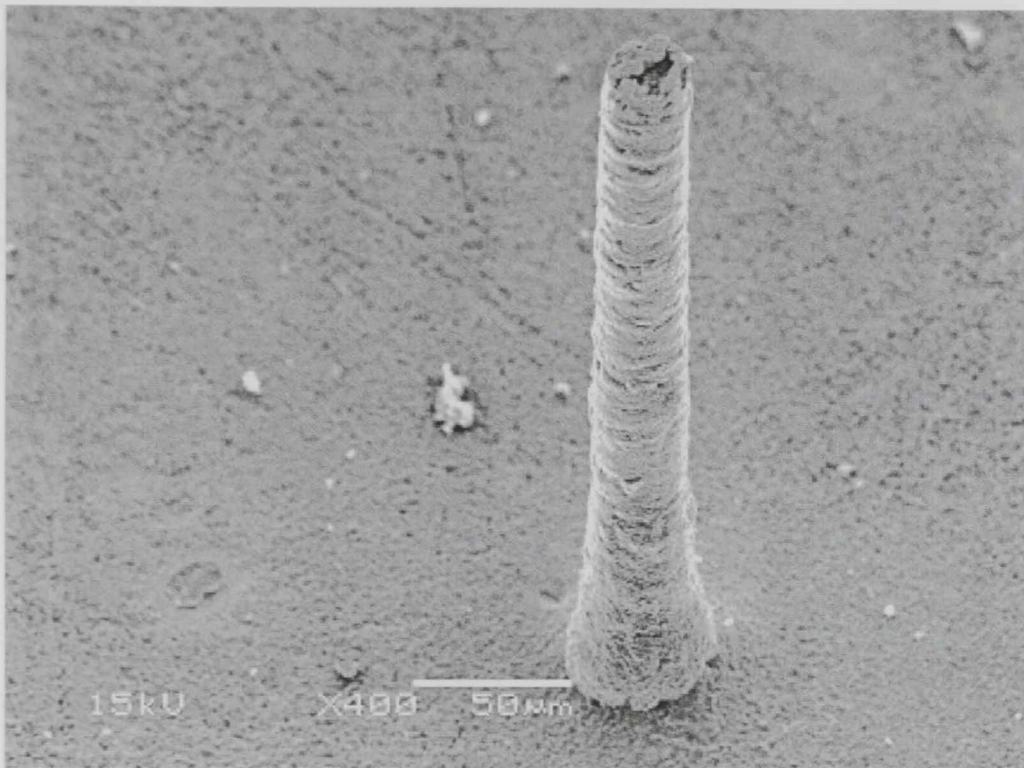


Figure 6.10: SEM image for a single copper column microstructure using the single tip microelectrode shown in figure 4.2. The height is programmed to be $400\ \mu\text{m}$; the thickness of the column equals $25\ \mu\text{m}$, which is the same as the tip diameter used. Note the base due to the fringing effect of the electrical field generated by the tip. The structure is better than previous structures with the porosity and resolution are enhanced. This structure is fabricated by maintaining fixed $0.5\ \mu\text{m}$ gap between the structure and the tip.

6.3.2 Serial deposition using single tip microelectrode

In figure 6.11, serial deposition/discrete algorithm was used to fabricate an array of 4 microstructures. In this algorithm, one structure was fabricated each time, and then the microelectrode was moved to the next location on the substrate by the aid of the picomotors and the written LabVIEW code. Due to the large insulation material surrounding the tip used, the resolution was limited by the insulation geometry (i.e. one

can not fabricate array structures with interspacing less than the microelectrode dimension which is normally much greater than the tip diameter due to the insulation). The maximum the insulation that was achieved was about $300\mu\text{m}$ when using a single tip in the heptode array shown earlier in figure 4.5.b. Also by implementing serial fabrication technique, every microstructure in the array requires a separate experiment by itself and all the microstructures are grown independently. Consequently, these 4 microstructures are not maintained under the same experimental conditions. If any vibrations in the electrode happened, the positioning of the electrode is changed and the distances between the microstructure will also vary. Also, if any microstructure failed to grow under a specific tip, the whole geometry will fail and the desired final array will not be produced. Some other serially fabricated arrays are shown in figures 6.12 and 6.13.

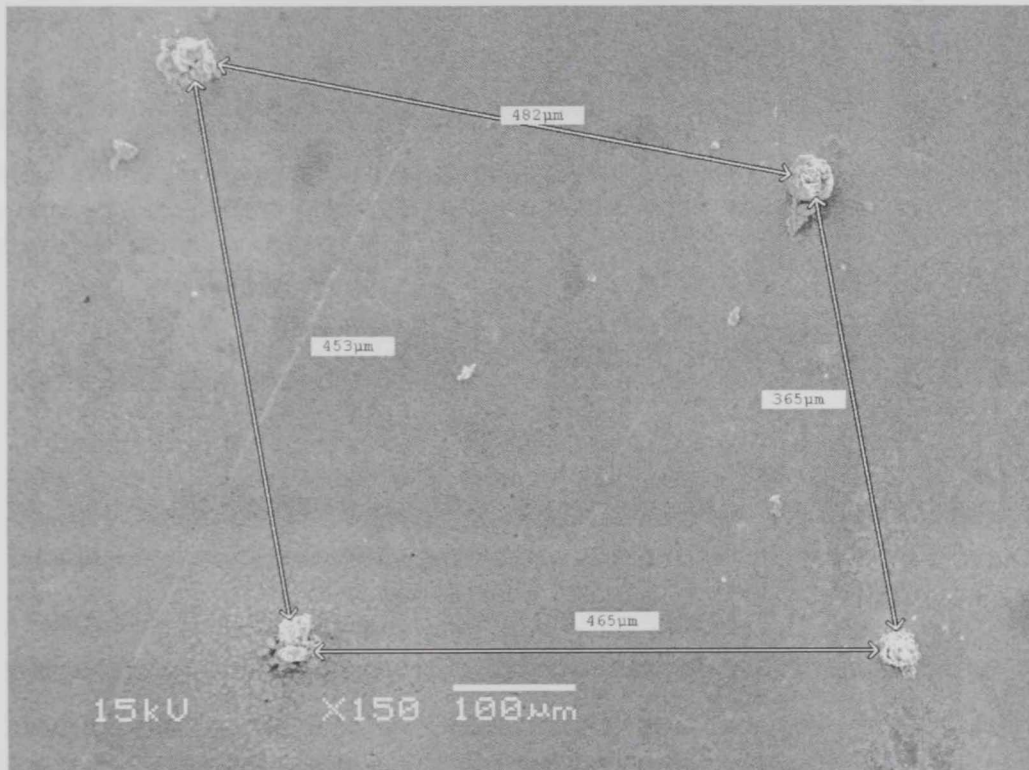


Figure 6.11: SEM image for 4 microstructures fabricated by serial deposition/discrete algorithm. Note the large distance between the microstructures as a result of the limitation imposed by the large insulation of the tip. The programmed height was $100\mu\text{m}$.

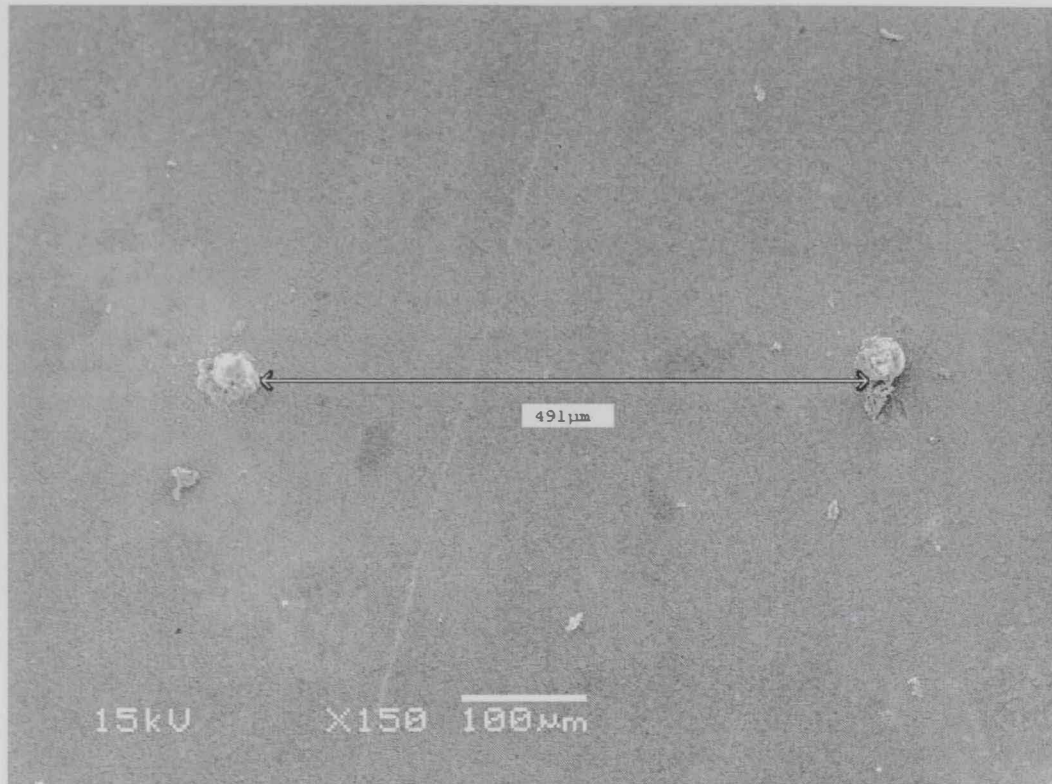


Figure 6.12: SEM image for 2 microstructures fabricated by serial deposition/discrete algorithm. Note that the minimum distance between the two tips is controlled by the electrode insulation geometry.

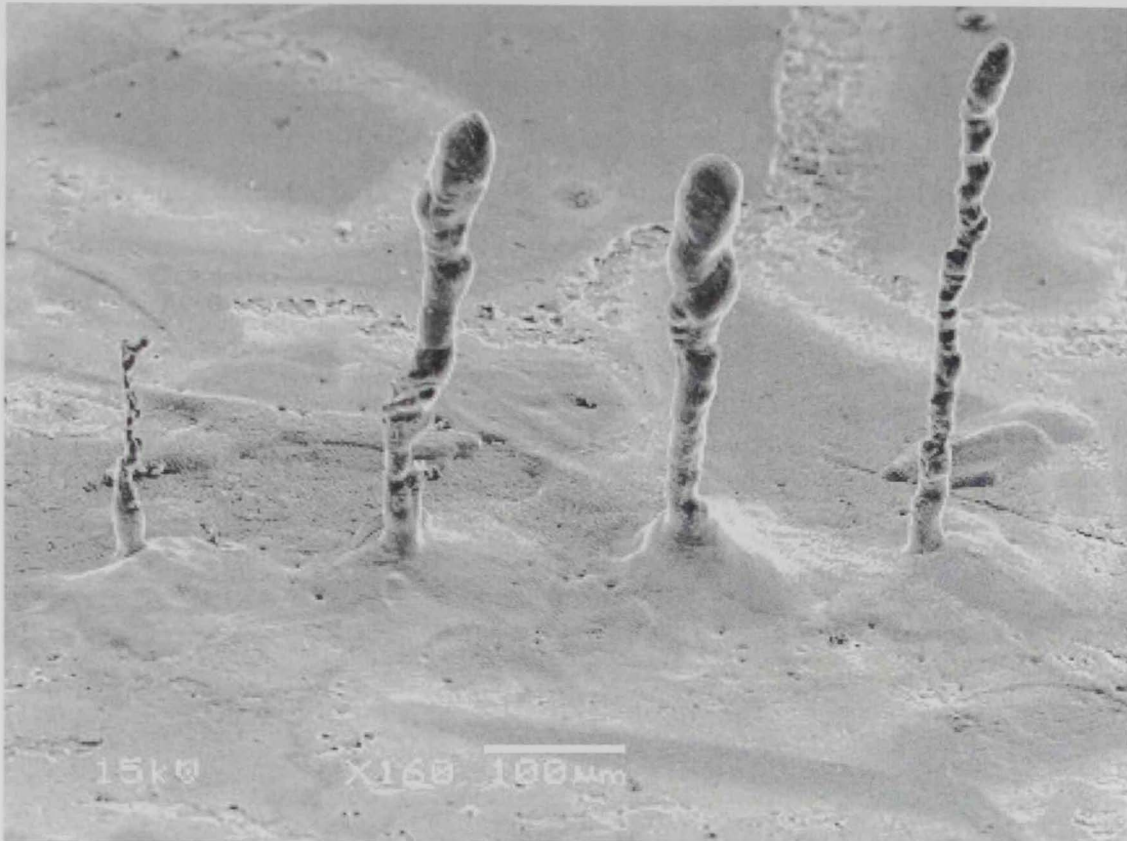


Figure 6.13: SEM image for 4 microstructures fabricated by serial deposition/discrete algorithm. Note the large base for the microstructures. Initially, all the structures were programmed to have $800\mu\text{m}$ heights. The fourth one however broken during the experiment and the deposition stopped which is one of the drawbacks of the serial fabrication technique.

The other discrete type of serial algorithm technique was also investigated. The single tip microelectrode was used to deposit at a certain position on the substrate and once enough deposition took place, the microelectrode was moved horizontally to deposit on another location, after both locations achieved enough deposition the microelectrode was moved away vertically by triggering the picomotor Z-axis. The microelectrode then was returned back again to its original location and start the process over. This process was controlled by LabVIEW code where the user can define the number of array elements required, the horizontal distance between them and the total height desired for all the array elements. As shown in the figures 6.14 and 6.15, although the two structures will approximately grow together, the deposition took a discrete form and the final structure was not homogeneous or confined due to the presence of porosity. Because of the movement of

the electrode forward and backward between the two structures, this may have affected the accuracy of the positioning of the microelectrode. Also this methodology takes long time due the time needed by the microelectrode to move from one location to another. This technique was found to be time consuming and its outcome was not symmetrical and the structures were suffering from high degree of porosity. The accuracy of the picomotors positioning was checked experimentally to investigate the positioning distance error of the microelectrode during this repeated movement.

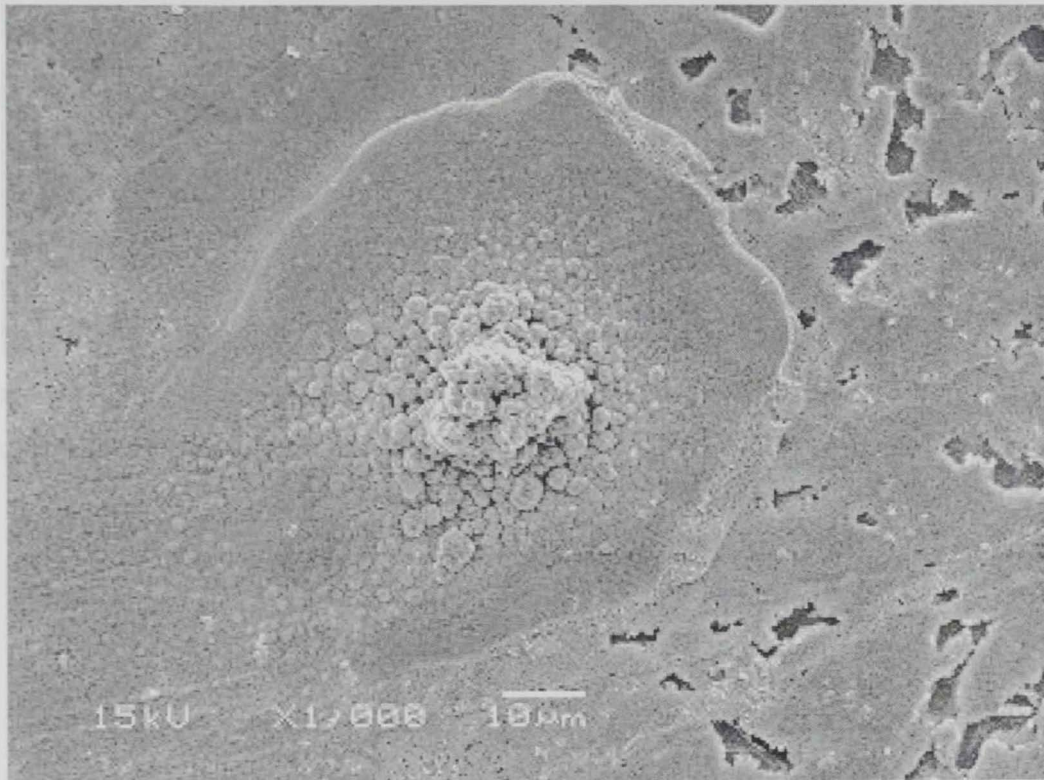


Figure 6.14: SEM image for a microstructure fabricated by serial deposition/continuous algorithm. The outcome of this technique is a highly porous structure with poor symmetry.

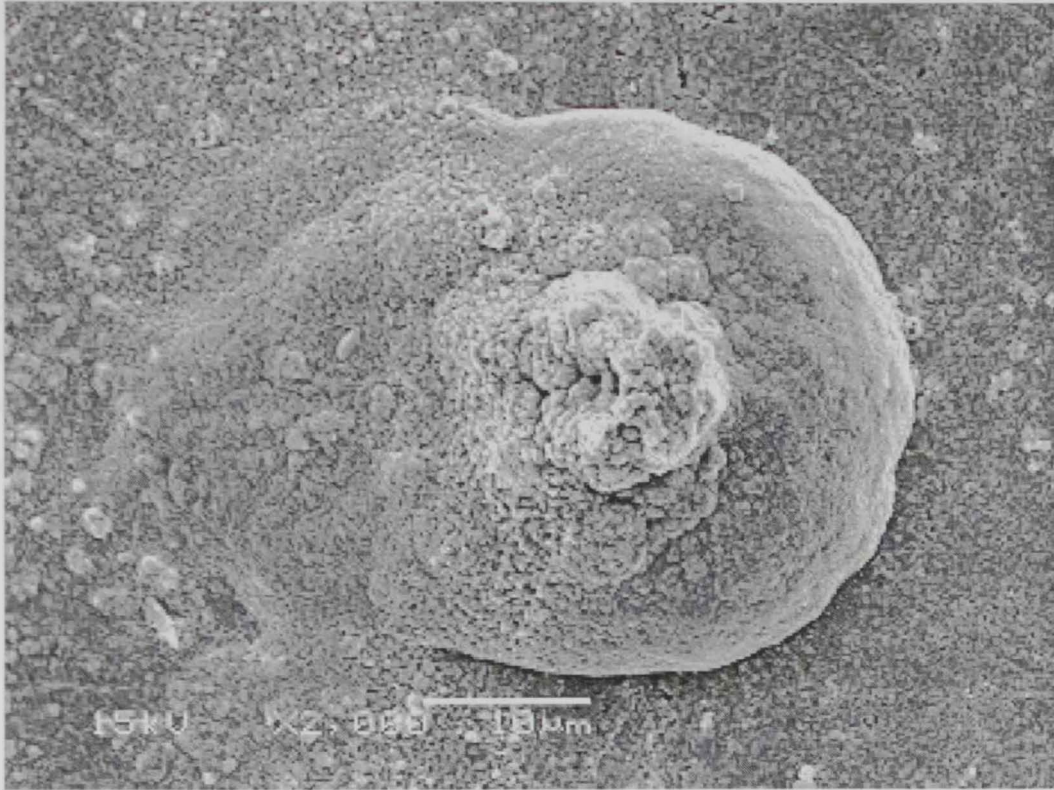


Figure 6.15: SEM image for another failed experiment to fabricate microstructures using serial/continuous deposition algorithm.

6.3.3 Parallel deposition by multi tip microelectrode

Several microelectrode arrays were used to realize parallel deposited structures. Figures 6.16 (A-C) show the outcome of some of these parallel deposition experiments. The heptode shown in figure 4.5 was used to realize these array microstructures. However, due to the very small separation distance between the array tips (around $7\mu\text{m}$), the output structure is not an array of several microstructures, rather it is a single column with diameter larger than the tip diameter. It can be noticed that the small distance between the tips is not sufficient to realize independent microstructures. These results agree with the simulation presented earlier in chapter 5.

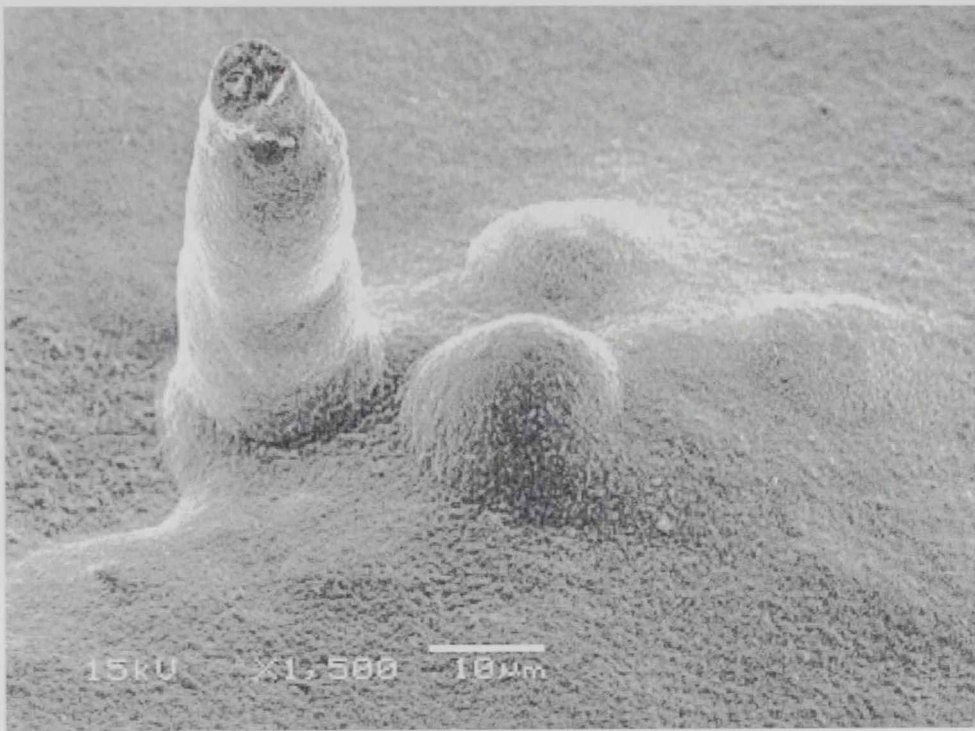


Figure 6.16-A: SEM image for a failed experiment of parallel deposition using the array in figure 4.5. Note at the base, the elements start to have a common large base and then grow up. These elements are so close to each other and approximately the width of each element equals to the tip diameter, which is around $7\mu\text{m}$. Only 4 tips were activated in this experiment.



Figure 6.16-B: SEM image for a parallel deposition by using the heptode shown in figure 4.5. All of the 7 tips were activated. Due to the small distance between the array elements, mutual effect is taking place and the output structure is not 7 independent structures, rather, it is composed of a one-column structure. Note that the width is greater than the tip diameter that is around $7\mu\text{m}$. These results agree with the simulation results presented earlier in chapter 5.



Figure 6.16-C: SEM image for a parallel deposition by using the heptode shown in figure 4.5. In this experiment not all of the heptode tips are active. Only 4 tips were activated. Actually the heptode was broken as the fiber containing the tips was very thin.

In figures 6.17 and 6.18, array microstructures were realized using the self-made microelectrode array. In figure 6.17, two microstructures separated by $100\mu\text{m}$ are fabricated using parallel deposition algorithm. The height is programmed to be $200\mu\text{m}$. The array used to fabricate these two structures shown in the corner of figure 6.18 is a two tips array made from nickel microwires of diameter $100\mu\text{m}$. From the figure of the array used, the separation between the two tips is approximately of around one tip diameter. The result in the SEM image matches this fact as shown in the figure below. The height of both microstructures was programmed to be $200\mu\text{m}$.

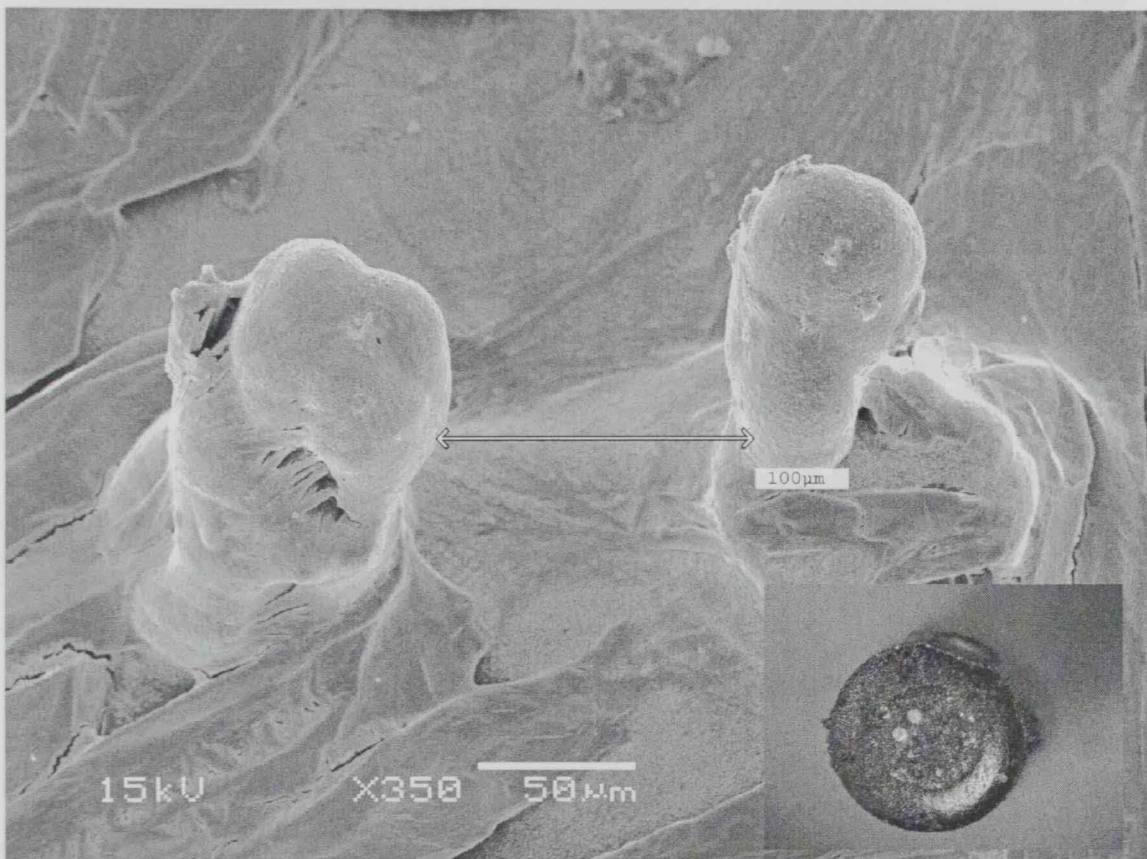


Figure 6.17: SEM image for 2 elements array microstructures made from copper and fabricated by parallel deposition algorithm using a multi tip array with two-nickel elements of $100\mu\text{m}$ diameter shown in the corner. Note the large area at the base. In this experiment these two elements are programmed to have the same height. Note the common large base of the two elements as a result of the mutual coupling of the field generated by the two tips. Note the distance between the two structures is $100\mu\text{m}$, which is the distance between the two tips in the array. Such a resolution is not possible using the serial deposition algorithm which illustrates the benefits of switching to parallel deposition algorithm.

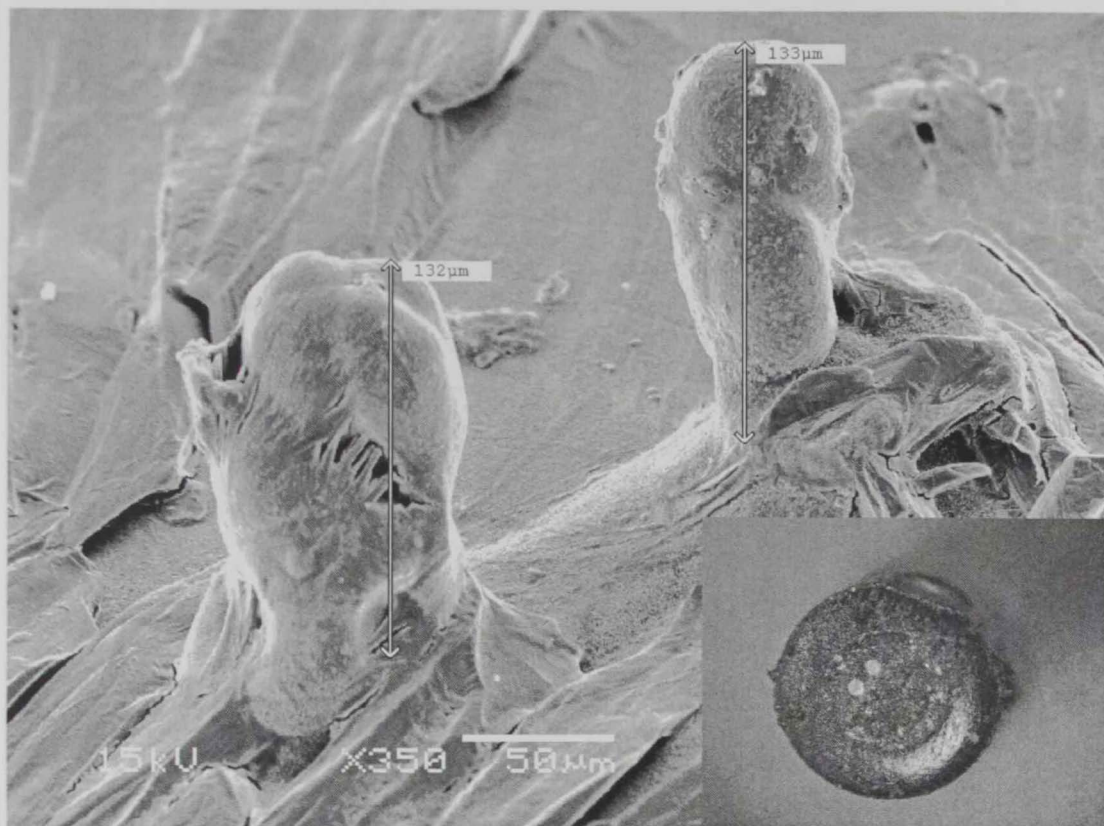


Figure 6.18: SEM image for the same array above with the height of about $130\mu\text{m}$. Note that both structures have almost the same height.

In figure 6.19, a copper microstructure array of 4 elements is fabricated using the microelectrode array shown in the corner of the figure. Initially, 5 elements were activated but later the fifth element was switched off as it took long time to initiate enough deposition. The programmed height was $150\mu\text{m}$. The tips involved in the process can be known by a close look to the geometry of the array. The parameters of the process like the threshold, tip potential and withdrawal speed of the picomotor has to be optimized to obtain confined and symmetrical structures.

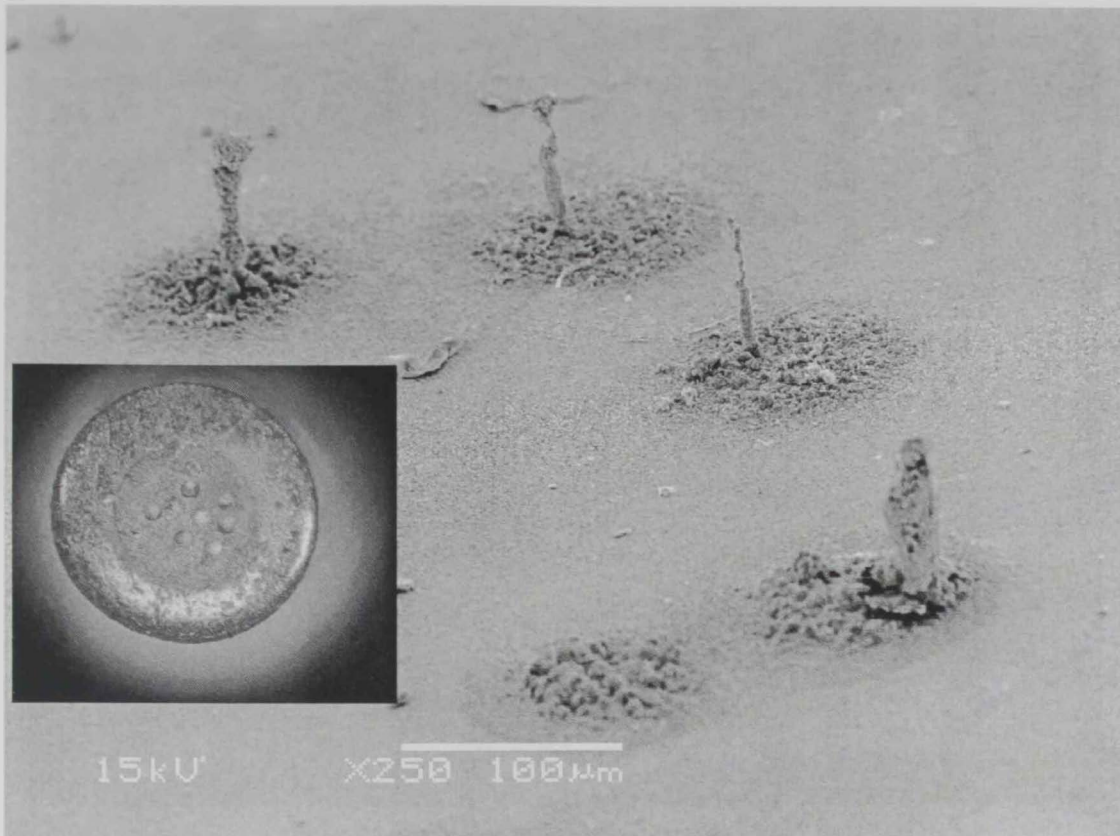


Figure 6.19: SEM image for 4 elements array copper microstructures fabricated by parallel deposition algorithm. These structures are fabricated using the 8 tips array shown in the corner where the tips are made from copper. Note the large area at the base of a diameter compared to the electrode tip diameter. Initially 5 tips were activated but the fifth elements excluded later as it took long time to finish deposition. In this experiment these elements are programmed to have the same height. Note the tips involved in this fabrication can be known by a close look to the tip used.

In figure 6.20, two-nickel microstructures fabricated by parallel deposition are shown using copper tips microelectrode shown in the corner of the figure. Note the knee at the middle of the two structures due to a little vibration of the microelectrode. Although the height is almost the same, the structure is porous due to the effect of the process parameters must be optimized further to enhance the structure geometry.

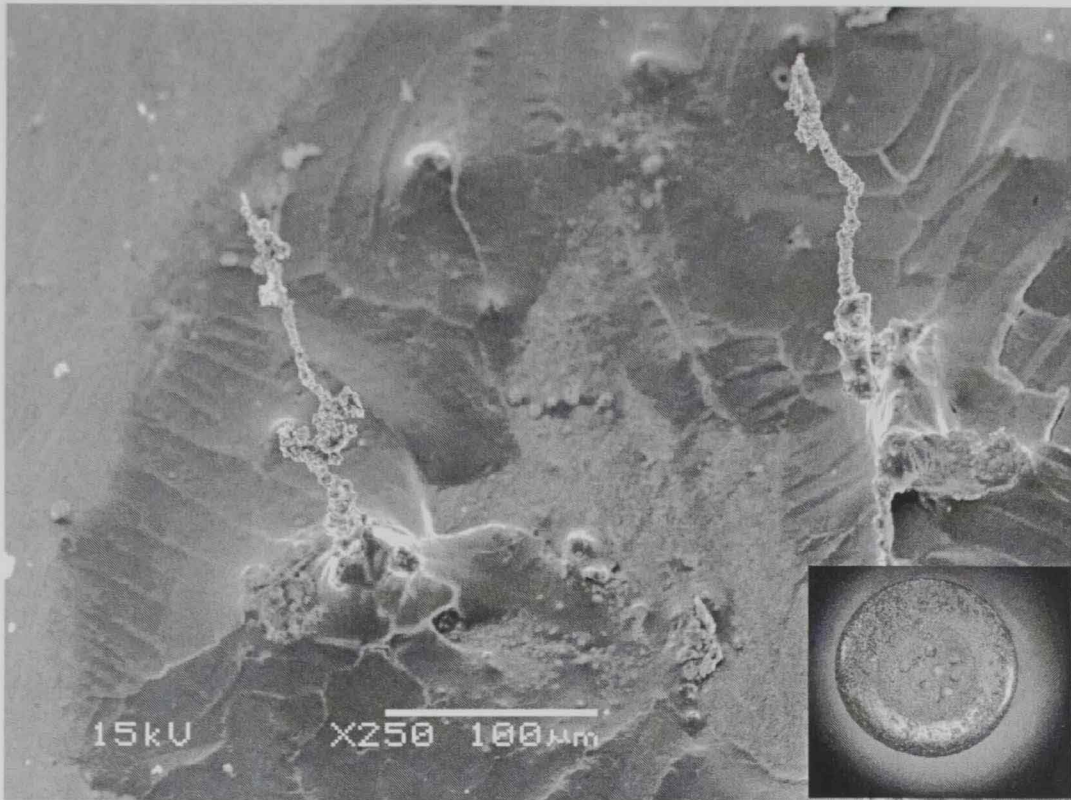


Figure 6.20: SEM image for two-nickel microstructures fabricated by parallel deposition. Although the height is almost the same, the structure is porous. As a result the fabrication process parameters must be optimized to improve the geometry of the deposited structure. The programmed height is $500\mu\text{m}$.

In figure 6.21, 6-nickel microstructures were fabricated by parallel deposition using a microelectrode of 24 nickel tips of diameters equal $100\mu\text{m}$ as shown in the corner. Note the microstructures are almost of the same height and the diameters of the microstructures equal the tip diameter especially in the base section. Still the resolution has to be enhanced further. Note that the structure is almost porous-free.

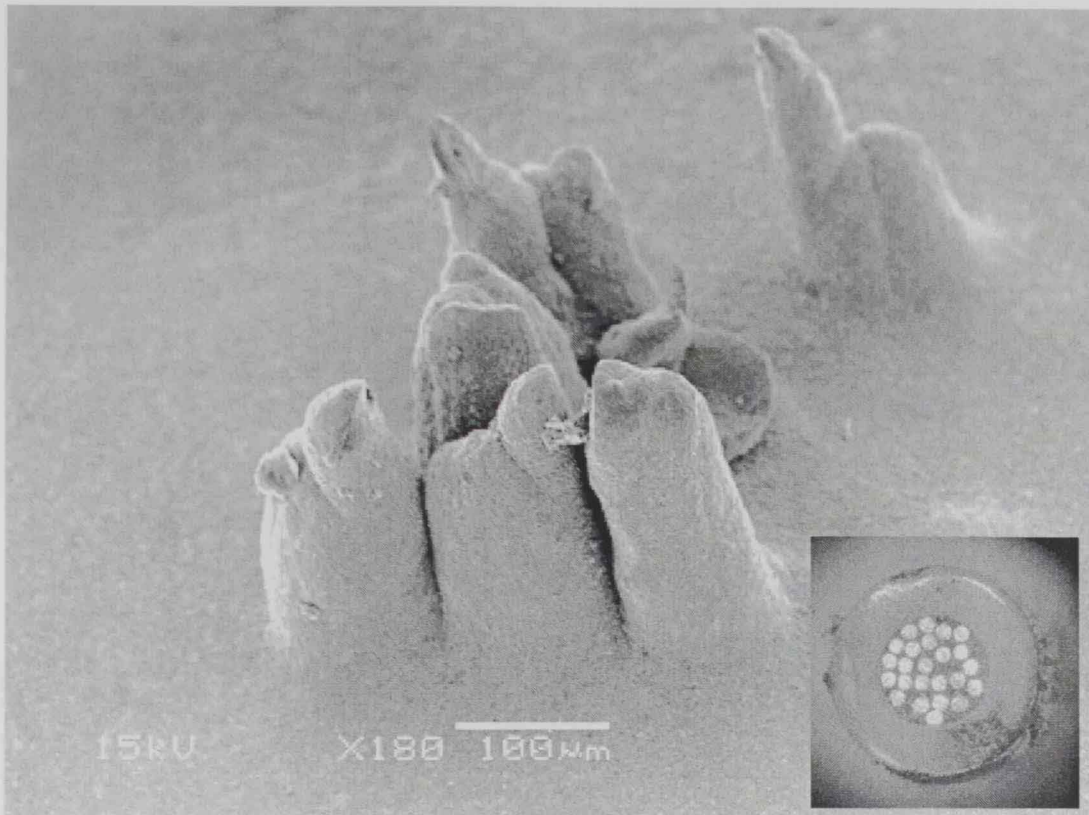


Figure 6.21: SEM image for 6-nickel microstructures fabricated by parallel deposition using a microelectrode of 24 nickel tips of diameters equal $100\mu\text{m}$ as shown in the corner. The programmed height was $400\mu\text{m}$.

In figures 6.22 and 6.23, a 6 elements copper array microstructure was fabricated by parallel deposition using a microelectrode of 55 Pt/Ir (90% 10%) tips of diameters equal $25\mu\text{m}$ as shown in the corner. Note the microstructures are almost of the same height. The diameters of the microstructures equal the tip diameter at the base and then it becomes less. These micro array antennas can be utilized in the upper GHz range applications. The fabrication process parameters must be optimized further to obtain confined and repeatable microstructures.

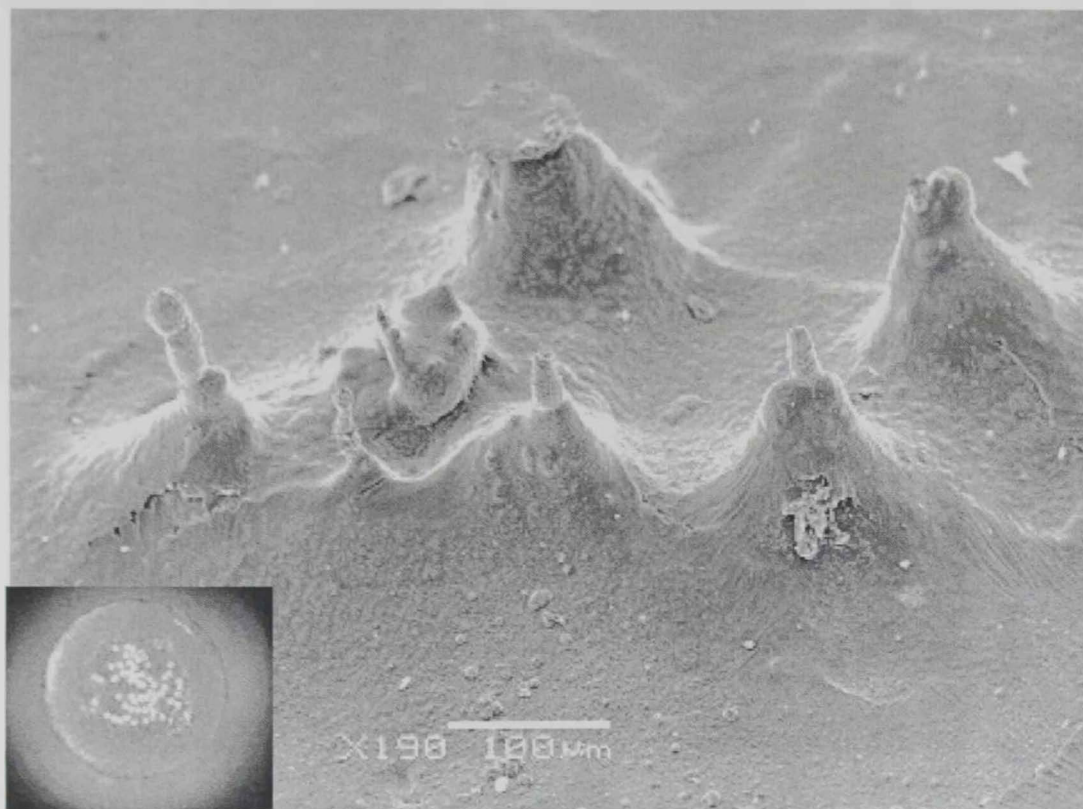


Figure 6.22: SEM image for a 6-elements copper array microstructure was fabricated by parallel deposition using a microelectrode of 55 Pt/Ir (90% 10%) tips of diameters equal $25\mu\text{m}$ as shown in the corner. The programmed height was $300\mu\text{m}$.

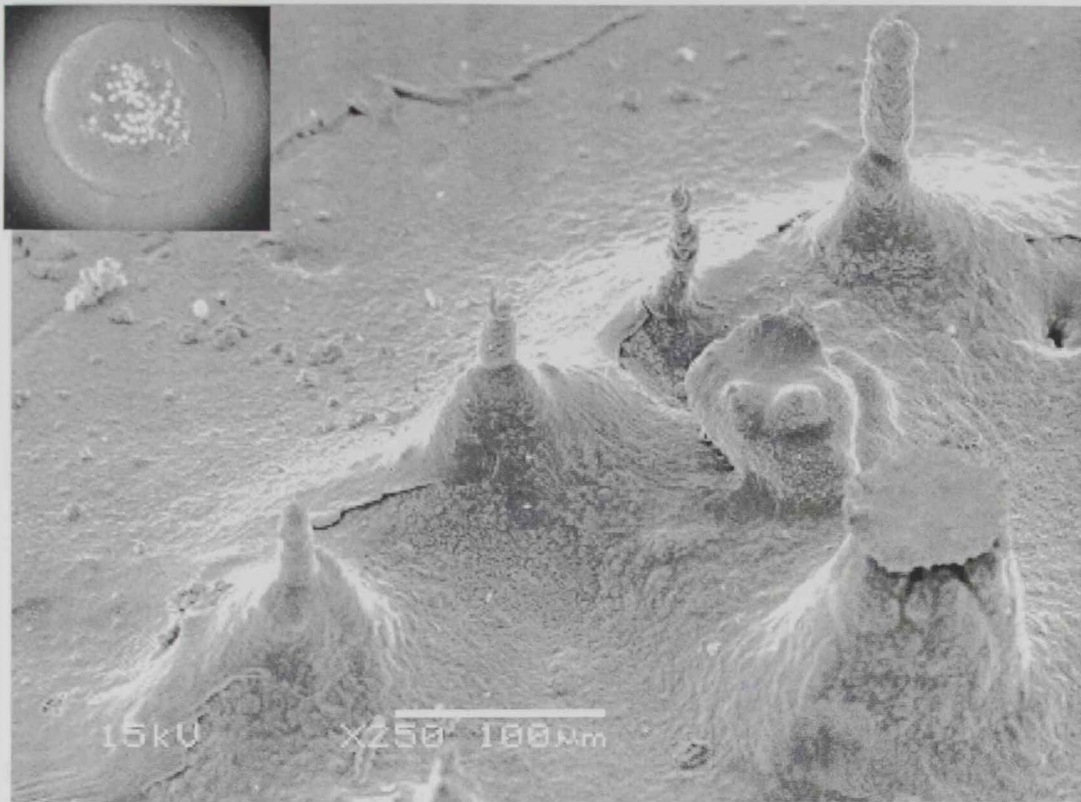


Figure 6.23: The array shown in the previous image from a different angle.

In figure 6.24, 3 elements copper array microstructure is fabricated by parallel deposition using a microelectrode of 55 Pt/Ir (90% 10%) tips of diameters equal $25\mu\text{m}$ as shown in the corner. Note the final microstructures are almost of the same height. However, the diameters and the resolution of the microstructures must be enhanced further.

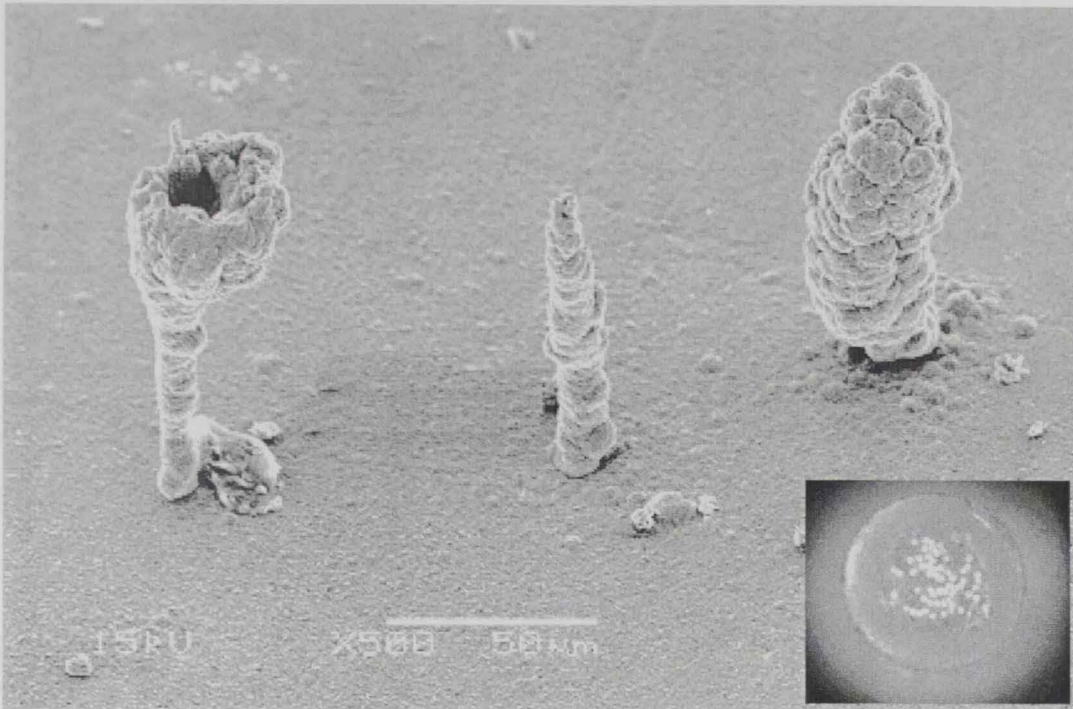


Figure 6.24: SEM image for a 3-elements copper array microstructure fabricated by parallel deposition using a microelectrode of 55 Pt/Ir (90% 10%) tips of diameters equal $25\mu\text{m}$ as shown in the corner. The programmed height is $140\mu\text{m}$.

In figure 6.25, an array of 5-nickel elements is fabricated by parallel deposition using a microelectrode of 55 Pt/Ir (90% 10%) tips of diameters equal $25\mu\text{m}$ as shown in the corner. Note the microstructures are almost of the same height except the one in the middle where the user inactivated the tip after starting the deposition process. However, the diameters, porosity and the resolution of the microstructures must be enhanced further.

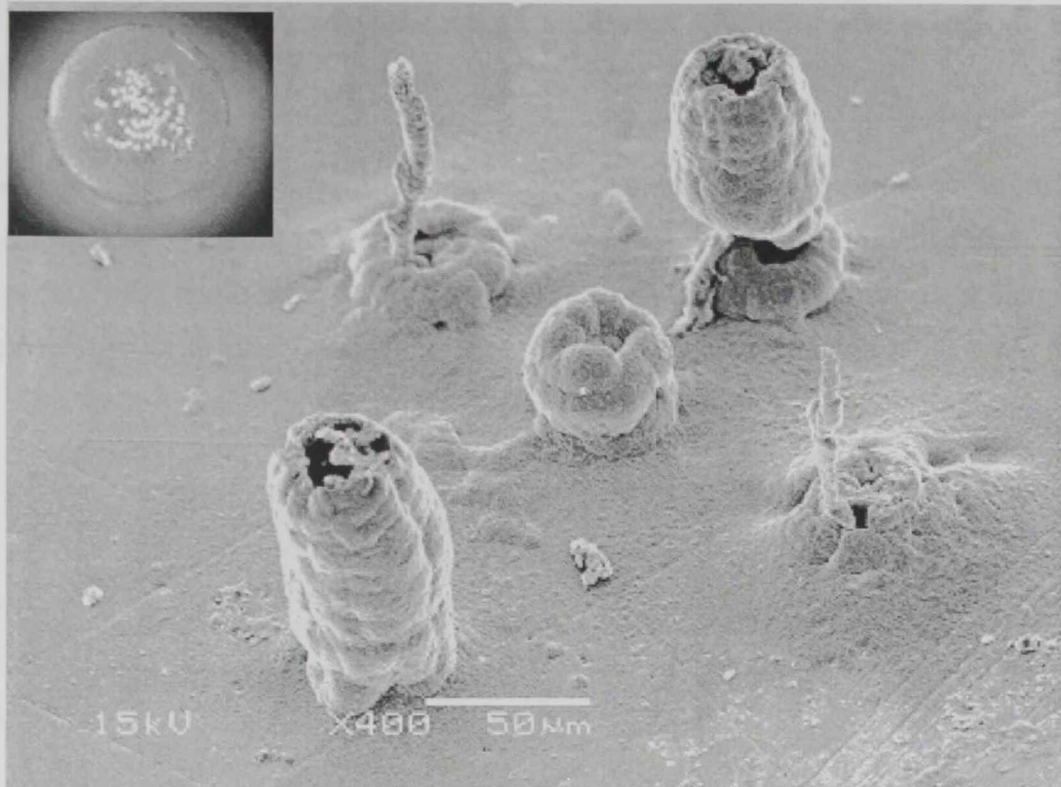


Figure 6.25: SEM image for a 5-elements nickel array microstructure fabricated by parallel deposition using a microelectrode of 55 Pt/Ir (90% 10%) tips of diameters equal $25\mu\text{m}$ as shown in the corner. The programmed height is $180\mu\text{m}$. Note the microstructures are almost of the same height except the one in the middle where the user switched the tip off after starting the deposition process. However, the diameters, porosity and the resolution of the microstructures must be enhanced further.

6.4 Error Analysis

In case of serial deposition algorithm, movement of the microelectrode is required between locations on the substrate. In order to test the actuator error during this process, a LabVIEW code was written where the picomotor was continuously moving between two locations on the substrate back and forth. The two locations separated by $500\mu\text{m}$ were identified on the substrate by the aid of the microscope. 40 movement loops were completed by the picomotor and the error was unnoticeable. The specification of the picomotors indicates error range of about $1\mu\text{m}$ per half-inch movement. Note that this

result indicates that the picomotors alone can be used with acceptable precision in the LED process.

The following tables show the vertical error resulting from the movement of the microelectrode in the Z-axis when enough deposition is achieved. During this work, open loop picomotor was used to move the microelectrode in the vertical direction. Note that the errors are taken roughly using the SEM images of the microstructures.

Table 6.1: Error analysis for single column deposition

Programmed Height (μm)	Average measured height of the microstructure (Using SEM) (μm)	% Error
400	401	0.25
800	700	13
400	350	13

Table 6.2: Error analysis for serial fabrication/discrete algorithm

Programmed Height (μm)	Average measured height of the microstructure (Using SEM) (μm)	% Error
100	100	0
800	500	38

Table 6.3: Error analysis for parallel fabrication algorithm

Programmed Height (μm)	Average measured height of the microstructure (Using SEM) (μm)	% Error
200	133	34
400	350	13
300	200	34
140	100	28
500	300	38

6.5 Effect of tip diameter

According to figures 6.17-6.25, table 6.4 shows the effect of the tip diameter on the fabrication of array microstructures. It can be seen that very small tips will introduce less fringing and less deposition base but higher diameters will introduce significant fringing and large deposition base. Tip diameter that is comparable with the distance between the tips will not improve the resolution of the array as shown in the case of the heptode array. The deposition success of the larger diameter was observed, as the area of the electrode available for oxidization reaction is greater.

Table 6.4: Effect of tip diameter on the fabrication of the array microstructures.

Electrode Tip Diameter (μm)	Fringing Effect	Resolution of the array	Deposition success rate
7	Low	--	-
25	Medium (at the Base)	++	+++
100	Large (at the Base)	+	+

6.6 Effect of tip material

According to the figures 6.16-6.25, table 6.5 shows the effect of the microelectrode tip material on the fabrication of array microstructures. It can be seen that platinum/Iridium tips are more successful in achieving deposition compared with copper and nickel. The structures are more symmetrical using the Pt/Ir microelectrode while the structures are very porous using the copper microelectrode tips. This is due to the fact that the Pt is inert material in the electrolyte and suitable for electrodeposition process, which illustrates why Pt microelectrodes are widely used in the LED research. As indicated earlier, the mechanism of deposition depends on the type of the used tip material, as it will affect the charge transfer that is taking place during the electrochemical reactions.

Table 6.5: Effect of electrode tip material on the fabricated microstructure.

Electrode Tip Material	Reaction Current (Fabrication Rate)	Porosity and Symmetry	Deposition success rate
Pt/Ir (90% 10%)	+	+	+++
Copper	-	-	-
Nickel	+	+	+

6.7 Effect of tips spacing

According to figures 6.16-6.25, table 6.6 shows the effect of the electrode tips spacing on the fabrication of array microstructures. It can be seen that when the tips are so close from each other as in the case of the heptode array, fringing will be significant and individual array microstructures cannot be realized. When increasing the tip spacing to more than twice the tip diameter, microstructures will grow more independently. The deposition rate is also higher in the case of large tips spacing.

Table 6.6: Effect of tip diameter on the fabricated microstructure.

Electrode Tips spacing (μm)	Mutual Coupling	Resolution	Deposition success rate
10	High	--	-
150	High/Medium	+/-	+/-
200	Medium	+	+

6.8 Effect of electrolyte

According to figures 6.17-6.25, table 6.7 shows the effect of the electrolyte type on the fabrication of array microstructures. It turned that copper sulphate and nickel sulphate can produce high aspect ratio structures. However, the nickel proved to be more successful to be deposited although the substrate was copper in the both cases. On the other hand, Rare earth metals deposition was not promising. The deposition was taking a dot or film look and localization does not impose microstructure growth. Further studies must be conducted in this regard.

Table 6.7: Effect of electrolyte material on the fabricated microstructure.

Electrolyte Material	Aspect Ratio	Deposition Current (Fabrication time)
Copper Sulphate	High	+
Nickel Sulphate	High	++
Rare earth metals (cerium carbide, Neodymium chloride and Erbium chloride)	Low "Dots"	-

From the above results, it is clear that LED can produce microstructure arrays from different materials and by different geometries and resolutions. In this work, copper, nickel and rare earth metals like cerium and erbium were investigated. The technique successfully produced array elements that can be implemented in microelectronics industry. However, the fabrication process parameters as the deposition threshold, electrode potential, withdrawal speed, electrolyte concentration and microelectrode array geometry must be optimized in order to obtain a confined structure with high degree of symmetry. The deposition of rare earth metals needs further investigation.

As shown also in the above results, LED can produce microstructures of different geometries. The resolution of the process is determined by the tip diameter. It is shown that LED can produce high aspect ratio microstructures of $100\mu\text{m}$ and $25\mu\text{m}$ diameters. If an application requires a mixture of different diameters, an array of variable tip diameter can solve this problem.

Compared with serial deposition, parallel deposition can realize array structure with less separation between the individual array elements. Also, by using parallel deposition algorithm, no time is wasted in moving the microelectrode between the desired locations. As a result, all structures will be under the same experimental conditions. Also the user has more freedom to choose the desired geometry by just switching some tips in the array off. Parallel deposition when implemented with optimized process parameters will lead to an increase in the overall production rate of microstructures. The disadvantage of parallel deposition is that some tips (especially on the edges of the microelectrode) may consume the electrolyte and block the electrolyte from diffusing to the other tips especially the inner tips in the array. This may cause some porosity in the inner elements

in the array. This may be solved by increasing the electrolyte concentration and continuously steering the electrolyte during the deposition process in order to allow the electrolyte to enter to the inner tips. However, further investigation must be performed to enhance the deposition profile of the technique.

Chapter 7:

Conclusion and Future Work

7.1 Conclusion

In this work, a new capability to localized electrochemical deposition (LED) technique was added. This capability is the ability of LED to fabricate array microstructures. In this work, different LED fabrication methodologies to fabricate array microstructures using serial and parallel deposition algorithms were investigated which in turn can be used as array micro antennas. In serial deposition technique, single tip microelectrode is used to create array microstructures serially (element by element). This process is time consuming, resolution-limited and suffers from the repeatability drawback. On the other hand, the methodology of parallel microfabrication using multi-tip microelectrode was investigated for the first time. This algorithm is based on using tip array microelectrode instead of single tip microelectrode to fabricate microstructures. Parallel deposition is based on gating the array tips on and off based on their individual deposition performance. All of the individual tips are monitored and if any tip produced sufficient deposition, it will be turned off to allow other tips to reach to this level. Once all the tips achieve enough and equal deposition level, the microelectrode will be pulled away from the substrate and the whole process is repeated until the total height of the elements is achieved. In this way all of the microstructures will grow simultaneously. The process is controlled via a controlling code written in LabVIEW, which is used to monitor the deposition current and compare it with the threshold value and trigger an actuator to move the array away from the substrate in the 3D space until the total desired height is achieved.

Parallel deposition algorithm can produce an array of microstructures of the same height. In this way, the outcome of this process will be useful as an array antenna used in gigahertz and terahertz frequency range. If the parallel deposition technique is programmed to yield variable segments heights then a discrete surfaces can be realized. These discrete surfaces maybe integrated as dish antenna or as structuring elements for MEMS applications. The geometry of the microelectrode array used for parallel deposition is very critical in the whole process and must be carefully designed in order to obtain confined structures. In this work, the fabrication process is totally automated and

the user interaction is kept to minimum. This will enhance the LED fabrication process towards full and complete standardization.

A comparison between the serial deposition and the parallel deposition algorithm is shown in the table 7.1. Parallel deposition can produce array microstructures faster than serial deposition. However, the porosity and confinement of the microstructure is suffering from poor feeding of the electrolytes to the inner tips in the array where the diffusion is interrupted by either the generated air bubbles or by the other deposited structures acting as a barrier for the electrolyte to diffuse freely to the inner tips in the array. Electrolytes concentration, electrode material, tip potential and other process materials must be optimized before serial deposition is replaced by the parallel deposition algorithm.

Table 7.1: Comparison between parallel and serial fabrication algorithms

	<i>Serial Deposition</i>	<i>Parallel Deposition</i>
<i>Microelectrode</i>	Single tip	Multi tip
<i>Fabrication rate</i>	-	+
<i>Porosity and confinement</i>	+	-
<i>Resolution</i>	-	+

During this work, copper and nickel microstructures were successfully deposited. Results show that there is a minimum tips separation distance below which array microstructure cannot be achieved. Investigation was also carried for the case of rare earth metals but further work must be done. Also, different tip geometries were investigated. LED proved that it can produce microstructures with various resolutions. The tip diameter controls the resolution of the process while the distances between the tips determine the distances between the microstructures within the array. During this work, microstructures with diameters of about the 100 μm and 25 μm were realized. The LED process proved that it can be a promising technique to fabricate arbitrary 3D microstructures, however further investigation and development must be performed in order to come up with a standard technology suitable for commercial use.

7.2 Future Work

In this work, a self-made multi-tip microelectrode was implemented. However, there was less control on the distance between the tips. For future work, I recommend the following:

- Design and machine a multi-tip microelectrode array with defined geometry and defined tips separation. The optimum design for this microelectrode array has a large number of tips (say 50×50). The user has the ability to program the microelectrode to work as 2×2 or 8×8 or even any structure by choosing which elements are to be activated. This will heavily reduce the cost for the LECD technique and will open the door for the micromachining of arbitrary structures.
- Design and implement a controller code that is able to control the fabrication process while enhancing the resolution, accuracy and repeatability of the structure.
- Implant the switching circuit on a microcontroller (for example simple PIC microcontroller) and integrate it with the microelectrode array.
- Implement further experiments to understand the parallel deposition technique and try to optimize its parameters to get various structures of 3D features.
- Create a mathematical model for the parallel deposition technique as the model available in literature is concerned with single tip microelectrode.

References

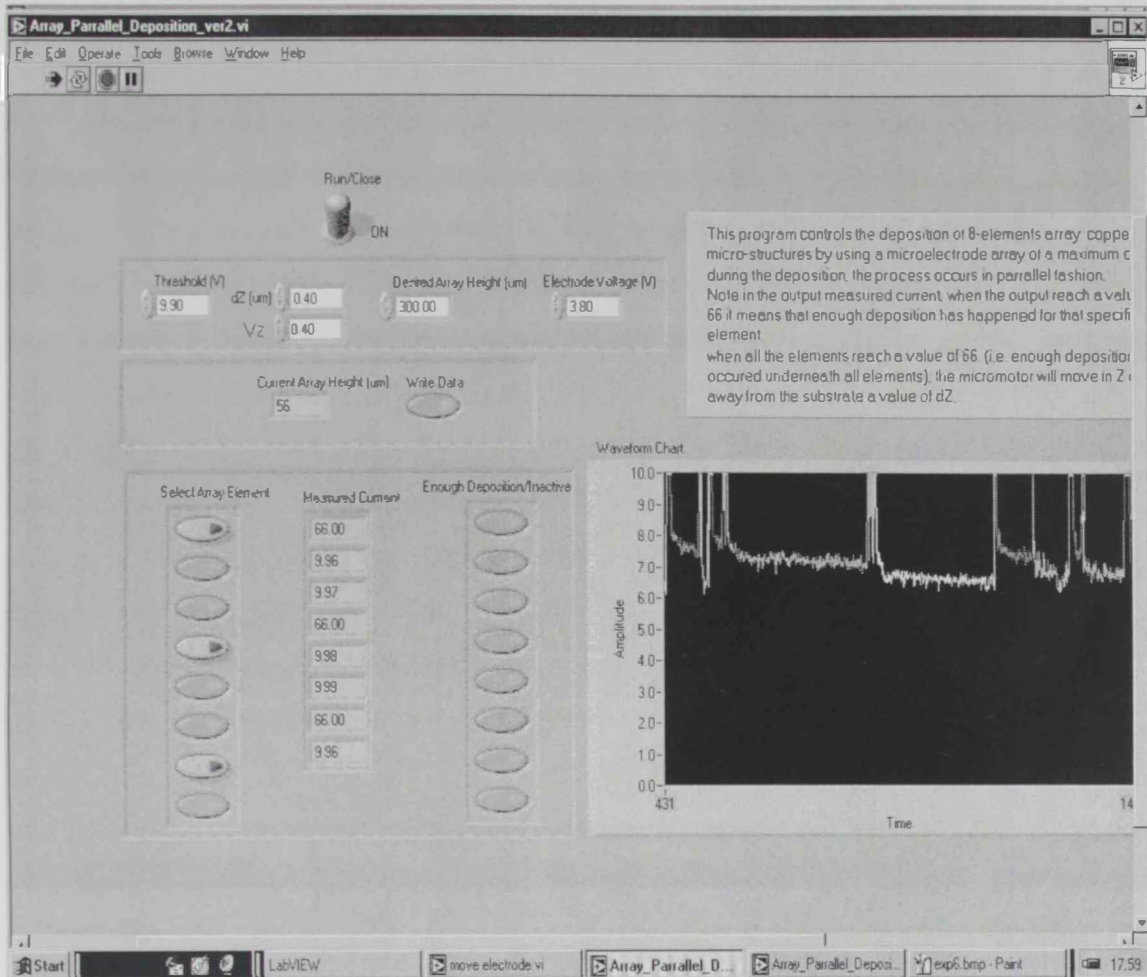
- [1] John D. Madden and Ian W. Hunter, Three-dimensional microfabrication by localized electrochemical deposition. *Journal of Microelectromechanical Systems*, 5, 24-32, 1996.
- [2] Salil S. Desai, Multiphysics analysis and optimization of 3 dimensional printing technology using nano fluidic suspensions, PhD dissertation.
- [3] Michael Hatzakis, Materials and processes for microstructure fabrication, *IBM Journal of Res. Develop.* Vol. 32, 4, 1998.
- [4] Greger Thornell and Stefan Johansson, Microprocessing at the fingertips, *Journal of Micromechanics and Microengineering*, 8, 251-262, 1998.
- [5] Wolfenbuffel R.F. and Van Mullem C.J., Microtechnology and Microsystems in measurement applications, *IEEE Trans. Instrum. Meas.*, 50, 1469, 2001.
- [6] Dean R., Nordine P. and Christodoulou C., 3-D helical THz antennas, *Microw. Opt. Tehnol. Lett.* 24, 106-11, 2000.
- [7] Gebhard M. and Benecke W., Microtechnologies for microscaled robots and components, *Proc. INRIA/IEEE Symp. On Emerging Technologies and Factory Automation*, 9, 1995.
- [8] Souteyrand E., Cloarec J.P., Martin J.R., Cabrera M., Bras M., Chauvet J.P., Dugas V., and Bessueille F., Use of microtechnology for DNA chips implementation, *Appl. Surface Sci.*, 164, 246, 2000.
- [9] Van Der Schoot B., Biollat M., and De Rooij N., Micro-instruments for life science research, *IEEE Trans. Instrum. Meas.*, 50, 1538, 2001.
- [10] Ikuta K., Hirowatari K. and Ogata T., Dimensional micro integrated fluid systems (MIFS) fabricated by stereo lithography, *Proc. IEEE Micro Mechanical Systems*, pp 1-6, 1994.
- [11] Robertson J. K. and Wise K. D., A nested electrostatically-actuated microvalve for an integrated microflow controller, *Proc. IEEE Micro Mechanical Systems*, pp 7-11, 1994.

- [12] Rebeiz G. M., Katehi L. P. B., Ali-Ahmad W. Y., Eleftheriades G. V. and Ling C. C., Integrated horn antennas for millimetre-wave application, *IEEE Antennas Propag. Mag.* 34, 7-16, 1992.
- [13] Herrick K.J., Yook J.G., and Katehi L.P.B., Microtechnology in the Development of Three-Dimensional Circuits, *IEEE Trans. Microwave Theory and Techniques*, 46, 1832, 1998.
- [14] Walker J.A., The future of MEMS in telecommunications networks, *Journal of Micromech. Microeng.*, 10, R1, 2000.
- [15] El-Giar E. M. and Thomson D. J., Localized electrochemical plating of interconnects for microelectronics, *WESCANEX 97: Proc. IEEE Conf. on Communications, Power and Computing*, pp 327-32, 1997.
- [16] Web reference: <http://www.wave-report.com/tutorials/MEMS.htm>
- [17] Vinay Kadekar, Weiya Fang, Frank Liou, Deposition Technologies For Microfabrication: A Review, *Journal of Manufacturing Science and Engineering*, November, Vol. 126/787, 2004.
- [18] Web reference: <http://www.darpa.mil/MTO/MEMS/>
- [19] Datta M., Applications of electrochemical microfabrication: An introduction, *IBM Journal of Res. Develop.* Vol. 42, 5, 1998.
- [20] Web reference: <http://www.ece.gatech.edu/research/labs/vc/theory/photolith.html>
- [21] Datta M., Microfabrication by electrochemical metal removal. *IBM Journal of Res. Develop.* Vol. 42, 5, 1998.
- [22] Becker E. W. et al, Fabrication of microstructures with high aspect ratios and great structural heights by synchrotron radiation lithography, galvanofarming, and plastic moulding (LIGA process), *Microelectron. Eng.* 4 35-36, 1986.
- [23] Henry Helvajian, *Microengineering Aerospace Systems*, Chapter 1, Introduction to MEMS.
- [24] Said R.A., Localized Electro-Deposition (LED): The march toward process development, *Institute of physics, Nanotechnology* 15, 649-659, 2004.
- [25] Timothy A., John P., Microelectrode Array Fabrication by Electrical Discharge Machining, *IEEE transactions on biomedical engineering*, Vol. 15, 6, 2004.

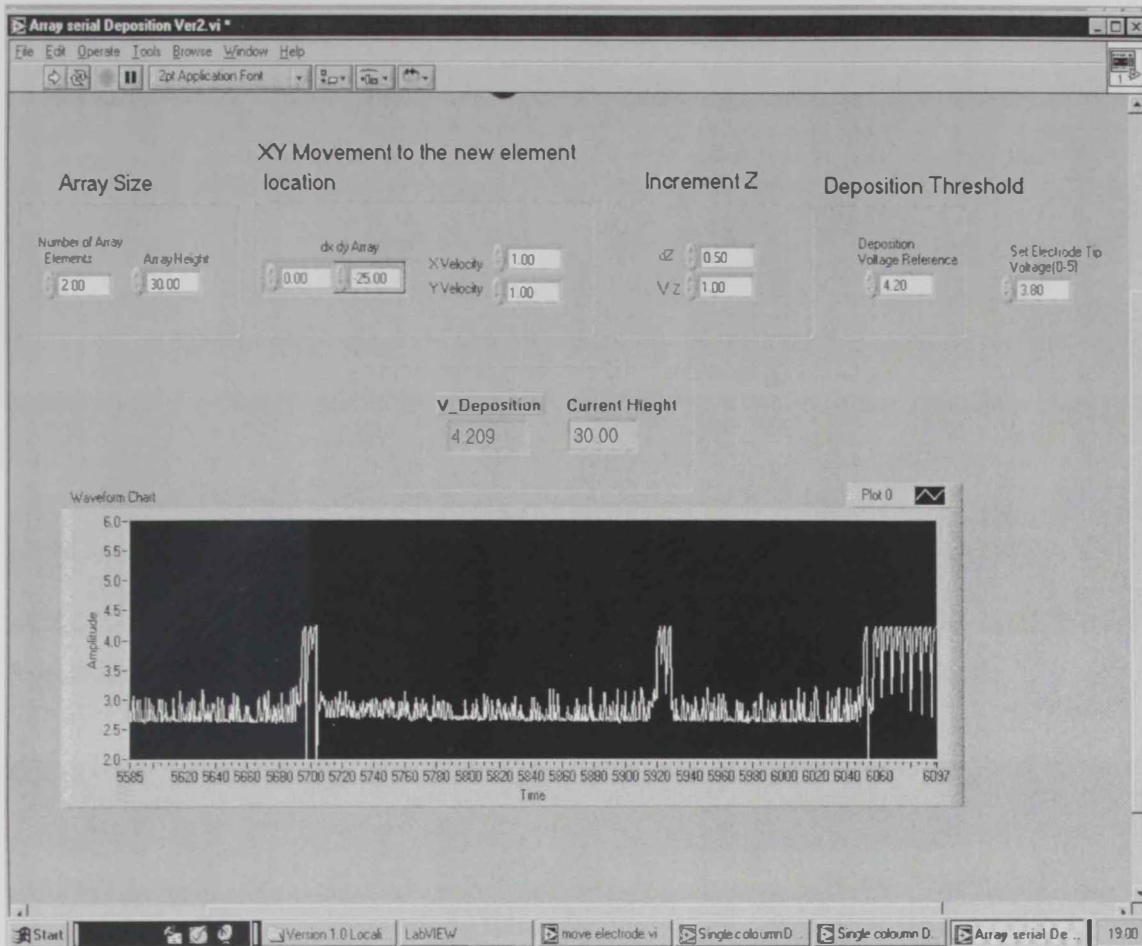
- [26] Hereen, Reynaerts, Brussel, Berurent, Larsson and Bertholds, Microstructuring of silicon by electro-discharge machining (EDM) - Part II: Application, Sensors and Actuators, A 61, pp. 379-386, 1997.
- [27] Said R.A., Shape Formation of Microstructures Fabricated by Localized Electrochemical Deposition, Journal of the Electrochemical society, 150, 8 1-0, 2003.
- [28] Jung Woo Park I, Shi Hyoung Ryu, and Chong Nam Chu, Pulsed Electrochemical Deposition for 3D Micro Structuring, Journal of Precision Engineering and Manufacturing, Vol. 6, 4, 2005.
- [29] Lin C.S., Lee C.Y, Improved copper microcolumn using localized electrochemical deposition, Electrochem. Solid-State Lett., Vol.8, 9, 125-129, 2005.
- [30] Said R. A., Forced convection magneto-electroplating for enhanced semiconductors metallization, Journal of Vac. Sci. Technol. A 22 452-60, 2004.
- [31] Andeas Hierlemann, Oliver Brand, Christoph Hagleitner, and Henry Baltes, Microfabrication Techniques for Chemical/Biosensors, Proceedings of the IEEE, Vol. 91, 6, 2003.
- [32] Karel Stulik, Christian Amatore, Karel Holub, Vladimir Marecek and Wlodzimierz Kutner, Voltammetric Microelectrodes: Definitions, characterization, and applications, Technical Report, Pure Appl. Chem., Vol. 72, 8, 1483-1492, 2000.
- [33] Jian Wul, Le Yan, William C. Tang and Fan-Gang Zeng, Micromachined Electrode Arrays with Form-Fitting Profile for Auditory Nerve Prostheses, Proceedings of the 2005 IEEE Engineering in Medicine and Biology 27th Annual Conference Shanghai, China, 2005.
- [34] Andrew C. Barton, Stuart D. Collyer, Frank Davis, Davinia D. Gornall, Karen A. Law, Emma C.D Lawrence, Danian W. Mills, Suzy Myler, Jeanette A. Pritchard, Mark Thompson, Seamus P.J Higson, Sonochemically fabricated microelectrode arrays for biosensors offering widespread applications: Part I, Journal of Biosensors and Bioelectronics, Vol. 20, 2, 328-337, 2004.
- [35] Rosemary Feeney and Samuel P. Kounaves, Microfabricated Ultramicroelectrode Arrays: Developments, Advances, and Applications in Environmental Analysis, Electroanalysis 2000, 12, 9, 2000.

- [36] Said R. A., Localized deposition of copper microstructures (II): artifacts of electrode-tip geometry, The Electrochemical society int. Semiconductor Technology Conf., Shanghai, China, pp 18-25, 2001.

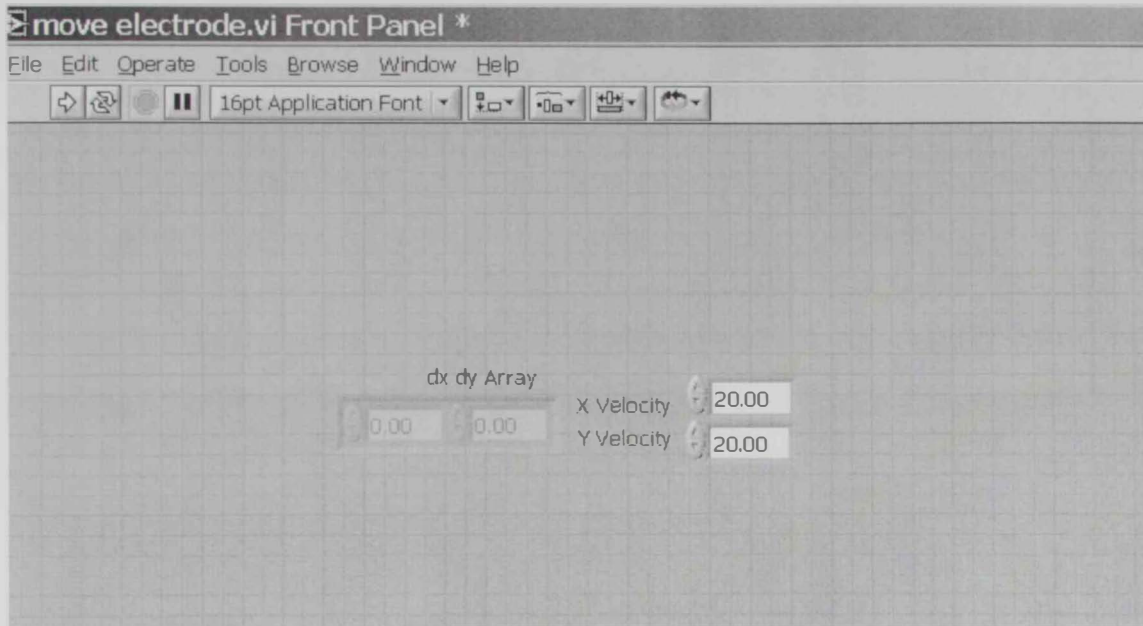
Appendix



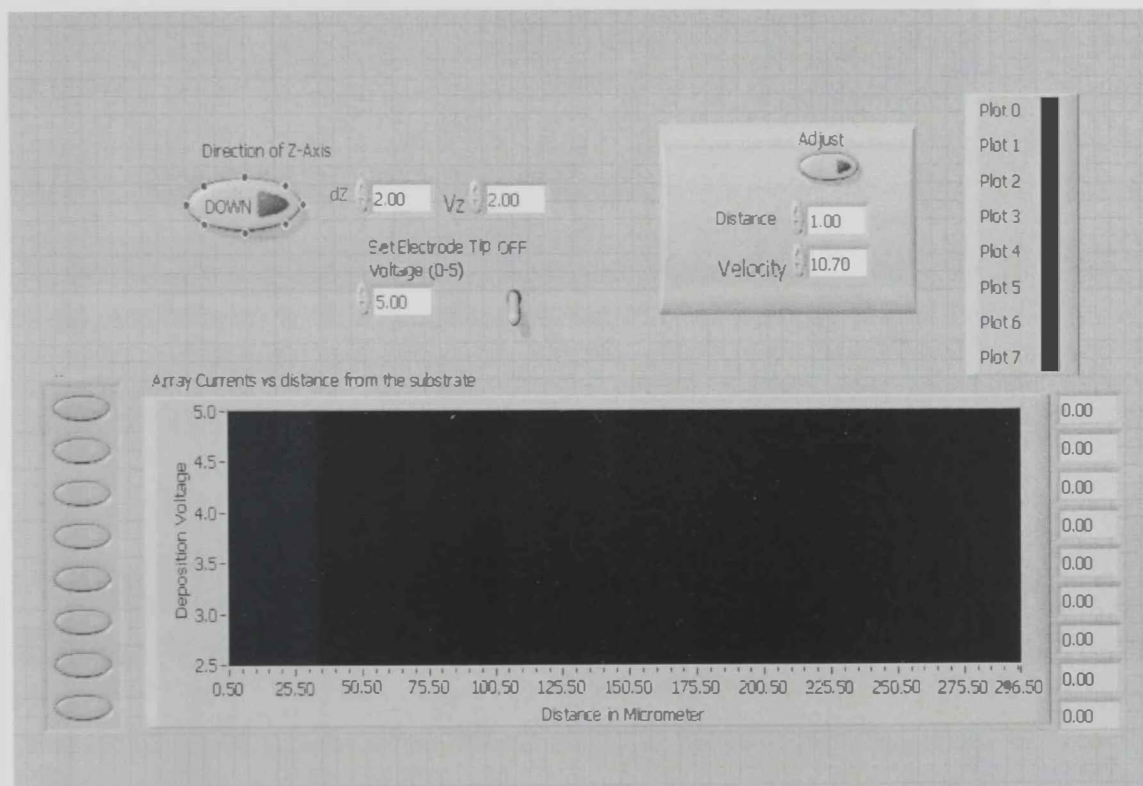
Appendix A: Block diagram code for the parallel deposition algorithm written in LabVIEW. The program is designed to allow the user to control and monitor the LED parallel deposition algorithm. Note when the current reaches a value more than the threshold indicating by the peak in the graph, it means that enough deposition has been achieved.



Appendix B: Block diagram code for the serial deposition algorithm written in LabVIEW.



Appendix C: Block diagram code used to move the microelectrode in the cell.



Appendix D: Block diagram code used for initial positioning of the microelectrode.

الخلاصة

لقد ازداد اهتمام الباحثين في مجال تكنولوجيا التصنيع الميكروسكوبي في استخدام الترسيب الكهربائي المركز وذلك بسبب إيجابيات هذه الطريقة بالمقارنة مع طرق التشكيل الميكروسكوبي التقليدية. هذه الإيجابيات تشمل بساطة النظام مما يقلل من كلفة تصنيع الأشكال الدقيقة، القدرة على تصنيع أشكال ميكروسكوبية ثنائية و ثلاثية الأبعاد و كذلك قابلية التشكيل من مواد مختلفة. ولكن إلى هذه اللحظة، لا تتوفر هذه التكنولوجيا على نطاق تجاري. الجهود الآن تتركز على محاولة توثيق التصنيع باستخدام الترسيب الكهربائي المركز من خلال وصف تأثير كل العوامل التي تؤثر في هذه العملية و التحكم فيها من أجل إنتاج أشكال ميكروسكوبية معقدة. هذه الأشكال بدورها يمكن أن تدمج في تطبيقات مختلفة مثل الإلكترونيات الدقيقة، الأجهزة الكهروميكانيكية الميكروسكوبية، الهوائيات و كذلك يمكن استخدامها كمجسات دقيقة في التطبيقات الحيوية و غيرها. من أجل توسيع قدرات الترسيب الكهربائي المركز التصنيعية، هذه الرسالة تقدم دراسة لامكانية تصنيع أشكال ميكروسكوبية متعددة باستخدام تكنولوجيا الترسيب الكهربائي المركز. هذه الأشكال المتعددة في شكل حزمه يمكن استخدامها كهوائيات في التطبيقات عالية التردد و في الأجهزة الكهروميكانيكية الميكروسكوبية.

في هذا البحث، لقد تم تقديم طريقتين لتصنيع الأشكال الميكروسكوبية المتعددة و هما التصنيع المتوالي و التصنيع المتوازي. تقوم فكرة التصنيع المتوالي على استخدام المجس الميكروسكوبي التقليدي في تشكيل الأشكال الميكروسكوبية في الحزمة بالتوالي، أي واحدا تلو الآخر. في الجهة الأخرى، يقوم التصنيع المتوازي بتشكيل الأشكال الميكروسكوبية في الحزمة دفعة واحدة وذلك باستخدام المجس الميكروسكوبي المتعدد. لقد تم دراسة تأثير مادة المجس، أبعاد المجس الهندسية و المادة المستخدمة في عملية الترسيب على الشكل الميكروسكوبي خلال عملية التصنيع.

إن طريقة الترسيب المتوازي التي تم اعتمادها في هذه التكنولوجيا لأول مرة تساعد على تطوير التشكيل باستخدام تكنولوجيا الترسيب الكهربائي المركز. لقد حسن الترسيب المتوازي من إمكانية تصنيع أشكال ميكروسكوبية متلاصقة مع تحسن في مدى نجاح التصنيع عند اعادته تحت نفس الظروف تقريبا. إن أحد الفوائد المهمة في الترسيب المتوازي بالمقارنة مع الترسيب المتوالي هي تقليل الوقت اللازم لصنع أشكال ميكروسكوبية على شكل حزم مما يسهل عملية إنتاج هذه الأشكال على نطاق واسع.



جامعة الإمارات العربية المتحدة
عمادة الدراسات العليا

تصنيع الأشكال الميكروسكوبية المتعدده باستخدام الترسيب الكهربائي المركز

رسالة مقدمة من :

نضال خلف الشواور

إشراف:

أ.د. يوسف حايك
قسم الهندسة الميكانيكية
كلية الهندسة- جامعة الإمارات العربية المتحدة

د. رافع أحمد سعيد
قسم الهندسة الكهربائية
كلية الهندسة- جامعة الإمارات العربية المتحدة

مقدمة لجامعة الإمارات العربية المتحدة استكمالاً لمتطلبات الحصول على درجة الماجستير في
علوم و هندسة المواد

2005-2006